Comprehensive Seismic Risk and Vulnerability Study for the State of South Carolina

URS Corporation
Durham Technologies, Inc.
Image Cat, Inc.
Pacific Engineering & Analysis
S&ME, Inc.

Final Report

10 September 2001

URS

FINAL REPORT

COMPREHENSIVE SEISMIC RISK AND VULNERABILITY STUDY FOR THE STATE OF SOUTH CAROLINA

Prepared for

South Carolina Emergency Preparedness Division
1100 Fish Hatchery Road
West Columbia, SC 29172-2024

Prepared by

URS Corporation
Durham Technologies, Inc.
ImageCat, Inc.
Pacific Engineering & Analysis
S&ME, Inc.

10 September 2001

51-D0111027.00

TABLE OF CONTENTS

TABLE OF CONTENTS

TABLE OF CONTENTS

TABLE OF CONTENTS

Figures

TABLE OF CONTENTS

TABLE OF CONTENTS

TABLE OF CONTENTS

Tables

Appendices

Acceleration - The rate of change of velocity of a reference point. Commonly expressed as a fraction or percentage of the acceleration due to gravity (g), where $g = 9.8\ m/sec^2$.

Acceleration Response Spectrum - A plot of the maximum acceleration response (to an earthquake record) of a series of linear single-degree-of-freedom (SDOF) systems. Many structures and soil deposits can be represented by one or more SDOF systems.

Aleatory Variability - Inherent or natural randomness in physical quantities.

Amplification Factor - Ratio of soil motion to rock motion. In this project the motion is defined as 5% damped response spectra.

Attenuation - A decrease in seismic-signal amplitude as waves propagate from the seismic source. Attenuation is caused by geometric spreading of seismic-wave energy and by the absorption and scattering of seismic energy in different Earth materials. Q and kappa are attenuation parameters used in modeling the attenuation of ground motions.

Band-Limited - An observation that strong ground motion amplitudes decrease rapidly at low and high frequency and are relatively uniform at intermediate frequencies (see **corner frequency**).

Building Types - The following building structural types are derived from FEMA's National Earthquake Hazards Reduction Program [FEMA 310, FEMA 356, etc.], and are used in the HAZUS methodology:

W1	Wood, Light Frame (5,000 sq. ft.)
W2	Wood, Commercial and Industrial (> 5,000 sq. ft.)
S1	Steel Moment Frame
S2	Steel Braced Frame
S3	Steel Light Frame
S4	Steel Frame with Cast-in-Place Concrete Shear Walls Low-Rise
S5	Steel Frame with Unreinforced Masonry Infill Walls Low-Rise
C1	Concrete Moment Frame Low-Rise
C2	Concrete Shear Walls Low-Rise
C3	Concrete Frame with Unreinforced Masonry Infill Walls Low-Rise
PC1	Precast Concrete Tilt-Up Walls
PC2	Precast Concrete Frames with Concrete Shear Walls Low-Rise
RM1	Reinforced Masonry Bearing Walls with Wood or Metal Deck Diaphragms Low-Rise
RM2	Reinforced Masonry Bearing Walls with Precast Concrete Diaphragms Low-Rise
URM	Unreinforced Masonry Bearing Walls Low-Rise
MH	Mobile Homes

(The complete NEHRP definition for each building structural type is presented in Appendix F.)

Corner Frequency - Frequency below which strong ground motion amplitudes rapidly decrease (see **band-limited**).

Damping - The loss or dissipation of energy in a system.

Deterministic Hazard Assessment - An assessment that specifies single-valued parameters such as maximum earthquake magnitude or peak ground acceleration, without consideration of likelihood.

Drift - The relative interstory displacement of a building subject to lateral loads.

Ductility - The ability to sustain deformation beyond the elastic limit (yield) without material failure.

Duration - The time interval in earthquake ground shaking during which motion exceeds a given threshold. For example, the measure of duration to be used as a measure of damage potential to buildings might be the time interval over which acceleration at the base of a building exceeds, say, 5 percent of the acceleration of gravity.

Earthquake Hazard - Any physical phenomenon associated with an earthquake that may produce adverse effects on human activities. This includes surface faulting, ground shaking, landslides, liquefaction, tectonic deformation, tsunami, and seiche and their effects on land use, manmade structures, and socio-economic systems. A commonly used restricted definition of earthquake hazard is the probability of occurrence of a specified level of ground shaking in a specified period of time.

Elastic Behavior - Elastic behavior describes a state of deformation under an externally-imposed load from which a member will return to its previous undeformed state completely, once the imposed loading is removed. If member responses are directly proportional to the amount of load applied, then the behavior is described as *linear elastic* response.

Epicenter - The point on the Earth's surface vertically above the point (focus or **hypocenter**) in the crust where a seismic rupture nucleates.

Epistemic Uncertainty - Lack of knowledge regarding the values of physical quantities.

Equivalent-Linear Approach - A widely used approximate solution to computing ground motions when the relationship between stress and strain depends on the level (amplitude) of strain (see **nonlinear**).

Fault - A fracture along which there has been significant displacement of the two sides relative to each other parallel to the fracture. Strike-slip faults are vertical (or nearly vertical) fractures along which rock masses have mostly shifted horizontally. Dip-slip faults are inclined fractures along which rock masses have mostly shifted vertically. If the rock mass above an inclined fault is depressed by slip, the fault is termed normal, whereas if the rock above the fault is elevated by slip, the fault is termed reverse (or thrust).

Fines Content - Soil particles that will pass through a No. 200 sieve.

Finite Source - An earthquake source whose areal extent of slip on the fault rupture surface is considered in estimating strong ground motions.

Frequency - In the context of risk analysis, frequency refers to how often an event or outcome will occur, given a specified exposure period. In the context of earthquake engineering and structural analysis, frequency is the inverse of a period of vibration.

g - See **Acceleration**.

Hazard - An event which threatens to cause injury, damage or loss, such as ground shaking, surface fault rupture, soil liquefaction, etc.

Holocene - Refers to a period of time between the present and 10,000 years before present. Applied to rocks or faults, this term indicates the period of rock formation or the time of the

most recent fault slip. Faults of this age are commonly considered active, based on the observation of historical activity on faults of this age in other locales.

Hypocenter - The point within the Earth where an earthquake rupture initiates.

Hysteretic - The relationship between stress and strain for nonlinear materials.

Intensity - A subjective numerical index describing the severity of an earthquake in terms of its effects on the Earth's surface on humans and their structures.

Irregularity *(see also* **Regularity***)* **-** Describes deviations from optimal seismic structural configuration. Common irregularities are divided into *vertical* and *plan* irregularities:

Plan Irregularities - Common cases include re-entrant corners, non-symmetric distribution of mass, strength or stiffness within any given story.

Vertical Irregularities - Abrupt changes in plan dimensions, weight, strength or stiffness from one story to another. One common vertical irregularity is the soft or weak story, often the first story, which may lead to structural collapse as earthquake ductility demands concentrate in one story, rather than distributing more uniformly over the height of the building.

Kappa - Parameter describing material damping in the shallow crust (depths of 1 to 2 km).

Lateral Flow (or lateral spread) - Liquefaction-induced ground failure where surficial soil is displaced downslope or towards a free face (e.g., a river channel) along a shear zone formed within liquefied soil.

Lifelines - Structures that are important or critical for urban functionality. Examples are roadways, pipeline, powerlines, sewers, communications, and port facilities.

Liquefaction - The soil behavior phenomenon in which a saturated sand softens and loses strength due to the development of high excess pore pressures during strong earthquake ground shaking.

Magnitude (M) - A number that characterizes the relative size of an earthquake. Magnitude is based on measurement of maximum motion recorded by a seismograph, corrected for attenuation to a standardized distance. Several scales have been defined, but the most commonly used are (1) moment magnitude (**M**), (2) local magnitude or Richter magnitude (M_L), (3) surface-wave magnitude (M_S), and (4) body-wave magnitude (m_b). The moment magnitude (**M**) scale, based on the concept of seismic moment is uniformly applicable to all sizes of earthquakes but is more difficult to compute than the other types. In principal, all magnitude scales could be cross-calibrated to yield the same value for any given earthquake, but this expectation has proven to be only approximately true, thus the need to specify the magnitude type as well as its value.

Moment - A traction which tends to cause rotation, e.g., a torque.

Bending Moment - The internal traction within a framing member which induces curvature (i.e., flexural deformation).

Natural Period of Vibration - The time required to complete one cycle of motion in harmonic vibration. A single-degree-of-freedom oscillator, such as a simple pendulum, has a single

natural period of vibration. A complex structure, such as a building, may vibrate in many different elastic modes, each having an associated period of vibration.

Nonlinear - In all materials, above a threshold strain, the relationship between stress and strain depends on the level (amplitude) of strain.

Parametric Uncertainty - Epistemic or aleatory uncertainty in parameter values of a physical process.

Peak Horizontal Acceleration (PHA) - An instrumental measure of earthquake ground motion intensity, normally taken from a triaxial earthquake accelerogram as the maximum value recorded from either of the two horizontally-oriented axes.

Plastic Behavior - Plastic behavior describes a state of deformation under an externally-imposed load from which a member will *not* return to its previous undeformed state completely once the imposed loading is removed. Some permanent residual *("plastic")* deformation will remain.

Pleistocene - The time period between about 10,000 years before present and about 1,650,000 years before present. As a descriptive term applied to rocks or faults, it marks the period of rock formation or the time of most recent fault slip, respectively. Faults of Pleistocene age may be considered active though their activity rates are commonly lower than younger faults.

Point Source - An earthquake source process where the areal extent of slip on the fault rupture surface is considered to occur at an idealized point in the earth in estimating strong ground motions.

Probabilistic Hazard Assessment - An assessment which stipulates quantitative probabilities of the occurrences of specified hazards, usually within a specified time period.

Random Vibration Theory (RVT) - Approximate relationship between the spectral and time domain of physical processes that display inherently random characteristics, e.g., the accelerations (forces) from an earthquake.

Regularity - For optimum seismic performance, a building structure should be *regular.* In general, regular structures have:

- balanced earthquake resisting elements (in strength and stiffness)
- symmetrical plan (to reduce torsion, or twisting)
- uniform cross section in plan and elevation
- maximum torsional resistance
- short member spans
- direct load paths
- uniform story heights
- redundancy (no single component failure should cause system failure)

Risk - The chance or probability that some undesirable outcome, such as injury, damage, or loss, will occur during a specified exposure period.

Seismicity - The geographic and historical distribution of earthquakes.

Shear - Generally speaking, seismic shear is the sum of the internal horizontal forces which develop within a building as the building responds to the horizontal displacement of its base in earthquake ground motion. Shear also refers to internal forces or stresses within building elements:

Shear Wall - a structural wall designed to resist lateral (i.e., sideways) forces which act parallel to the plane of the wall.

Beam or Slab Shear - the internal member force acting perpendicular to the length of the beam or plane of the slab.

Shear Wave (or S-wave) - A seismic wave with direction of propagation that is at right angle to the direction of particle vibration.

Shear-Wave Velocity - The velocity at which a shear wave is transmitted through a media. The shear wave velocity is mathematically related to stiffness. In earthquake engineering, the in-place shear wave velocity is used to determine the stiffness of the soil and rock at very small strains.

Spectral Acceleration - Response of a suite of single-degree-of-freedom oscillators to an earthquake, used to represent forces on a structure.

Stochastic - Randomly varying, e.g., earthquake forces, particularly at high (> 1 Hz) frequency. Although the peak amplitudes of strong motions (accelerations) from large earthquakes are predictable with reasonable accuracy, when the peaks occur in time is unpredictable or stochastic.

Tectonic - Refers to rock-deforming processes and resulting structures that occur over regional sections of the Earth's crust and uppermost mantle.

Vulnerability - A facility's susceptibility to damage or loss from a specific hazard.

At 9:50 p.m. on 31 August 1886, one of the largest known earthquakes to have occurred in eastern North America struck Charleston, South Carolina. The event lasted less than a minute but resulted in 60 deaths and extensive damage in Charleston. The earthquake also caused minor to moderate damage throughout the southeastern U.S. In this report, we describe a comprehensive seismic risk assessment of the State of South Carolina performed for the South Carolina Emergency Preparedness Division (SCEPD). The purpose of the study is to evaluate the potential losses from four earthquake scenarios using HAZUS (FEMA'S state-of-the-art loss estimation model). These results will provide a basis for the State to effectively plan and prepare for future damaging earthquakes. The four earthquake scenarios considered were a moment magnitude (**M**) 7.3 "1886 Charleston-like" earthquake, **M** 6.3 and **M** 5.3 events also from the Charleston seismic source, and a **M** 5.0 earthquake in Columbia. The evaluation was carried out in ten tasks: (1) review of current South Carolina emergency management plans, including the Emergency Operations Plan, the Hazard Mitigation Plan, and the Hurricane Plan, (2) characterization of geologic site response categories, (3) calculations of scenario earthquake ground motions, (4) evaluation of liquefaction and earthquake-induced landslide potential, (5) compilation and evaluation of building inventory, (6) compilation and evaluation of lifeline and essential facility data, (7) compilation and evaluation of HAZMAT data, (8) evaluation of a dam database, (9) HAZUS calculations and analysis, and (10) development of maps.

Ground motion estimates for the four scenario earthquakes were computed at a high-resolution 2x2-km-grid spacing of the entire State using a state-of-the-art numerical modeling approach which incorporated region-specific seismic source, path, and site effects as well as their uncertainties. Because there is considerable uncertainty regarding the source of the 1886 Charleston earthquake, fault rupture parameters were varied and the resulting calculated pattern of ground motions and probability of liquefaction were compared against the 1886 observations. Based on these comparisons, the final fault parameters were selected which resulted in the most favorable comparison to the 1886 earthquake. The rupture plane of the **M** 7.3 event was generally modeled as a north-northeast-trending strike-slip fault 100 km in length coincident with the Woodstock fault. The possibility that the fault was only 50 km long was also included in the ground motion estimates.

The **M** 6.3 and **M** 5.3 Charleston scenario earthquakes were assumed to occur on the same fault source as the **M** 7.3 event but with smaller rupture dimensions. The **M** 6.3 rupture area was generally modeled as being 20 km in length and 10 km in width. The **M** 5.3 rupture area was assumed to have the dimensions of about 5x5 km. Although the specific sources of earthquakes are unknown in the Piedmont, we assumed that the scenario earthquake in Columbia was an event that could occur along a segment of the Eastern Piedmont fault system with rupture dimensions of about 3x3 km.

An extensive effort was made to characterize the subsurface geology of the State for the purposes of quantifying the effects of soil on ground motions and corresponding liquefaction potential. The type of geologic material, thickness, shear-wave velocities, and dynamic material properties of units were evaluated along with their respective uncertainties. For evaluating liquefaction, the degree of water saturation was also analyzed. Based on the characterization of the surficial geology, the State was divided into four site response categories: Blue Ridge/Piedmont, Savannah River, Myrtle Beach, and Charleston. Based on the rock ground motion calculations, State-wide maps for estimates of the surficial ground shaking characterized by four parameters (peak horizontal acceleration and velocity and 0.3 and 1.0 sec spectral

acceleration) were produced by multiplying the rock motions by soil amplification factors. These factors were computed for each site response category and were a function of soil thickness and input rock motion.

Both the ground motions and factor of safety against liquefaction reflect best estimate median values due to uncertainties in seismic source, path, and site properties. Actual ground motions as well as liquefaction occurrence then have a 50% chance of being larger or smaller than median estimates presented for each of the scenario earthquakes. Thus the results of the HAZUS analysis are based on our best estimates of the ground shaking and liquefaction hazards associated with the four scenario earthquakes. Higher estimates of losses would result from considering other estimates of the hazards with lower probabilities of being exceeded (e.g., 84th percentile).

The highest median ground motion estimates were calculated for the **M** 7.3 scenario event. Peak horizontal accelerations as high as 0.6 to 0.7 g on soil were estimated in the vicinity of the modeled rupture. For the **M** 6.3 and 5.3 Charleston scenarios, peak horizontal accelerations are estimated to be > 0.3 g and 0.20 to 0.25 g, respectively. A **M** 5.0 in Columbia could result in peak values greater than 0.2 g. For each of the four scenario earthquakes, isoseismal maps expressed in terms of Modified Mercalli intensity were also developed.

The potential for liquefaction was evaluated for the entire State and mapped. The soil resistance to liquefaction was estimated based on the average shear-wave velocity profile for each site response category. The earthquake demand (in terms of cyclic shear stress) was then determined by the site response analysis. The ratio of the cyclic resistance to the cyclic demand (adjusted for earthquake magnitude) is the factor of safety against liquefaction, and can be also related to both ground movement potential as well as probability of liquefaction. As evidenced by the widespread liquefaction that occurred in 1886, the potential is moderate to high along the Coastal Plain. Considering the age of the residuum (weathered bedrock) in the Piedmont and Blue Ridge areas of South Carolina, the liquefaction hazard was considered very low, and thus, liquefaction-induced settlement and lateral spreading during an earthquake was considered very unlikely. However, younger sediments (e.g., loose Pleistocene sands) are considered susceptible to liquefaction. Based on the ground motions, the liquefaction and earthquake-induced landslide hazards were quantified and input into HAZUS at the 2x2 km grid spacing.

HAZUS databases for the building inventory were updated using current values tabulated by occupancy. Furthermore, the algorithms that map occupancy-related building value into structural vulnerability were customized to better reflect the types and quality of building construction found in South Carolina. The customized inventory and vulnerability modeling were deemed extremely important, because the distribution and characteristics of South Carolina's building stock are markedly different from the national averages for building types and from California damage experience used in the default data provided with HAZUS.

First, South Carolina's choices of building type are often quite different from typical selections in California. For example, concrete tilt-up buildings are very often the building type of choice for light industrial facilities in California, but are seldom used in South Carolina. Light steel construction is largely preferred by South Carolina engineers and contractors for such applications. Second, building damagability (vulnerability) relationships will vary considerably from California to South Carolina, where very vulnerable unreinforced masonry, constructed without seismic design, was prevalent in most South Carolina counties until eight years ago. The

seismic performance of such URM will be much poorer than that of California reinforced masonry that has been designed for seismic forces. However, because of the incidence of hurricane force winds in a roughly 50 mile coastal strip, light construction (such as wood and light steel framing) that has been designed for such wind forces may perform quite well seismically in such South Carolina coastal areas.

To update and refine the census and building value data, the Project Team utilized six sources of information: (1) the 2000 Census data at a census block resolution level, (2) the 2000 occupancy square footage data processed by Dun and Bradstreet also at a census block resolution level, (3) collected assessor's files for Greenville and Berkeley counties, (4) historical demographic growth data to approximate the age of buildings, (5) county business pattern for the economic data, and (6) data reprocessed at more than 21,138 (2x2 km) grid cells instead of the current 854 census tracts. In addition to the improved HAZUS default data, the State provided an inventory listing for all State buildings greater than 3,000 square feet in area.

A limitation of HAZUS and this analysis is that the influx of tourists into the State, particularly during the summer months, is not explicitly accounted for in our loss estimates. If a large earthquake were to occur in the summer, the losses could be significantly higher.

The Project Team drew upon the expert opinion of local building officials and structural design professionals, visual surveys in Charleston and other urban areas, and records from the 1886 Charleston earthquake as a basis for updating structural vulnerability relationships within HAZUS. Occupancy and vulnerability assignments were developed for the following specific cases:

- Charleston's historical district,
- General urban areas (Charleston, outside of the historical district, and other areas statewide having a population density greater than 500 persons per square kilometer),
- General nonurban areas, and
- Coastal resort areas.

For each case, building values-at-risk from each occupancy class were distributed to HAZUS structural classes. Seismic design levels were specified, and seismic "quality" assigned. Age breakdowns were established where appropriate. As a result of the inventory revisions and the improved structural vulnerability modeling, the HAZUS model for South Carolina much more accurately represents the exposures and their damage potential. Based on these tasks, the information on the built environment was aggregated at the 2x2 km grid for the State.

Lifelines include water and sewage systems, electric power and communication systems, natural gas facilities (including pipelines), transportation systems, airports, and port and harbor facilities. Essential facilities include police and fire stations, hospitals and emergency operations centers. Supplemental data was collected for all data types. In the vast majority of cases, we were able to substantially increase the amount and accuracy of data. The data collection effort contributed to a much more accurate loss assessment.

Very detailed hazardous materials databases were collected from the South Carolina Department of Health and Environmental Control and reformatted to adhere to a HAZUS format. This process included such tasks as the elimination of duplicate records, GIS projection and many database queries.

Because of the potential severe consequences of dam failures in South Carolina, a detailed inventory of dams was compiled. From the National Inventory of Dams (NID), we collected general information on over 4,500 dams in the State and adjacent states. Dams from neighboring states were considered as their failure could cause loss of life or material losses in South Carolina. We assigned various risk factors to each dam and combined them into a site- and structure-specific "Total Risk Factor" (TRF). We also developed simple seismic vulnerability functions for each type of dam based on the worldwide performance of dams during historic earthquakes. The vulnerability functions, ground motion estimates, and other factors, such as dam size, year when constructed or modified, reservoir volume and downstream hazard were used to obtain the TRF. We then ranked the dams within and outside the State by decreasing TRF's and assigned to each dam a risk class, ranging from "Low" (Class I) to "Extreme" (Class IV).

Three South Carolina dams have been assigned the Extreme Risk Class IV. These are Pinopolis West Dike, Lake Murray, and Clearwater Lake. Ninety-four South Carolina dams fall into the High Risk Class III, and 2,047 dams within the Moderate Risk Class II. Outside of South Carolina, four tailings dams were assigned the Extreme Risk Class IV. Bonsal Tailings Dam, North Carolina and Winson Impound Dam No. 1, Georgia, were ranked one and two, respectively. We assigned the Class III to 478 dams, while 1,682 more belong to Class II. The risk classification will provide guidance to the Dams and Reservoirs Safety Section of the Department of Health and Environmental Control and other agencies to select appropriate evaluation procedures for the most critical dams and will facilitate the assignment of priorities for future safety evaluations.

Based on the above input, the HAZUS calculations and analysis were performed. The findings highlight several critical factors that have important implications for earthquake risk reduction, planning, preparedness, emergency response, and disaster recovery. Results indicate, not surprisingly, that the **M** 7.3 Charleston scenario by far would be the most destructive and disruptive to the State, followed by the **M** 6.3 scenario. Results from the **M** 7.3 scenario include:

- Economic losses due to building damage alone are estimated to be over $14 billion (2000 dollars) with ground failure effects included, compared to the $2 billion for the **M** 6.3 event. Losses to lifelines would result in more than $1 billion for the **M** 7.3 event.
- About $10.9 billion or about 77 percent of the total economic losses will occur in the Tri-County region (Charleston, Berkeley, and Dorchester Counties).
- The building damage alone will cause over $4.2 billion in losses due to business interruption in the State. These losses correspond to rental income losses, lost business income, wage losses, and expenses associated with relocation. Secondary business interruption losses related to lost revenues to suppliers and wholesalers are not included.
- A daytime event will cause the highest number of casualties. Of the estimated 45,000 casualties, close to 9,000 or about 20 percent will be major injuries (injuries requiring hospitalization) and fatalities (about 900). Most of these casualties will occur in Charleston, Dorchester, and Berkeley counties.
- Nearly 70,000 households, or about 200,000 people are expected to be displaced, with an estimated 60,000 people requiring short-term shelter.

- Fire following a **M** 7.3 earthquake in the Charleston area will be concentrated primarily in the Tri-county region. The scenario earthquake is expected to cause over 250 fires. The lack of operational firefighting equipment and a supply of water for fighting fires after a large earthquake may become a major concern in effectively fighting these fires.
- Due to insufficient seismic building code standards and the vintage of the building stock, the majority of the structures in the State, in particular schools and fire stations are vulnerable to damage. Indeed, it is estimated that over 220 schools (not considering the extensive damage to the relocateable school buildings) and over 100 fire stations will experience significant damage. This may lead to some potential issues with respect to providing reliable shelters for immediate use in emergency response and sheltering and with respect to responding effectively to the 250 fires, expected from this scenario. Schools are expected to suffer significant damage in the case of the **M** 6.3 scenario, as well. Furthermore, there could be some safety issues related to school children, teachers, and other persons in school buildings. The catastrophic failure or partial collapse of one or more school buildings during school periods could greatly increase the casualty estimates. Restoration of the schools for the emergency sheltering of the homeless and other contingency service will be demanding.
- Over 36 million tons of debris will be generated, including an estimated 10 million tons of Category II debris, which includes concrete and steel – materials that require special treatment in "deconstruction" and disposal. Debris disposal, therefore, may pose a major challenge in the recovery phase. This total does not include biomass.
- Hospitals will likely suffer significant building damage that could result in more than 30 hospitals out of the 108 (about 30%) being nonfunctional. Over half of these affected hospitals may experience extensive damage. The **M** 6.3 event will result in about 10 hospitals suffering considerable damage. Since most of this damage will be concentrated in the Tri-county area, the region may be faced with the serious issue of how to provide the needed care to existing patients and potential thousands of earthquake victims from the affected communities.
- Close to 800 bridges are expected to suffer enough damage to make them inaccessible, thus, hampering even further the recovery efforts. In addition, certain communities in the greater Charleston area are that are only accessible by bridge routes may be cut off.
- A good portion of the Charleston area is susceptible to liquefaction. However, ground failure effects contribute only about 5% or less to losses.
- Of all the utility systems, electric power is arguably the most critical, as many other lifelines depend on it. It is expected that about 63 electric power facilities, (51 substations out of the total of 380 and 12 power plants out of the total of 53) will suffer at least moderate damage and nearly 300,000 households will be without power, right after the earthquake.
- In potable water pipes greater than 12 inches, over 1100 repairs will be needed, or about a repair for every two kilometers of these pipes. Over half of these are expected to be breaks. Widespread water failure may drain water within minutes or hours from the distribution system, thus preventing adequate water supply for fire suppression. In addition, about 80% of the urban households in the affected area will be deprived of water. It will take weeks, if not months, to restore the serviceability of the water systems. Therefore, significant external augmentation would be required to provide and sustain such a high repair level.

In the event of a **M** 6.3 earthquake in Charleston, approximately 136,000 buildings will sustain slight to moderate damage and 25,000 will be extensively damaged. Total building loss including capital stock and income losses will exceed $2 billion. Approximately 30 to 60 people will be killed and from 2,000 to more than 3,000 people will suffer minor to major injuries.

In the **M** 5.3 Charleston scenario earthquake, the losses and casualties decrease significantly. Injuries will number less than 100 with no estimated deaths. Total loss to buildings will be about $230 million.

If a small earthquake of **M** 5.0 were to occur in Columbia, approximately 400 buildings would sustain slight or moderate damage with a total loss of $310 million. Less than 10 people will be injured and only with minor injuries.

In summary, a repeat of the **M** 7.3 Charleston earthquake in South Carolina, at least in the early aftermath, may cause the State to be overwhelmed by widespread damage as well as the disruption of lifelines. The impact from this event demonstrates the scope of the problem and reinforces the need to implement structural and non-structural mitigation measures as a central feature in long-term initiatives to reduce seismic risk. Affected communities will be coping with the trauma and demands of immediate response and early recovery.

Early Federal assistance, along with first-tier support drawn from the non-affected regions, will be of highest priority. Still, a well-coordinated, pre-planned response involving all levels of government, along with the private sector and other groups, will be required to deal effectively with the consequences of an event of this magnitude. Establishing centralized communications, command, and control to coordinate rescue efforts will be immediately critical. Transporting the injured to hospitals will require priority action. Directing firefighting efforts to the most essential facilities and to control the spread of fires will require prompt action to minimize casualties and property loss. The emergency inspection and repair of minimum critical water pipeline segments must be well focused in coordination with the fire department. Directing debris removal may require priority for passage of emergency vehicles.

By characterizing the nature and scope of potential impacts, this report represents a starting point in this effort and provides a planning baseline for coordination, capability development, training and strategic planning for SCEPD.

RECOMMENDATIONS

Given the nature and scope of impacts that a major seismic event will have on South Carolina, the obvious question is “what can be done?” The impacts of a major earthquake are indeed overwhelming. However, a better understanding of the impacts revealed by this study will significantly improve the ability of decision makers to judge how best to proceed.

Several areas appear to lend themselves to follow-on study, do not require major expenditures, and appear to be the purview of State government. The Project Team has outlined several such recommendations for follow-on study that will allow the State to gain a significantly better understanding of some of the key impacts of such seismic events, and also of what the possibilities, costs, and benefits of various mitigative actions might be.

1) The HAZUS study should be updated, once the balance of the 2000 census data is available.

2) The HAZUS study may be refined for certain geographical areas of interest such as Charleston (e.g., areas with larger populations, greater amounts of industry, etc.). Further research and collection of subsurface data could be performed to achieve a greater resolution for the different soil conditions using a smaller grid size. Because the liquefaction resistance depends on the characterization of the subsurface conditions, any refinements will also influence the results of the liquefaction hazard evaluation.

3) A series of studies could be performed to quantify the seismic risk in specific areas and to develop concepts for reducing that risk. Such quantification of risks and the benefits afforded by risk reduction measures would allow a prioritization of which measures are the most cost-effective in reducing casualties, damage, etc. The areas for such focused follow-on study include seismic vulnerability/risk audits for critical and important structures and facilities such as bridges, schools, fire stations, police stations, emergency response centers, hospitals, water systems, waste water systems, and airport and power generating facilities. State and local government buildings could also be included. Initially, such studies should focus on the more seismically active areas, such as the Tri-County area.

4) Analyses could be carried out on the feasibility and the benefit/cost ratios of anchoring of Charleston historical wood residential buildings to their foundations, and the bracing of URM parapet walls, and the anchorage of URM walls to roofs and floors in the Tri-County area. This latter recommended study should consider whether the promotion of such measures should be by legal mandate, or by offering governmental "incentives". Unlike the public structures and facilities above, this recommendation addresses private buildings.

5) A more detailed analysis could be performed to quantify the level of hazardous materials release and the impact that these releases have on the general public. The database for this analysis should build on the work detailed in the "Handbook for Conducting a GIS-Based Hazards Assessment at the County Level", prepared for SCEPD by the Hazards Research Laboratory at USC.

6) A more detailed analysis could be performed to address specific transportation loss issues (evacuation, traffic congestion, etc.) using specifically designed software.

7) A more detailed analysis could be performed to study the impact that large earthquakes have on local and regional tourism including developing a more accurate model of hotel occupancy in the Tri-County area. To assess the actual costs or losses to the tourism industry, a study of both short- and long-term impacts should be conducted.

The 31 August 1886 moment magnitude (**M**) 7.3 earthquake which struck Charleston, South Carolina, is the largest event to have occurred in the southeastern U.S. and the most destructive (Bollinger, 1977; Bollinger *et al.*, 1991). It damaged or destroyed the large majority of buildings in Charleston and killed 60 people. Structural damage was widespread, extending as far as Alabama, Ohio, and West Virginia. Liquefaction was extensive in the epicentral area (Obermeier *et al.*, 1985; Amick and Gelinas, 1991; Talwani *et al.*, 1999). The maximum Modified Mercalli (MM) intensity was X. Summerville, which is now a rapidly growing urban area, was subjected to strong ground shaking that resulted in many houses either being displaced off their foundations, settled differentially, or had their chimneys destroyed. To this day, the source of the 1886 earthquake remains controversial.

Obviously a repeat of the 1886 earthquake or even a smaller moderate-sized event could be catastrophic to the State, particularly to the City of Charleston and the surrounding areas. Based on the recently developed 1996 U.S. Geological Survey national hazard maps (Frankel *et al.*, 1996), the Charleston area is only second to the New Madrid zone in terms of hazard in the eastern U.S. In recognition of its exposure to the earthquake hazard, the South Carolina Emergency Preparedness Division (SCEPD) has taken a major, unprecedented step (outside of the State of California) to undertake a comprehensive *statewide* analysis of its earthquake risk.

Thus, at the request of the SCEPD, URS Corporation and its partners Durham Technologies, Inc., ImageCat, Inc., Pacific Engineering Analysis, and S&ME, Inc. have performed a comprehensive seismic risk and vulnerability study for the State of South Carolina. In this evaluation, we have estimated the potential losses from four scenario earthquakes using FEMA's geographical information system (GIS) software HAZUS99. The four scenarios include three potential earthquakes generated by the source of the 1886 Charleston event: a **M** 7.3 repeat of the 1886 event and two smaller events of **M** 6.3 and **M** 5.3; and a **M** 5.0 earthquake resulting from rupture of a segment of the Eastern Piedmont fault system near Columbia.

Recent large earthquakes in the world have raised the awareness of the State of the damage potential of even a moderate-size event striking South Carolina. Four fundamental questions are at the center of this awareness:

1) What are the probabilities of damaging earthquakes in the State;
2) Where are the probable locations for such damaging events;
3) What structures are likely to be damaged; and
4) How would transportation and utility infrastructures be impacted.

Given the four scenario earthquakes considered in this study, we have attempted to answer the last two questions. The results of this study will allow the State to better understand its earthquake risk and vulnerabilities and to prepare the earthquake elements of its preparedness, response, and mitigation plans.

1.1 OBJECTIVE

The objective of this study was to estimate the losses resulting from four scenario earthquakes that may occur in South Carolina sometime in the future. As specified by SCEPD, we have estimated the following earthquake losses for each of the four scenarios. The effect of secondary hazards such as fires, dam/dike failures, and hazardous material (HAZMAT) release and spills

are included in these losses. Quantitative estimates of these losses will be calculated and they will be illustrated on HAZUS-generated maps.

- Number of casualties
- Number of persons requiring medical aid
- Number of uninhabitable homes
- Number of uninhabitable commercial and public buildings
- Amount of debris
- Economic impact in terms of dollars and recovery time summarized by county and state
- Functional loss of critical facilities and services including but not limited to
- Hospitals
- Schools
- Emergency response facilities
- Transportation facilities such as highways, airports, railroads, and ports
- Communication facilities such as telephone and radio
- Lifeline facilities such as electricity, natural gas, water supply and wastewater treatment
- Timeline for response and recovery.
- Casualty and homeless distribution forecast map.

In addition to the above quantitative estimates, we have produced the following map products for each earthquake scenario as requested by SCEPD. Each map displays the locations of critical and important facilities (e.g., hospitals, schools, military installations, etc.), roadways and highways, railways, airports, HAZMAT areas, and lifeline systems and facilities.

- Statewide isoseismal map
- Coastal Plain and Piedmont isoseismal map
- Ground shaking maps
- Liquefaction potential map
- Earthquake-induced landslide potential map
- Active fault map

1.2 USE OF THIS STUDY

This study is unique in its scope and in its involvement of nationally recognized experts in seismic hazard and risk assessment, and building, lifeline, and dam vulnerability. As outlined above, the result of this multidisciplinary effort is a comprehensive analysis of the impact of four scenario earthquakes on the State of South Carolina – its people, its buildings and lifelines, and its economy.

The outputs from the analysis can be used in a variety of ways:

- To assess the vulnerability of South Carolina's built environment to earthquakes of various magnitudes;
- To provide emergency managers at all levels with detailed estimates of damages and losses (outlined in Section 1.1), information that can be used to identify resource requirements for an effective, intergovernmental response and recovery operations;
- To specifically enable emergency managers to scale the mission requirements for "Emergency Support Functions." For example, the study provides the U.S. Army Corps of Engineers with estimates of the volume of debris that can be expected for different scenario earthquakes, information that can be factored into resource requirements for the agency's debris removal and disposal mission.
- To develop a statewide public awareness and education campaign that describes in details the consequences of different scenario earthquakes;
- To support the development and prioritization of mitigation strategies in a long-term effort to reduce the vulnerability of South Carolina to earthquakes; and
- To promote business–government coordination and collaboration in preparing for a major earthquake in South Carolina. For example, the HAZUS outputs on the functionality of lifelines, including electric power, water supply, and transportation (notably the functionality of bridges), can be valuable information in carrying out a business impact analysis.

1.3 SCOPE OF WORK

To accomplish the above objective, we have performed a series of 12 tasks as described below (Figure 1-1). The description of Tasks 1 to 9, their objectives, approach, and results are contained in the remaining sections of this report. The products of Task 10 are described in the respective sections.

- Review of Current Emergency Management Plans (Task 1)
- Characterization of Site Response Categories (Task 2)
- Calculations of Earthquake Scenario Ground Motions (Task 3)
- Evaluation of Liquefaction Earthquake-Induced Landslide Potential (Task 4)
- Compilation and Evaluation of Building Inventory (Task 5)
- Compilation and Evaluation of Lifeline and Essential Facility Data (Task 6)
- Compilation and Evaluation of HAZMAT Data (Task 7)
- Evaluation of Dam Database (Task 8)
- HAZUS Calculations and Analysis (Task 9)
- Development of Maps (Task 10)
- Final Report (Task 11)
- Project Management (Task 12)

1.4 PROJECT ORGANIZATION

The Project Team consists of individuals from URS Corporation and its partners. The following lists the Team members and their primary responsibilities.

Name	Responsibility
John O'Brien	Program Manager
Jeff Rouleau	Project Manager
Tara Engles	Assistant Project Manager
Ivan Wong	Technical Director and Tasks 10 and 11 Leader. Assisted in Tasks 2, 3, and 4.
Mike Swigart	Task 1 Leader
Tim Siegel	Task 2 Leader. Co-Leader for Task 4.
Billy Camp	Task 2 Advisor. Assisted in Task 4.
Dr. Walter Silva	Task 3 Leader. Co-Leader for Task 4. Assisted in Task 2.
William Graf	Task 5 Leader
Allan Porush	Task 5 Advisor
Charlie Huyck	Tasks 6 and 7 Leader
Ron Eguchi	Tasks 6 and 7 Advisor. Assisted in Tasks 6 and 7
Gilles Bureau	Task 8 Leader
Dr. Jawhar Bouabid	Task 9 Leader
Dr. Ron Andrus	Technical Advisory and Review Panel
Dr. Martin Chapman	Technical Advisory and Review Panel
Dr. Thomas Durham	Technical Advisory and Review Panel
David Fenster	Technical Advisory and Review Panel
Dr. Richard Lee	Technical Advisory and Review Panel
Dr. Stan Lindsey	Technical Advisory and Review Panel

1.5 HAZUS METHODOLOGY

Acknowledging the need to develop a standardized approach to estimating losses from earthquake and other hazards, FEMA embarked on a multi-year program to develop a GIS-based regional loss estimation tool under a cooperative agreement with the National Institute of Building Sciences. FEMA first released HAZUS in 1997 followed by an updated version in 1999. HAZUS is a tool that local, state and federal government officials and other can use for earthquake-related mitigation, emergency preparedness, response and recovery planning, and disaster response operations. The methodology in HAZUS is comprehensive. It incorporates state-of-the-art approaches for: 1) characterizing earth science hazards including ground shaking, liquefaction, and landslides; 2) estimating damage and losses to buildings and lifelines; 3) estimating fires following earthquake; 4) estimating casualties, displaced households, and shelter requirements; and 5) estimating direct and indirect economic losses.

The HAZUS technology is built upon an integrated GIS platform that produces regional profiles and estimates of earthquake losses. The methodology addresses the built environment, and categories of losses, in a comprehensive manner. HAZUS is composed of seven major modules,

which are interdependent and are shown in Figure 1-2. This modular approach allows different levels of analysis to be performed, ranging from estimates based on simplified models and default inventory data to more refined studies based on detailed engineering and geotechnical data for a specific study region, such as this one.

A brief description of each of the seven modules is presented below. Detailed technical descriptions of the modules can be found in the HAZUS technical manual (FEMA, 1999).

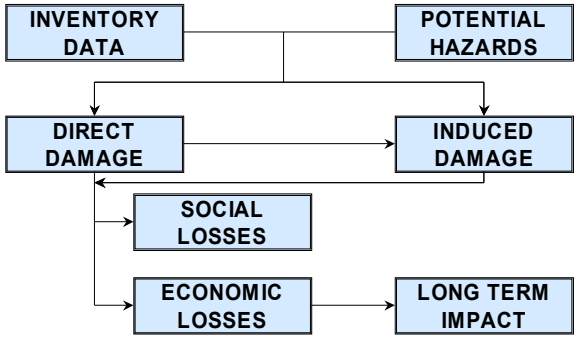

Figure 1-2. HAZUS Modules

Module 1 Potential Earth Science Hazard (PESH)

The Potential Earth Science Hazard module estimates ground motion and ground failure (landslides, liquefaction, and surface fault rupture). Ground motion demands in terms of spectral acceleration (SA) and peak horizontal ground acceleration (PGA) are typically estimated based on the location, size and type of earthquake, and the local geology.

For ground failure, permanent ground deformation (PGD) and probability of occurrence are determined. GIS-based maps for other earth science hazards, such as tsunami and seiche inundation, can also be incorporated. In the current study, the hazard data developed specifically for four scenarios is used.

Module 2 Inventory and Exposure Data

Built into HAZUS is a national-level basic exposure database that allows a user to run a preliminary analysis without having to collect any additional local data. The general stock of buildings is classified by occupancy (residential, commercial, etc.) and by model building type (structural system and material, height). The default mapping schemes are state-specific for single-family occupancy type and region-specific for all other occupancy types. They are age and building-height specific.

The four inventory groups are: a) general building stock, b) essential and high potential loss facilities, c) transportation systems, and d) utilities. The infrastructure within the study region must be inventoried in accordance with the standardized classification tables used by the methodology. These groups are defined to address distinct inventory and modeling characteristics. A description of the four inventory groups and HAZUS default mapping schemes can be further examined in Chapter 3 of the HAZUS technical manual. In this project and as described in great details in Sections 6, 7, and 8, inventory information related to the building

infrastructure, essential facilities, transportation networks, and utility systems has been substantially enhanced.

Default population data is based on the 1990 U.S. census, however in this project the demographic information is updated using the 2000 census data. Estimates for building exposure are based on default values for building replacement costs (dollars per square foot) for each model building type and occupancy class, in addition to certain regional cost modifiers. This data was drawn from Dun and Bradstreet and RS Means and also updated to year 2000.

Module 3 Direct Damage

This module provides damage estimates for each of the four inventory groups based on the level of exposure and the vulnerability of structures (potential for damage at different ground shaking levels).

For HAZUS, a technique using building fragility curves based on the inelastic building capacity and site-specific response spectra was developed to describe the damage incurred in building components (Kircher *et al.*, 1997). Since damage to nonstructural and structural components occurs differently, the methodology estimates both damage types separately. Nonstructural building components are grouped into drift-sensitive and acceleration-sensitive components.

For both essential facilities and general building stock, damage state probabilities are determined for each facility or structural class. Damage is expressed in terms of probabilities of occurrence of specific damage states, given a level of ground motion and ground failure. Five damage states are identified - none, slight, moderate, extensive and complete.

Module 4 Induced Damage

Induced damage is defined as the secondary consequence of an event. This fourth module assesses dams and levees for inundation potential, and hazardous materials sites for release potential. Fire following an earthquake and accumulation of debris are also assessed.

Module 5 Direct Social Losses

HAZUS provides estimates for social losses in terms of casualties, displaced households, and short-term shelter needs. The output of the casualty module includes estimates for four levels of casualty severity (minor to dead) by time (2:00 a.m., 2:00 p.m., and 5:00 p.m.) for four population groups (residential, commercial, industrial, and commuting). Casualties, caused by secondary effects such as heart attacks or injuries while rescuing trapped victims, are not included.

Homelessness is estimated based on the number of structures that are uninhabitable, which in turn is evaluated by combining damage to the residential building stock with utility service outage relationships.

Module 6 Direct Economic Losses

HAZUS provides estimates for economic include structural and nonstructural damage, costs of relocation, losses to business inventory, capital-related losses, income losses, and rental losses.

Module 7 Indirect Losses

This module evaluates the long-term effects on the regional economy from earthquake losses. The outputs in this module include income change and employment change by industrial sector.

1.6 LIMITATIONS

In this study, we have divided the State of South Carolina into 2 by 2 km grid cells to evaluate the subsurface geology and hence the ground shaking and liquefaction hazards. Based on this spatial resolution, we have calculated losses using HAZUS. It would be ideal if the geologic conditions pertinent to earthquake ground shaking and liquefaction were consistent within such a grid resolution, and that such conditions were confirmed with thorough subsurface data. In reality, subsurface conditions can vary significantly within the grid spacing used in this study, and while the near-surface conditions of South Carolina have been extensively characterized in some isolated areas, very little high-quality subsurface data is available for much of the state. Therefore, in consideration of the state-wide nature of this study and the level of detail involved in the characterization, some simplification based on engineering judgement was necessary. The simplifications applied in this study are intended to result in conservative estimates within the HAZUS model, and thus are considered appropriate for the purposes of this study. In light of this, it is emphasized that no conclusions should be drawn from this HAZUS study for a specific location without confirmation by a site-specific study including detailed geotechnical testing and subsurface characterization. It is recognized that the results of such a site-specific study may be significantly different from the conclusions inferred from results of this more general HAZUS study.

1.7 ACKNOWLEDGMENTS

Many Project Team members assisted in this study and we wish to acknowledge their contributions: Robyn Schapiro, Lenica Castner, and Doug Wright. Our thanks to Dr. Bill Clendenin, Dr. Pradeep Talwani, and Dr. Richard Lee for providing us data and information. Our sincere appreciation to John Knight and Tammie Dreher of SCEPD for their support and assistance in this study. The study was performed under SCEPD Contract 48651-001-028. Melinda Lee, Fumiko Goss, Carol Zuver, Deborah Fournier, and Rachel Griener assisted in the preparation of this report and we appreciate their assistance.

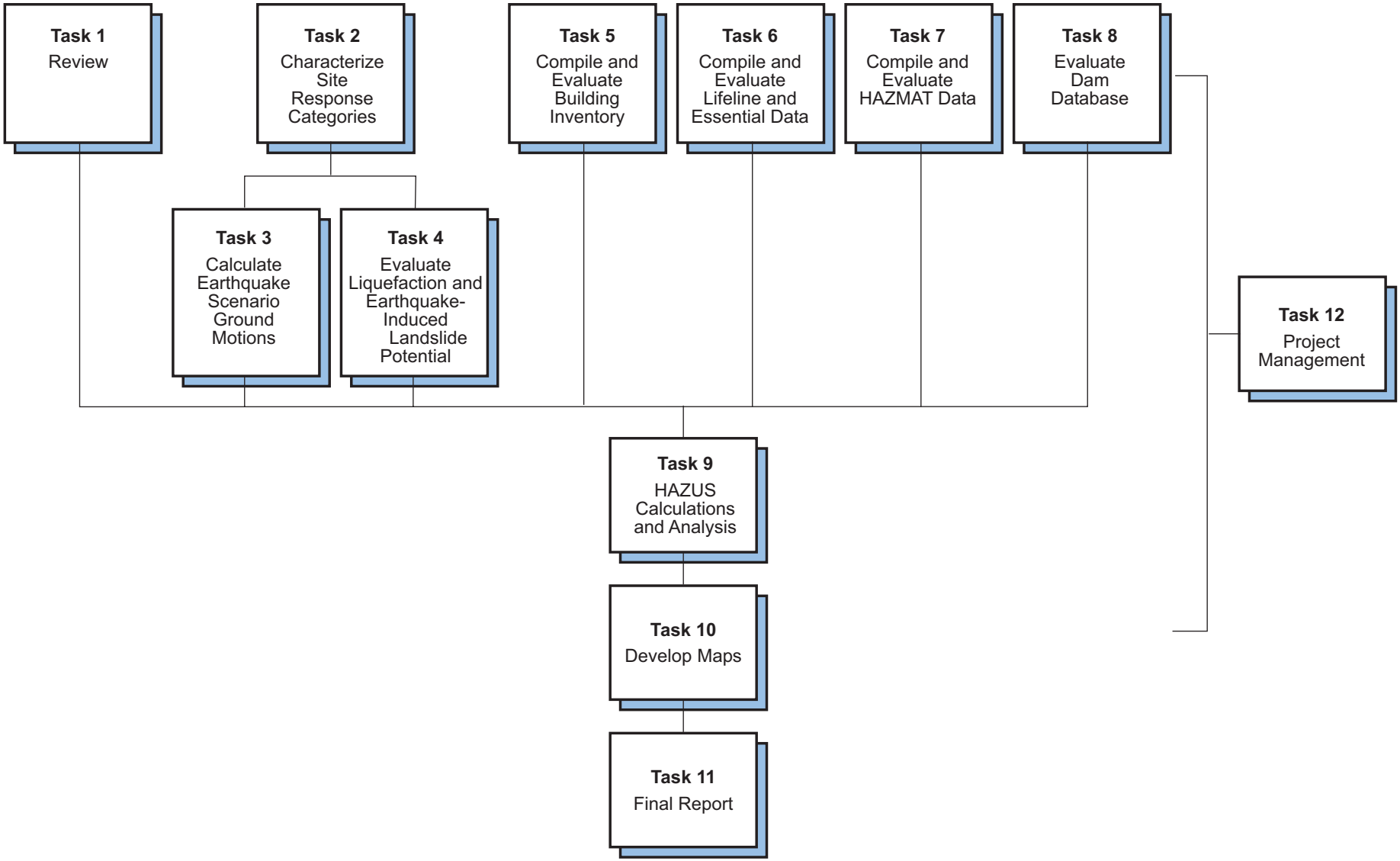

Figure 1-1. Project Approach

The HAZUS results that include maps and tabular data will provide State and local emergency management officials, as well as other practitioners, with a comprehensive, current analytical baseline estimate of the effects of four scenario earthquakes on the State of South Carolina. Additionally, improved HAZUS default data specific to South Carolina is incorporated in this study providing a customized version of HAZUS that will allow SCEPD to run any desired scenario. It is anticipated that the customized default database will also be extremely useful to SCEPD as additional HAZUS models become available such as the Wind and Flood Models.

The HAZUS analysis encompasses virtually every aspect of community vulnerability including population, buildings, critical facilities, lifelines, economic impacts, and earthquake-induced impacts (flooding, hazardous materials accidents, fires, and debris). This information will be very useful to State and local planners, hazards researchers, and others in planning for potential earthquake events.

This section of the report focuses on three key documents in South Carolina:

- The South Carolina Emergency Operations Plan (SCEOP)
- The South Carolina Hazard Mitigation Plan
- The South Carolina Hurricane Plan

The results of each plan review are discussed in detail below. The intent of each review was to identify sections within each plan that should be updated based on the results of this HAZUS study.

2.1 SOUTH CAROLINA EMERGENCY OPERATIONS PLAN

The SCEOP assists the SCEPD in the planning and execution of emergency management functions before, during and after a disaster ensuring a coordinated and efficient delivery of resources. The SCEOP defines roles and responsibilities regarding mitigation, preparedness, response, and recovery activities. The SCEOP is divided into three parts:

1. The Executive Order
2. The Basic Plan
3. The Annexes

Our review of the Basic Plan and Annexes indicates that the following sections need to be updated based on the results of this study.

2.1.1 Basic Plan

Section II, Part A. 1., *Vulnerability Analysis*, should be updated based on the 2000 census data that has been utilized in the HAZUS study. Additionally, Part 2.e., *Earthquakes,* should be updated based on the results of the four scenarios analyzed in this study. We recommend that secondary effects from an earthquake, such as fires, transportation, and hazardous material spills also be considered in updating the earthquake vulnerability.

Section IV, *Concept of Operations,* details what is expected of each organizational level of emergency management, namely local, state, and federal. Specifically, Part F.2., *Strategic Planning,* and F.3. detail how each level will plan and prepare for future events through the five-

year strategic plan, the South Carolina Hazard Mitigation Plan, and hazard-specific training exercises. We recommend that all three of these preparedness components be reviewed and updated accordingly based on the results of this study.

Section VI, *Evacuation,* details the levels of, and activities associated with evacuation. SCEPD has a detailed evacuation plan (South Carolina Hurricane Plan) in the event of a hurricane. We recommend that this be used as a model to develop a formal earthquake evacuation plan. This will be discussed further in the Hurricane Plan review section.

Section VII, *Public Information*, details how information concerning a disaster will be disseminated to the public before, during, and after a disaster. We recommend that this section be reviewed, as an earthquake will occur with little or no warning. The review should consider the results of this study and the effects on mechanisms to disseminate information.

Table 1, *Hazard Rating Summary*, should be reviewed, although the rating for an earthquake appears to be adequate.

2.1.2 Annexes

The Annexes of the plan provide guidelines and establish responsibility to develop appropriate measures to facilitate efficient and quick deployment of resources in any disaster. State agencies identified in the annexes as having functional responsibility are required to develop Standard Operating Procedures (SOPs) which detail operation procedures for each assigned annex. We recommend that Annexes 1 to 25 and the associated SOPs be reviewed to ensure consistency with the results of this study.

Specifically, Annex 25-C-1, *Earthquake Preparedness*, addresses response to earthquakes. We recommend that Sections I, II, and III of this Annex be updated based on the results of this study.

We also recommend that county level Emergency Response Plans and associated SOPs are consistent with and address the results of this study.

2.2 SOUTH CAROLINA MITIGATION PLAN

As part of the preparedness effort outlined in the SCEOP, SCEPD has developed the South Carolina Hazard Mitigation Plan (Mitigation Plan). The Mitigation Plan establishes a permanent method for cooperation between state agencies and organizations that are delegated responsibility for mitigation. The Mitigation Plan's intent is to develop a more disaster-resistant community both at a state and local level. The plan accomplishes this by defining the concepts, roles, and responsibilities of mitigation and prevention. Additionally, the plan identifies the state's hazards and vulnerabilities.

Our review of the Mitigation Plan indicates that the following sections need to be updated based on the results of this study.

Section 2, *Hazards Threatening South Carolina*, details the major hazards associated with the State. This section provides a baseline for developing mitigation priorities. Specifically, Part 2.2.1.7 details earthquake vulnerability. We recommend that this part of Section 2 should be updated based on the results of this study. Additionally, we recommend that item number 5, *Developing, Implementing, and Enforcing Codes*, of the potential mitigation measures should be placed higher on the list most likely before item number 2, *Professional Education*. This

recommendation is based on the success of similar programs during the recent Nisqually Earthquake. Proactive seismic programs considerably reduced damage from that earthquake. We agree that *Public Awareness and Education* should remain the number one priority.

Section III, *Hazard Analysis*, identifies significant hazards to South Carolina. Specifically, Annex D details earthquake hazards in the State. Based on our review, we recommend that Parts I, II, and III be updated based on the results of this study. Section III, *Vulnerability*, should be updated to reflect the results of the four scenarios analyzed in this study. We also recommend that SCEPD consider developing a separate Earthquake Plan similar to the existing Hurricane Plan.

2.3 SOUTH CAROLINA HURRICANE PLAN

The purpose of the South Carolina Hurricane Plan (Hurricane Plan) is to establish specific policies and procedures for responding to the threat of a hurricane approaching the State and immediately after impact.

The Hurricane Plan outlines the threat, operations and sheltering terminology, the utilization of the Hurricane Evacuation Study, evacuation decision timeline, and phased evacuation decision factors. The Hurricane Plan divides the state into four conglomerates to facilitate evacuation from the coast. Each conglomerate section serves as the general operational plan for that conglomerate.

Each conglomerate section provides guidance on Operating Condition Levels (OPCON), Traffic Management, and Shelter Management. The OPCON levels are intended to maximize advance warning and increase an Emergency Operations Center level of readiness based on pre-determined criteria. The Traffic Management portion establishes evacuation routes and necessary staff and equipment to monitor execute the evacuation. The Shelter Management portion establishes potential number of evacuees requiring shelter, planning shelter space, and coordinating shelter resources and openings.

We recommend that SCEPD consider the development of an earthquake plan similar to the existing Hurricane Plan. Although the Hurricane Plan is hurricane specific, the information could be utilized to develop a similar earthquake plan. The conglomerate concept could be modified or used as basis to develop areas that would need to be evacuated due to an earthquake. Items such as evacuation routes and shelters would need to be pre-identified and assessed for vulnerability to seismic activity. The results of this study present potential facilities such as structures or bridges that are likely to be adversely affected by the scenario earthquakes. These results should be used as a basis for facilities requiring further site specific analysis.

We also recommend that SCEPD consider the results of this study to review the structures critical to a hurricane response such as shelters and evacuation routes, for adverse affects should an earthquake occur just prior to or during hurricane season.

In summary, all three plans are well prepared and thorough. However, the results of this study provide more detailed data that should be incorporated as discussed above.

Observations of the effects of surficial geology on ground shaking during earthquakes have a long history. Del Barrio (1855), in the Proceedings of the University of Chile states[1] "...a movement.... must be modified while passing through media of different constitutions. Therefore, the earthquake effects will arrive to the surface with higher or lesser violence according to the state of aggregation of the terrain which conducted the movement. This seems to be, in fact, what we have observed in the Colchagua Province (of Chile) as well as in many other cases." In 1862, Mallet (1862) noted the effect of geology upon earthquake damage. Milne (1908) observed that in soft "damp" ground it was easy to produce vibrations of large amplitudes and long duration, while in rock it was difficult to produce vibrations of sufficient amplitude to be recorded.

Wood (1908) and Reid (1910), using apparent intensity of shaking and distribution of damage in the San Francisco Bay area during the 1906 earthquake, gave evidence that the severity of shaking can be substantially affected by the local geology and soil conditions. Gutenberg (1927, 1957) developed amplification factors representing different site geology by examining recordings of microseisms and earthquakes from instruments located on various types of ground.

3.1 EFFECTS OF NEAR-SURFACE SOIL CONDITIONS ON STRONG GROUND MOTIONS

Figure 3-1 shows average spectral shapes (response spectral acceleration divided by peak acceleration) computed from recordings made on rock and soil sites at close distances to earthquakes in the magnitude range of about **M** 6 to 7. The differences in spectral shapes are significant and depend strongly upon the general site classifications. These variations in spectral content represent average site-dependent ground motion characteristics and result from vertical variations in soil material properties (Hayashi *et al.*, 1971; Mohraz, 1976; Seed *et al.*, 1976). Due primarily to the limited number of records from earthquakes of different magnitudes, spectral content in terms of response spectral shapes was for some time, interpreted not to depend upon magnitude nor distance, but primarily on the stiffness and depth of the local soil profile. However, with an increase in the strong motion database, it has become apparent that spectral shapes depend strongly upon magnitude as well as site conditions (Joyner and Boore, 1982, Idriss, 1985; Silva and Green, 1989), and distance (Silva and Green, 1989), and that site effects extend to rock sites as well (Boatwright and Astrue, 1983; Campbell 1981, 1985, 1988; Cranswick *et al.*, 1985; Silva and Darragh, 1995; Silva *et al.*, 2000).

Examples of differences in spectral content largely attributable to one-dimensional site effects at rock sites can be seen in comparisons of response spectral shapes computed from motions recorded in both active (e.g., western North America, primarily California) and stable tectonic regions, eastern North America, (Silva and Darragh, 1995). Figure 3-2 shows average spectral shapes (Sa/amax) computed from recordings made on rock at close distances to large and small earthquakes. For both magnitudes (**M** 6.4 and 4.0), the motions recorded in eastern North America (ENA), a stable tectonic region, show a dramatic shift in the maximum spectral amplification toward higher frequencies compared to the western North American (WNA) motions. These differences in spectral content are significant and are interpreted as primarily

[1] Translated from the old Spanish by Professor Ricardo Dobry.

resulting from differences in the shear-wave velocity and damping in the rocks directly beneath the site, soft rock in WNA and hard rock in ENA (Boore and Atkinson, 1987; Toro and McGuire, 1987; Silva and Green, 1989; Silva and Darragh, 1995). Also evident in Figure 3-2 is the strong magnitude dependency of the response spectral shapes. The smaller earthquakes show a much narrower bandwidth. This is a consequence of higher corner frequencies for smaller magnitude earthquakes (Boore, 1983; Silva and Green, 1989; Silva and Darragh, 1995).

The difference in spectral content due to soil site effects, as shown in Figure 3-1, and due to rock site effects, as shown in Figure 3-2, are dramatic and illustrate the degree to which one-dimensional site conditions (vertical variations in dynamic material properties) control strong ground motions.

In order to capture these geologically controlled differences in ground motions, site amplification factors (Section 4.4) were developed for regions in South Carolina where surficial geological conditions give rise to distinctly different ground motions due to differences in shear-wave velocity, depth to basement material, as well as nonlinear dynamic material properties. The amplification factors were developed for 5% damped response spectra (values at 100 Hz apply to peak acceleration) and are relative to a generic hard crystalline rock site condition. The factors accommodate nonlinear soil/ soft rock response and are produced as a function of expected hard rock peak acceleration values. They may be applied to any size earthquake at any distance with knowledge only of the expected rock peak acceleration as soil response does not depend strongly on magnitude, for fixed expected rock outcrop peak acceleration (EPRI, 1993). The factors are considered appropriate for rock outcrop peak accelerations over 1.00 g and over the frequency range of 0.1 to 100.0 Hz. At long periods, due to possible basin effects, care should be exercised in applying the factors to deep soil sites at frequencies less than about 0.5 Hz for distant (> 50 km) earthquakes.

3.2 DATA COMPILATION AND EVALUATION

The characterization of site response categories (Task 2) involves development of distinct subsurface soil properties that affect both strong ground motion and liquefaction susceptibility. The categories are intended to reflect the range in soil conditions throughout the State and are used to develop ground motion amplification factors (Task 3) as well as provide assessments of liquefaction potential (Task 4).

Although a number of soil attributes, such as plasticity, grain size, geologic age, and depositional/formation environment affect how surficial soils respond to earthquake shaking, the primary controlling factors are soil stiffness (shear-wave velocity), depth to hard rock conditions, and nonlinear dynamic material properties. Additional factors which affect a soil's susceptibility to fail or liquefy are geologic age and degree of saturation (depth of water table). The site response categories were developed to capture these properties and their variability across the state, as an expression of "between" category variability. The "within" category variability is accommodated by randomizing the material properties of each category and computing estimates of median response for ground motions (Section 4) as well as liquefaction probability (Section 5).

Subsurface characterization for the development of site response categories and liquefaction assessment involved collecting and interpreting data from the following sources:

a) S&ME project files from offices located in Charleston, Columbia, and Spartanburg;

b) PE&A profile database which contains profiles from South Carolina as well as other regions with similar characteristics as South Carolina soils;

c) South Carolina Department of Natural Resources; and

d) Publications from the USGS and other sources.

3.3 DEVELOPMENT OF SITE RESPONSE CATEGORIES

Recent development of site amplification factors (Bonila *et al.*, 1997; Hartzell *et al.*, 1998; Borcherdt and Glassmoyer, 1992) found stable and distinct differences in amplification from recorded ground motions based on surficial geology. Additionally, good agreement has been found between amplification factors based on recorded ground motions and those computed using surficial geology-based shear-wave velocity profiles and the same computational approach implemented in this project (Silva *et al.*, 1999). As a result, development of the site response categories began with an assessment of South Carolina surficial geology (Figure 3-3).

In general, the surficial geology for South Carolina may be broadly characterized into two regions: the Coastal Plain and the Piedmont/Blue Ridge physiographic provinces (Hunt, 1967, Horton, 1991), which are divided by the Fall Line (Figure 3-3). The Coastal Plain lies southeast (below) of the Fall Line and may be generally typified as soft Quaternary soils ranging to relatively stiff Tertiary soils, with depth to hard rock increasing from near zero at the Fall Line to nearly 3,000 ft (914 m) at the coast (Figure 3-4). Above the Fall Line (northwest) lie the Blue Ridge and Piedmont physiographic provinces, which consist largely of residual soils over hard rock, apart from river deposits. Soil covering tends to be quite shallow above the Fall Line, a region of moderate topography with hills and narrow valleys and patches of outcropping rock (Figure 3-4).

Site response categories for this study were developed based on the distinction between the Coastal Plain and the Piedmont/Blue Ridge physiographic provinces. The Coastal Plain soils were further categorized into three zones based on the surficial geology and trends in subsurface data: the Charleston, Myrtle Beach, and Savannah River site response categories (Figure 3-5). An additional categorization is introduced for the somewhat slower shear-wave velocities observed in Triassic age basins underlying the Coastal Plain soils: South Georgia Basin, Florence Basin and the Dunbarton Basin. These soil and bedrock combinations result in seven site response categories, each of which is further refined by the thickness of soils in each site response category.

For evaluation of site response, each of the seven soil response categories is evaluated for several discrete ranges of soil column thickness. The soil column thickness ranges are 10-50, 50-100, 100-200, 200-500, 500-1000, 1000-2000 and 2000-4000 ft. The site response categories and soil column thickness ranges are shown in Table 4-7.

3.3.1 Triassic Basins and Depth to Hard Rock

For this study, hard rock is defined as pre-Cretaceous basement bedrock. Within Mesozoic (Triassic) basins in South Carolina, the pre-Cretaceous basement is composed of hard sedimentary and igneous rocks (Olsen *et al.*, 1991) which overlies the crystalline basement

complex. Beyond the limits of the Mesozoic basins, Triassic basement units are absent and the pre-Cretaceous basement is composed of Paleozoic crystalline rock. The three known Mesozoic basins, which are buried below the Coastal Plain sedimentary wedge, are: (1) the South Georgia Basin (also referred to as the Summerville Basin in South Carolina), (2) the Dunbarton Basin and (3) the Florence Basin. For this study, the boundaries of the basins, as well as the depth to the pre-Cretaceous basement, were developed from published information (Ackerman, 1983; Gohn *et al.*, 1983; Colquhoun *et al.*, 1983; Newcome, 1989; Olsen *et al.*, 1991; Snipes *et al.*, 1993; Leutgert *et al.*, 1994; Domoracki *et al.*, 1999; and Wheeler and Cramer, 2000).

Figure 3-5 shows the outlines of the Mesozoic basins along with contours of depths to hard rock within the Coastal Plain. As shown, the depth is very shallow at the Fall Line (northwestern limit of the Coastal Plain) and quickly increases toward the coast. In the vicinity of Charleston, the depth to hard sedimentary rock within the South Georgia Basin is approximately 2750 ft (838 m). The increase in depth from the Fall Line to the coast results from a thickening of the coast plain sedimentary wedge.

Northwest of the Fall Line, Figure 3-4 does not show any contours for depth to hard rock. In this region, Paleozoic rock or residual soil derived from the weathering of Paleozoic rock is either outcropping or covered by a very thin layer of recent sediments. For this region, which includes both the Piedmont and Blue Ridge physiographic provinces, depth to crystalline rock is assumed not to exceed 50 ft (15 m), with a variability of 10 to 50 ft (3.0 to 15 m) (see Section 4.4).

3.3.2 Piedmont/Blue Ridge Site Response Category

The Piedmont physiographic comprises nearly the entire area above the Fall Line in South Carolina. The Appalachian Mountains begin in the northeastern portion of the State and reflect the Blue Ridge physiographic province. The Blue Ridge area is typified by a thin veneer of residuum overlying partially weathered crystalline rock. The residuum derived by the in-place weathering of the parent crystalline rock is typically a micaceous silty sand or sandy silt. The upper rock is typically weathered, but maintains its rock-like fabric (i.e., it is saprolitic). As the depth increases, the rock becomes less weathered and transitions into crystalline basement. The Piedmont area is similar to the Blue Ridge except that it has a thicker residuum overburden, although hard rock can extend to the near surface (Fletcher, 1982). Blue Ridge characteristics also occur within the Piedmont province but are characterized as isolated pockets or patches, the Chauga Belt and gabbro shown in Figure 3-3. Because they both reflect shallow soil over hard rock and few measured profiles were available to distinguish the two, the Blue Ridge and Piedmont provinces were combined into a single category (Figure 3-5) with the profile shown in Figure 3-6. For each site response category smooth model profiles are developed as base case profiles. The base case profiles represent a smooth average profile from which individual profiles are generated for site response analyses (Section 4). The smooth model is only loosely based on the median profile since only three soil profiles were available. The shallow portion of the model (top 25 to 30 ft [7.6 to 9.1 m]) is taken to be consistent with the Opelika (Alabama) National Geotechnical Engineering Site, which shows a lower velocity than our other two Piedmont residual soil profiles. The Opelika site is well studied and considered typical of residual Piedmont soils (Schneider *et al.*, 1999; Hoyos and Macari, 1999; Borden *et al.*, 1996; Macari and Hozos, 1996). Unfortunately, the only profile that extends into hard basement material is the Catawba nuclear power station, located in north-central South Carolina. The site consists of stiff (about 1,200 ft/sec [366 m/sec]) sandy silts which overlie weathered rock,

saprolite, and grades into hard Paleozoic basement rock. The saprolitic zone extends in depth from about 30 to about 50 ft (9.1 to 15.2 m), the moderate gradient shown in Figure 3-6. Below about 50 ft (15.2 m), the steep gradient in Figure 3-6 is moderately weathered bedrock with the profile ending in hard rock, with a shear-wave velocity of about 8,000 ft/sec (2438 m/sec). The model profile uses this steep gradient but extends the partially weathered zone, with a constant shear-wave velocity near 3,500 ft/sec (1067 m/sec) to about 100 ft (50.5 m). This was done to be able to consider two depth categories for the Piedmont/Blue Ridge: 100 ft (30.5 m) to hard rock (top of steep gradient) as well as 50 ft (15.2 m) to hard rock. Additionally, the deepest layer in the base case profile shear-wave velocity was increased to about 11,000 ft/sec (3.40 km/sec) to be consistent with the top layer of the crustal model (Section 4). As with all the category profiles, they are placed on top of the crustal model to compute the amplification factors relative to hard crystalline rock (top of crustal model).

3.3.3 Savannah River Site Response Category

The Savannah River category is based entirely on in-situ velocity measurements at the U.S. Department of Energy Savannah River Site (WSRC, 1997). The site straddles the Dunbarton Basin along the Savannah River and is located within the Tertiary (Paleocene, Eocene, and Miocene) geologic units (Figure 3-3). The model profile (Figure 3-7) is based on over 100 shear-wave velocity measurements with several extending into pre-Cretaceous basement (both crystalline and Triassic) at depths near 1,000 ft (305 m). The profile is stiff near the surface with shear-wave velocities exceeding 1,000 ft/sec (305 m), a deep soft zone exists from about 50 to 150 ft (15.2 to 45.7 m) below which the velocities increase with depth, reaching about 3,000 ft/sec (914 m/sec). The Savannah River profile is assumed to be appropriate for the entire Paleocene, Eocene, and Miocene areas (Figures 3-3 and 3-5), so it was extended in depth to 4,000 ft (1219 m/sec) (using the deepest shear-wave velocity). It is then placed on top of both the crystalline and Triassic crustal models (Section 4).

3.3.4 Charleston Site Response Category

The Charleston profile has about 70 ft (21.3 m) of soft soil overburden above a stiffer, lightly-cemented material (e.g., the Cooper Group). As indicated by the shear wave velocity profile (Figure 3-8), the soil overburden is relatively soft or loose. The shear-wave profile is well constrained over the top 70 to 100 ft (21.3 to 30.5 m) with measured data from about 20 sites. The lower portion of the profile, to a depth of about 350 ft (107 m), is constrained by test data from two borings. Below 350 ft (107 m), the profile was extended to about 600 ft (183 m) where it was merged with the Savannah River profile. The extension to 4,000 ft (1219 m), based on the deepest (1,000 ft [305 m]) measured velocities at the Savannah River site, is consistent with measured compressional-wave velocities as well as stratigraphy at the Clubhouse Cross Roads deep test hole (Gohn, 1983) in addition to deep measurements in similar materials from other regions (Pacific Engineering & Analysis profile database). The profile steps up at 500 ft (152 m) to a shear-wave velocity of about 2,500 ft/sec (762 m/sec) to a depth of about 600 ft (183 m) where it again increases to near 2,700 ft/sec (823 m/sec). Near a depth of 700 ft (213 m), the velocity again increases to about 3,000 ft/sec (914 m/sec) and remains constant to a depth of 4,000 ft (1219 m).

To provide conservative estimates of low-frequency (< 1 Hz) amplification in view of the lack of region-specific data, these deeper (> 500 ft [152 m]) shear-wave velocities are considered to likely reflect slightly lower than expected median values. The proper mechanism to address this issue in epistemic uncertainty (Appendix C) is to develop separate amplification factors for a range in best-estimate median profiles (2 to 3 median profiles) and then envelop the results. Experience in developing amplification factors in a number of projects has shown that the lower velocity profile generally governs the amplification, provided material nonlinearities are not dominating the response. Since the profiles are assumed to behave linearly at depths exceeding 500 ft (152 m) (Section 4.4), potential unconservatism in amplification at high frequency due to excessive nonlinearity (high material damping) from the potentially low velocities is minimized.

The aerial extent of the Charleston category is based on boring log data as well as surficial soil conditions and is depicted in Figure 3-5. The category comprises much of the Pleistocene soils (Figure 3-3) within about 50 km of the coast from the Georgia border northeast to near Myrtle Beach.

3.3.5 Myrtle Beach Site Response Category

The Myrtle Beach site response category covers the Coastal Plain area from the Charleston category boundary to the Fall Line, with the exception of the Savannah River Category area (Figure 3-5). In general, based on borehole log data and surficial soil conditions, as few measured velocity profiles exist, the Myrtle Beach category area is expected to be typified by shallow soils that are somewhat stiffer than those in the Charleston zone while deeper velocities are expected to be similar. The boundary between the Myrtle Beach category and the Charleston category was determined based on borehole log data and interpolation of soil conditions between borehole locations. The shear-wave velocity profile adopted for the Myrtle Beach category is the same as Charleston with the top 30 ft (9.1 m) removed. The profile is shown in Figure 3-9 and is consistent with the available data consisting of only two profiles.

3.3.6 Water Level Depth

Water level depth is an essential parameter for liquefaction analysis, as only saturated soils (i.e., soils below the water table) are considered as potentially liquefiable. Available published information (U.S. Dept. of Agriculture, 1994) divides South Carolina into four regions with water levels of 0 to 2 ft (0. to 0.61 m), 2 to 4 ft (0.61 to 1.22 m), 4 to 6 ft (1.22 to 1.83 m), and 6+ ft (1.83+ m). On the basis of this information, an average water level depth of 2 ft (0.61 m) was conservatively used in the liquefaction analysis for most of the Coastal Plain. The exception is the Savannah River site response category, which used a water level depth of 20 ft (6.1 m). The water level in the Savannah River site category ranges from 0 to over 100 ft based on the information in Hiergesell (1998).

3.3.7 Liquefiable Zone

Based on available borehole information (soil type, plasticity, grain size, and blow counts), potentially liquefiable soils generally exist between the water table depth and about 40 ft (12.2 m) for the Myrtle Beach and Charleston site response zones. For the Savannah River category, due to the generally deeper water table and the presence of the soft zone, liquefiable

soils are considered present to a depth of 70 ft (21.3 m) (Dr. Richard Lee, Westinghouse Savannah River Site, personal communication, 2001).

Note that, although soil is present in the Blue Ridge and Piedmont categories, soils in these two regions are considered to have a very low risk of liquefaction considering published relationships between soil age, depositional environment, and historical evidence of liquefaction (Youd and Perkins, 1978). For this study, we have neglected base Holocene riverbank deposits above the Fall Line. These deposits are highly localized along the rivers and require a more site specific approach to assess liquefaction potential of engineering significance. Table 3-1 summarizes the potentially liquefiable zones for each site response category.

Table 3-1
Depth Ranges For Liquefaction Assessment

Site Response Category	Liquefaction Zone (ft)
Piedmont/ Blue Ridge	NL*
Myrtle Beach	2 - 40 (0.6 to 12.2 m)
Charleston	2 - 40 (0.6 to 12.2 m)
Savannah River Site	20 - 70 (6.1 to 21.3 m)

* Non Liquefiable

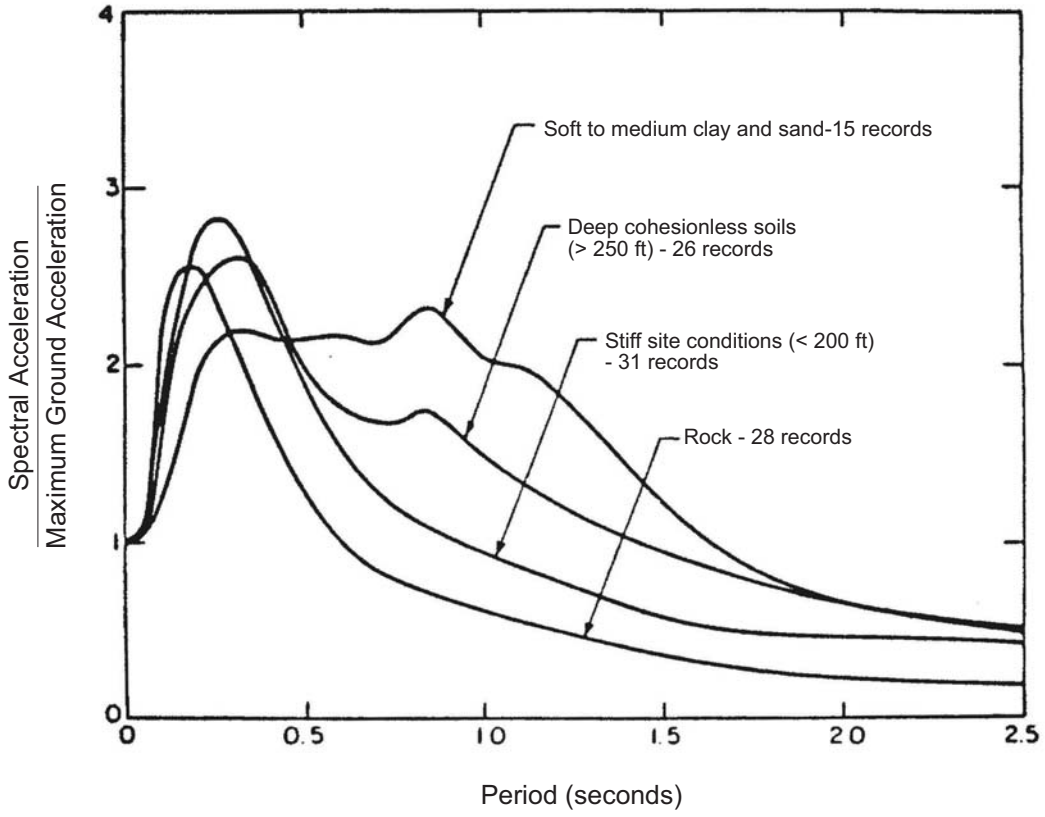

Source: Seed et al., 1976

Figure 3-1. Effects of near surface soil conditions on 5% damped response spectral shapes.

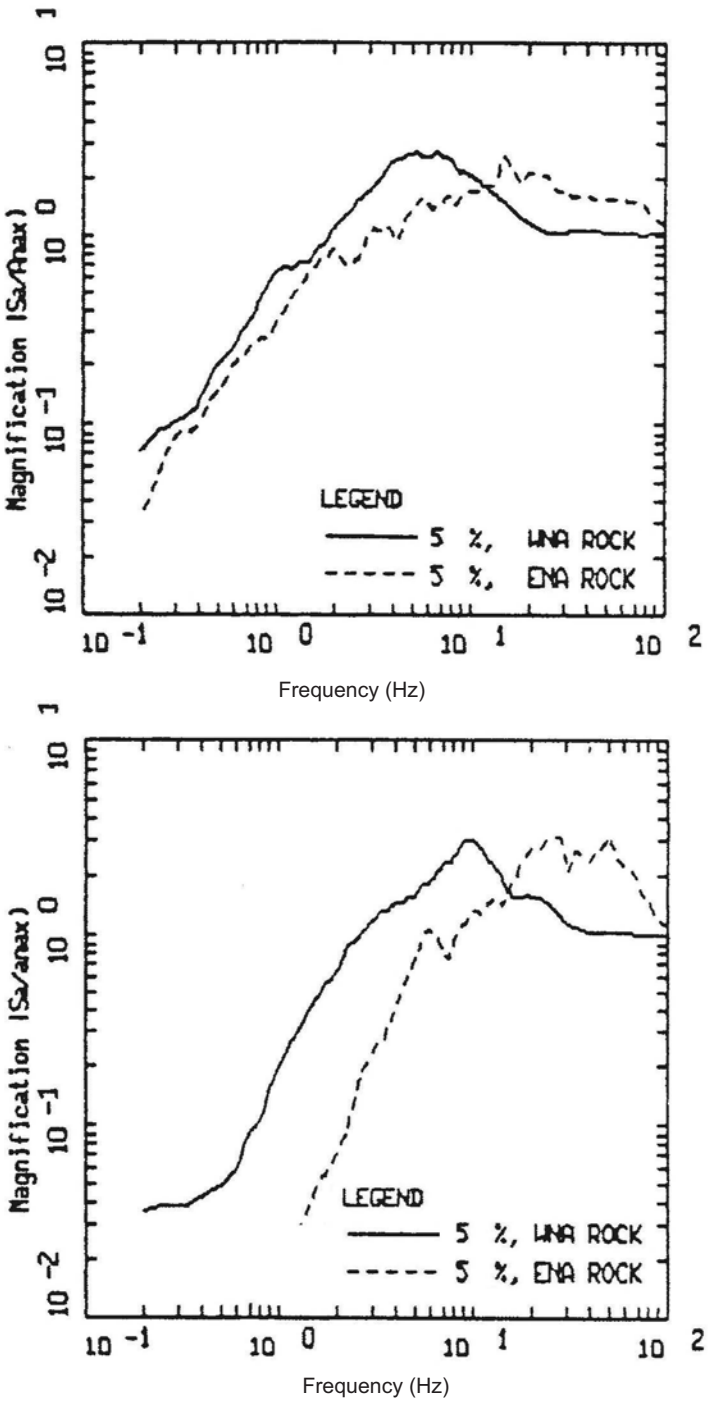

Source: Silva and Darragh, 1995

Figure 3-2. Effects of hard and soft rock site conditions and magnitude on 5% damped response spectral shapes for earthquakes with M ~6.5 (upper) and M ~4.5 (lower).

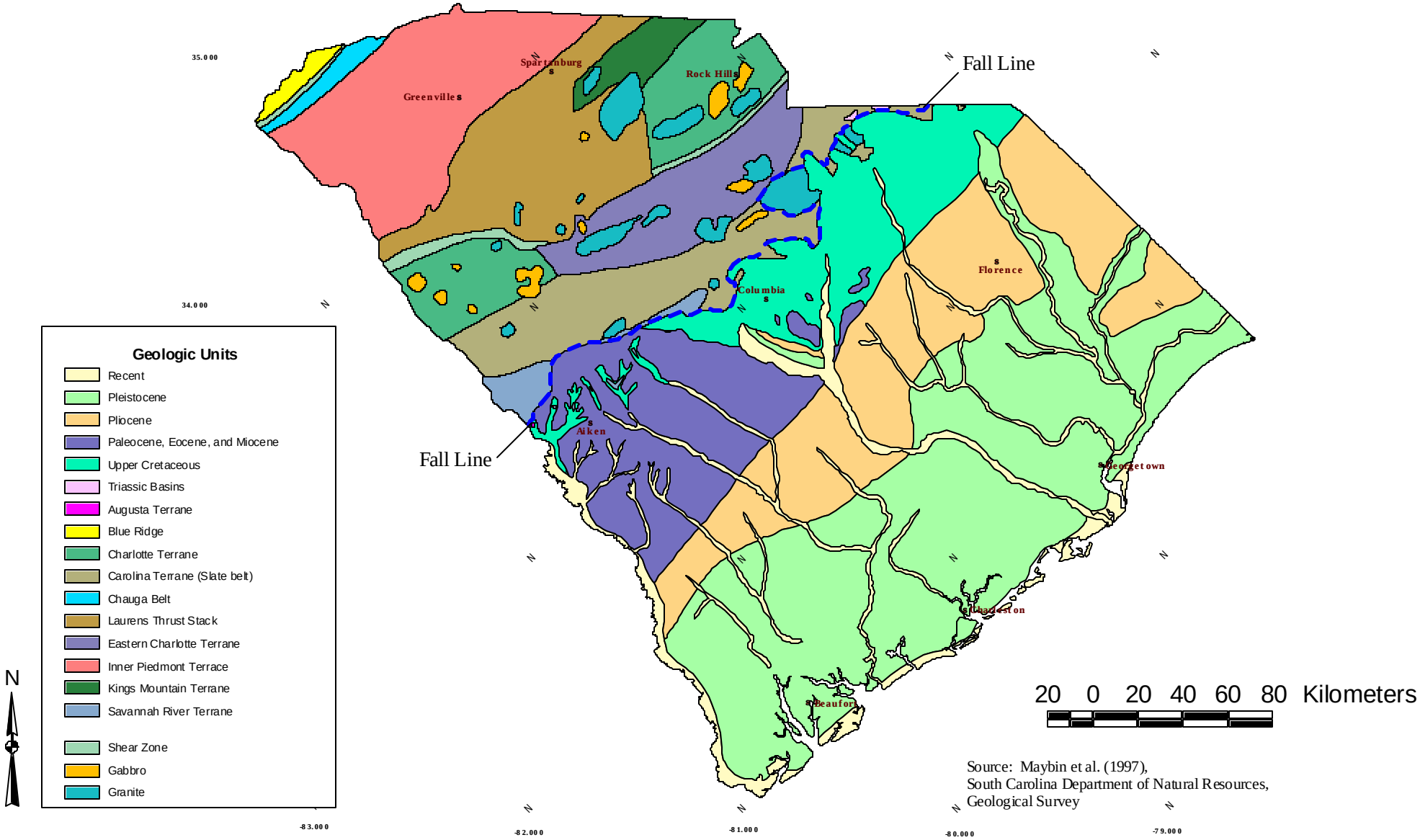

Figure 3-3. Generalized geologic map of South Carolina.

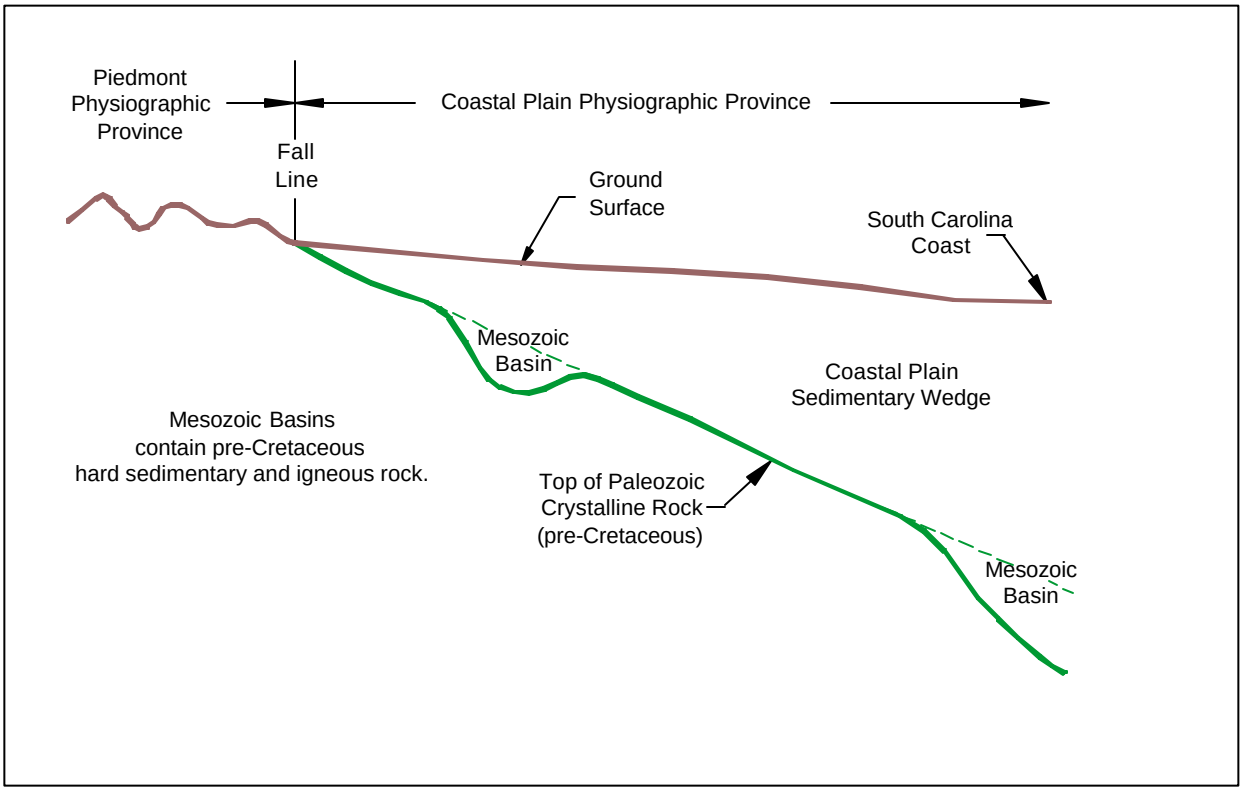

Figure 3-4. Conceptual profile of South Carolina Coastal Plain sedimentary wedge.

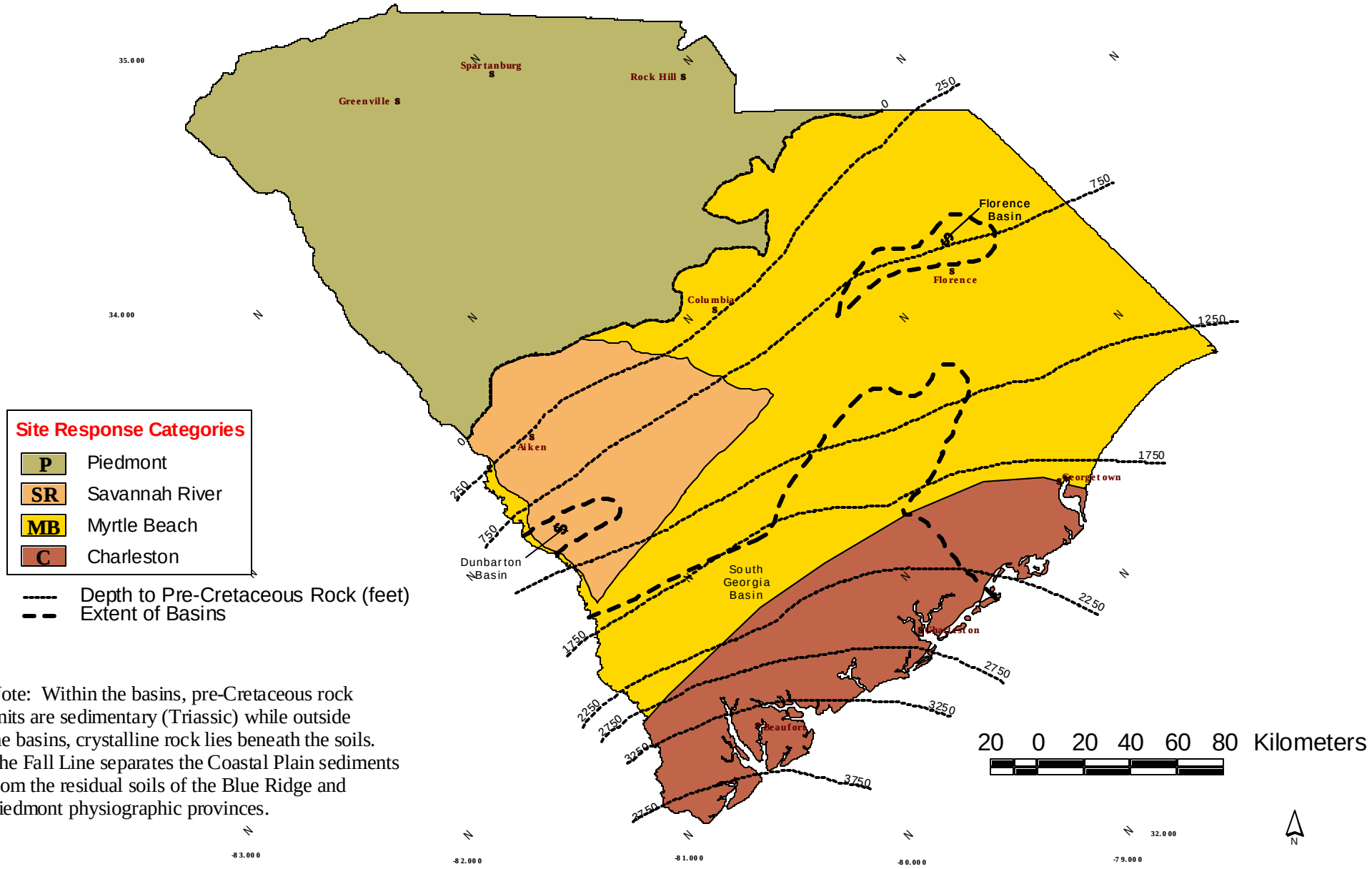

Note: Within the basins, pre-Cretaceous rock units are sedimentary (Triassic) while outside the basins, crystalline rock lies beneath the soils. The Fall Line separates the Coastal Plain sediments from the residual soils of the Blue Ridge and Piedmont physiographic provinces.

Figure 3-5. Site Response categories and depth to pre-Cretaceous rock.

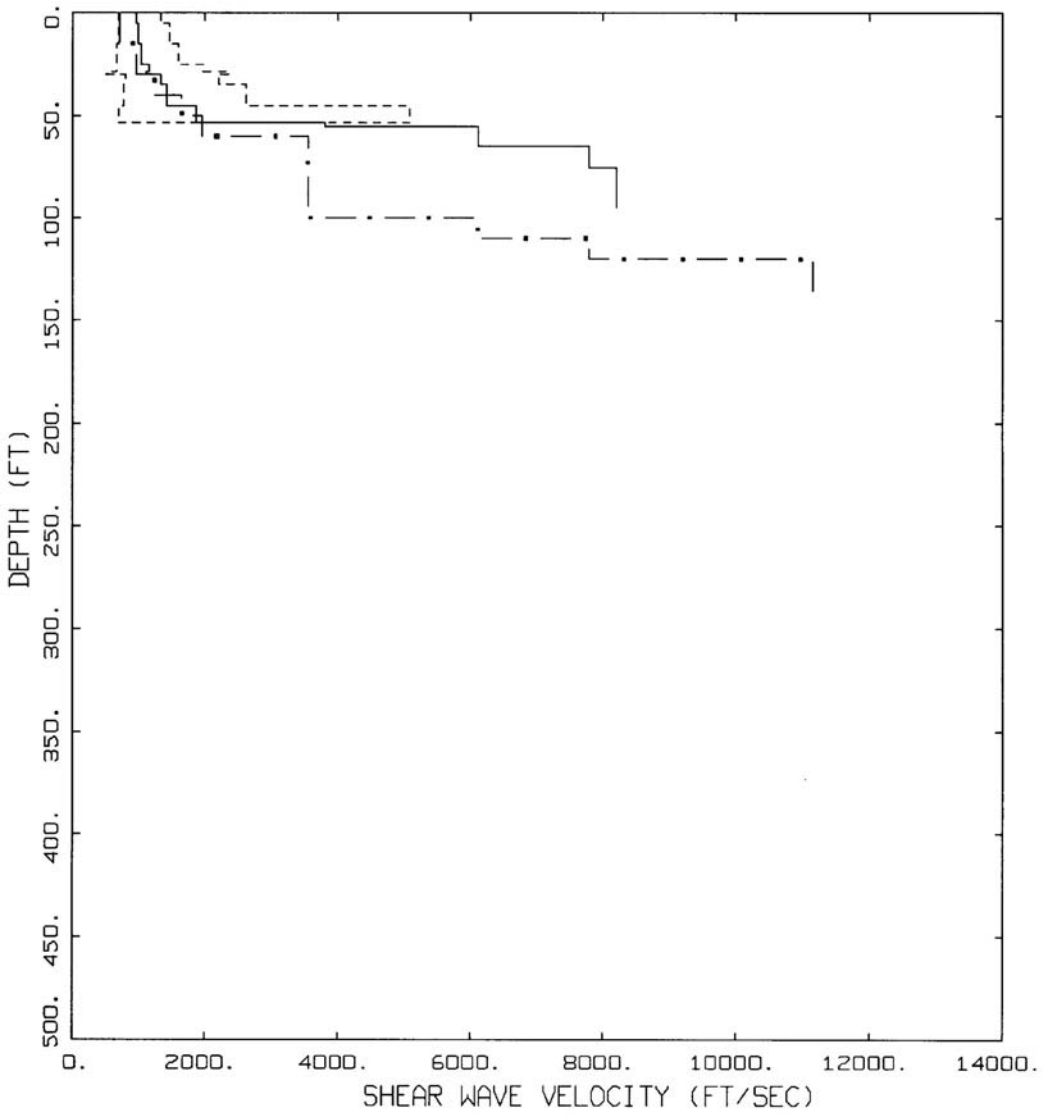

Figure 3-6. Base case shear-wave velocity profile for the Piedmont/Blue Ridge site response category along with median and $\pm 1\sigma$ available shear-wave velocity profiles.

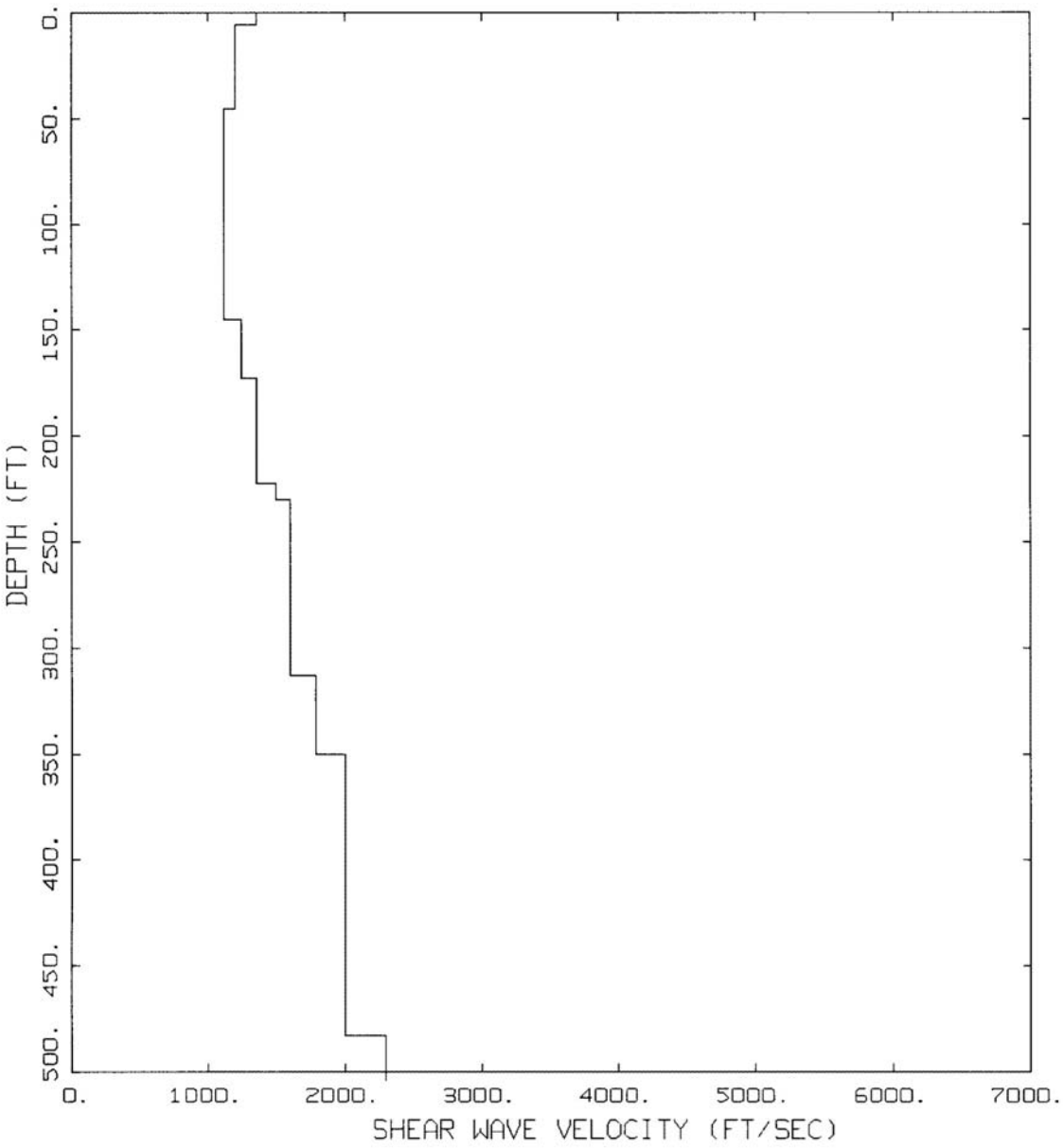

Figure 3-7. Base case shear-wave velocity profile for the Savannah River site response category.

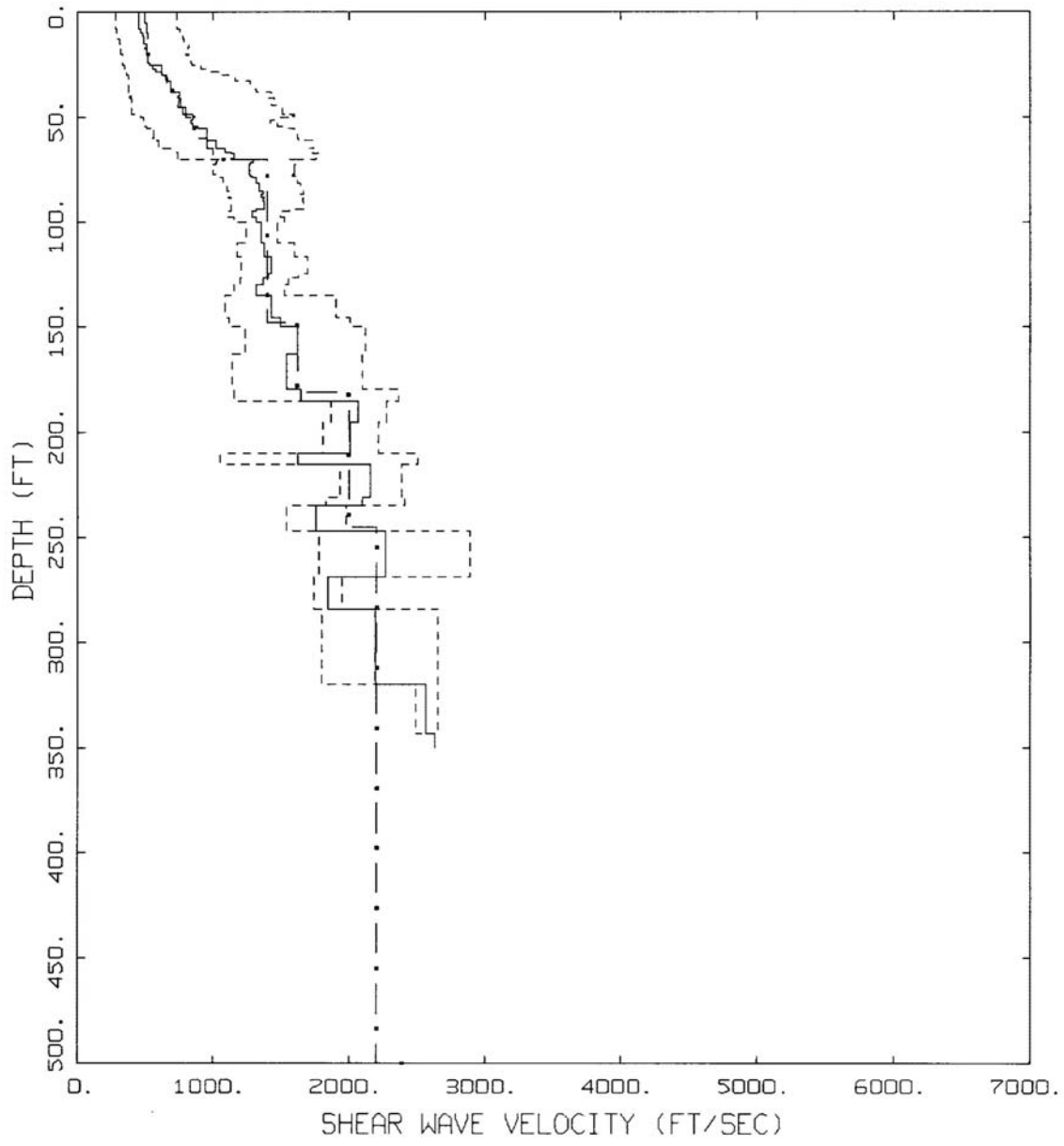

Figure 3-8. Base case shear-wave velocity profile for the Charleston site response category along with median and ±1σ available shear-wave velocity profiles.

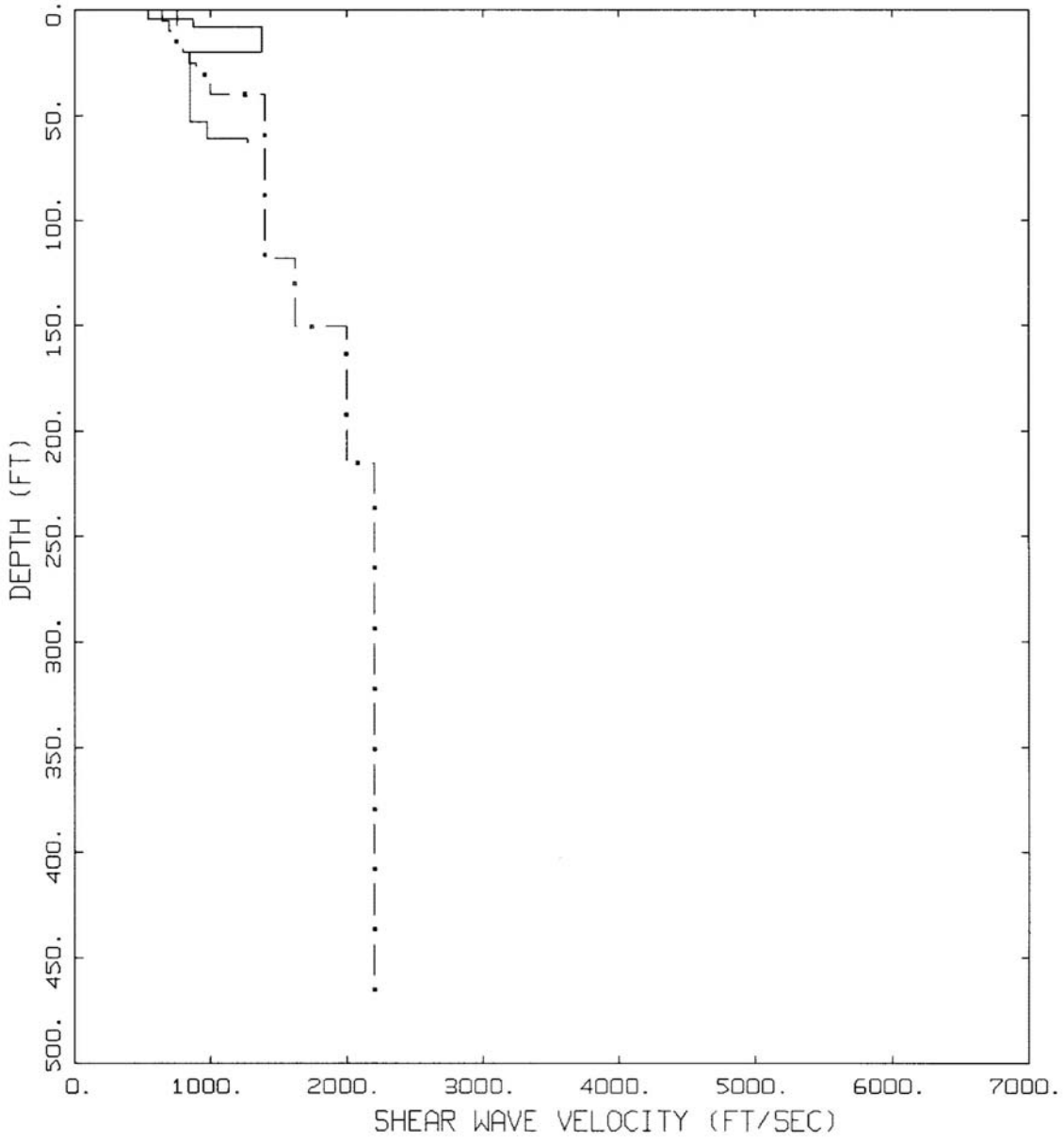

Figure 3-9. Base case shear-wave velocity profile for the Myrtle Beach site response category along with available profiles.

HAZUS requires as basic input, estimates of the seismic hazards to be considered. In Task 3, the ground shaking from the four scenario earthquakes was calculated. A fundamental limitation encountered in this task is the lack of strong motion recordings not only for South Carolina but the entire central and eastern U.S. The use of empirical attenuation relationships based on the recordings of strong motion is the traditional and most appropriate approach in estimating ground motions from future earthquakes. In this study, we have utilized a widely-accepted state-of-the-art numerical ground motion modeling technique as described below and in Appendix C. The four scenario earthquake modeled in this study are: a **M** 7.3 repeat of the 1886 event and two smaller Charleston events of **M** 6.3 and **M** 5.3; and a **M** 5.0 earthquake near Columbia possibly resulting from rupture of a segment of the Eastern Piedmont fault system.

4.1 SEISMICITY AND SEISMIC SOURCES IN SOUTH CAROLINA

An examination of the historical earthquake record for South Carolina, which dates back almost 300 years, clearly shows that the 1886 Charleston earthquake dominates the seismicity of the State. However, geologic evidence, though very sparse, and the historical earthquake record indicate that there are other seismic sources in South Carolina which have the potential to generate earthquakes of **M** 5.0 and possibly larger than **M** 6.0 (Figure 4-1).

The largest earthquake in the State outside of Charleston was an event on 1 January 1913 near Union County (Figure 4-1). The earthquake was felt throughout the western part of the State as well as in North Carolina, Georgia, and southern Virginia (Figure 4-2). The size of this event has been estimated to be body-wave magnitude (m_b) 4.8 based on an estimate of its felt area (Stover and Coffman, 1993). The earthquake knocked down chimneys in Union County and damaged plaster and stonewalls. Items were knocked off shelves. Many people were terrified and ran into the streets. The lone casualty was a pig killed by a falling chimney. A loud roaring sound was reported to accompany the earthquake. The maximum intensity assigned to the 1913 earthquake was Modified Mercalli (MM) intensity VII (Rossi-Forel intensity VIII on Figure 4-2) (Stover and Coffman, 1993). See Table 4-1 for an explanation of the MM intensity scale and equivalent Rossi-Forel intensities.

4.1.1 1886 Charleston Earthquake

Outside of the 1811-1812 New Madrid sequence in the central U.S., which consisted of three principal earthquakes greater than **M** 7 (**M** 7.2-7.3, 7.0 and 7.4-7.5; Hough *et al.*, 2000), the 1886 Charleston earthquake is the largest known event to have occurred in the eastern U.S. The 1886 event was felt throughout the eastern U.S. and in such distant locations as Boston, Massachusetts; Chicago, Illinois; Milwaukee, Wisconsin; Cuba, and Bermuda (Dutton, 1889; Bollinger, 1977; Stover and Coffman, 1993) (Figures 4-3 and 4-4). Minor to moderate structural damage was sustained several hundred kilometers from Charleston and long-period effects were observed at distances of more than 100 km. Few buildings escaped damage in Charleston (Figures 4-5 and 4-6). Liquefaction was widespread throughout the epicentral area (Figure 4-7). Sand craterlets as large as 6.4 m in diameter were observed. In addition, lateral spreading was observed along the Ashley River. In Summerville, then a town of 2,000 people, houses were displaced and subsided. Chimney damage was extensive.

Because the earthquake occurred prior to the advent of seismographic instrumentation, a precise measure of its magnitude has been lacking. A large range of values has emerged over time

which also vary with the magnitude scale used. The currently accepted magnitude of the 1886 earthquake is **M** 7.3 ± 0.26 (Johnston, 1996).

Table 4-1
Abridged Modified Mercalli Intensity Scale

I	Not felt except by a few under especially favorable circumstances (RF* I)
II	Felt only by a few persons at rest, especially on upper floors of buildings. Delicately suspended objects may swing. (RF I to II)
III	Felt quite noticeably indoors, especially on upper floor of buildings, but many people do not recognize it as an earthquake. Standing motorcars may rock slightly. Vibration like passing of truck. Duration estimated. (RF III)
IV	Felt indoors by many, outdoors by few during the day. Some awakened at night. Dishes, windows, door disturbed; walls make creaking sound. Sensation like heavy truck striking building. Standing motorcars rocked noticeably. (RF IV to V).
V	Felt by nearly everyone, many awakened. Some dishes, windows, and other fragile objects broken; cracked plaster in a few places; unstable objects overturned. Disturbances of trees, poles, and other tall objects sometimes noticed. Pendulum clocks may stop. (RF V to VI)
VI	Felt by all, many frightened and run outdoors. Some heavy furniture moved; a few instances of fallen plaster and damaged chimneys. Damage slight. (RF VI to VII)
VII	Everybody runs outdoors. Damage negligible in buildings of good design and construction; slight to moderate in well built ordinary structures; considerable in poorly built or badly designed structures; some chimneys broken. Noticed by persons driving cars. (RF VIII)
VIII	Damage slight in specially designed structures; considerable in ordinary substantial buildings with partial collapse; great in poorly built structures. Panel wall thrown out of frame structures. Fall of chimneys, factory stacks, columns, monuments, walls. Heavy furniture overturned. Sand and mud ejected in small amounts. Changes in well water levels. Persons driving cars disturbed. (RF VIII + to IX)
IX	Damage considerable in specially designed structures; well designed frame structures thrown out of plumb; great in substantial buildings; with partial collapse. Buildings shifted off foundations. Ground cracked conspicuously. Underground pipes broken. (RF IX +)
X	Some well built structures destroyed; most masonry and frame structures destroyed with foundations; ground badly cracked. Rails bent. Landslides considerable from river banks and steep slopes. Shifted sand and mud. Water splashed, slopped over banks. (RF X)
XI	Few, if any, [masonry] structures remain standing. Bridges destroyed. Broad fissures in ground. Underground pipelines completely out of service. Earth slumps and land slips in soft ground. Rails bent greatly.
XII	Damage total. Waves seen on ground surface. Lines of sight and level distorted. Objects thrown into the air.

* Equivalent Rossi-Forel (RF) intensities.

4.1.2 Paleoliquefaction Evidence

The distribution and timing of paleoliquefaction features has added considerable data to constrain the source location and recurrence of 1886-like earthquakes and possibly other seismic sources. The first systematic search for liquefaction features in South Carolina was conducted by Cox and Talwani (1983) and Cox (1984). Subsequently, extensive studies were performed by the U.S. Geological Survey (e.g., Obermeier *et al.*, 1985), Ebasco Services (e.g., Amick and Gelinas, 1991), and the University of South Carolina (e.g., Cox and Talwani, 1983). In a recent study by Talwani and Schaeffer (2001), they offer two models to explain the distribution of paleoliquefaction features (Figure 4-8) based on a reanalysis of 15 years of data. In Model 1, three seismic sources exist along the Coastal Plain of South Carolina: at Charleston where the events are **M** 7 ± and sources near Georgetown and Bluffton with **M** ~ 6. In Model 2, the only source is at Charleston with **M** 7 +. They estimate the recurrence time for 1886-like earthquakes is 500 to 600 years based on analyzing the timing of the past three episodes of paleoliquefaction in the last 2000 years. Earthquakes prior to 1886 at Charleston occurred about 546 ± 17 and 1021 ± 30 years before present (Talwani and Schaeffer, 2001).

The uncertainty in recurrence at Charleston is large because it is essentially based on only the last three events. Observations worldwide demonstrate that earthquakes, more often than not, occur at irregularly-spaced time intervals clustered in time. Thus, although only 115 years have elapsed since the last Charleston earthquake, the data are inadequate to state that the next event is several hundred years in the future.

4.1.3 Source of the 1886 Earthquake

The 1886 earthquake has been the subject of extensive studies and research since its occurrence and it is still unclear what the source of the event was. A key factor for this issue is that no surface faulting was observed as a result of the earthquake. A number of hypotheses and models have been put forth and yet no definitive data has emerged to favor one model exclusively over another.

In most previous studies, a large areal source zone has been used to model the 1886 earthquake. For example, in the recent development of the national hazard maps by the U.S. Geological Survey (Frankel *et al.*, 1996), an areal source zone was used to encompass a narrow source zone defined by Dr. Pradeep Talwani and a larger source zone suggested by S. Obermeier and R. Weems, based on the extent of paleoliquefaction sites.

Johnston (1996) postulated that the source of the 1886 earthquake may have been the result of rupture along a fault whose length varied from 20 to 160 km and widths of 16 and 25 km. He assumed a magnitude of **M** 7.3. His preferred models have rupture lengths of 30 and 50 km with corresponding widths of 25 km and 16 km and static stress drops (Brune) of 120 and 110 bars, respectively (Johnston, 1996).

In order to explain the contemporary seismicity observed near Summerville in the past three decades, Talwani (1982) postulated the existence of two buried faults: a northwest-striking structure that he called the Ashley River fault and a north-northeast-trending structure referred to as the Woodstock fault (Figure 4-9). Both are delineated by small magnitude earthquakes. Subsequent studies suggested that the Woodstock fault may be part of a more extensive fault zone which may be associated with a zone of river anomalies which indicate Quaternary uplift

and deformation (Marple and Talwani, 1993). Additional analyses using Landsat imagery, aerial photography, and geophysical and topographic data led Marple and Talwani (2000) to suggest that the Woodstock fault and the zone of river anomalies in the Coastal Plain in South Carolina is part of a 600 km-long fault system which extends from Charleston north-northeast to near Richmond, Virginia (Figure 4-10). The southern end of this "East Coast fault system" may be the source of the 1886 Charleston earthquake and other large prehistoric events (Marple and Talwani, 2000). The evidence suggests that the system has an oblique right-lateral strike-slip sense of displacement.

4.1.4 Other Seismic Sources

The historical earthquake record indicate that there are other seismic sources in addition to the 1886 Charleston source elsewhere in the State such as within the Piedmont (Figure 4-1). Bollinger *et al.* (1991) classify the seismicity in the southeastern U.S. based on their occurrence within the three geologic provinces which comprise the region: Appalachian Highlands (the Valley and Ridge and Blue Ridge), the Piedmont, and the Coastal Plain. Although the largest event outside the Coastal Plain has only been an estimated m_b 4.8 (1913 Union County earthquake) within the Piedmont of South Carolina, it is believed that events such as the 1897 Giles County, Virginia, earthquake are possible. This event had a maximum intensity of MM VIII and has been estimated to be m_b 5.8 in size based on felt area (Bollinger *et al.*, 1991). Giles County is located within the Appalachian Highlands Province. Two earthquakes of m_b 5.0 and m_b 5.2 occurred in the western half of North Carolina in 1861 and 1916 also in the Appalachian Highlands (Stover and Coffman, 1993).

Seismicity in the southeastern U.S., as elsewhere in the central and eastern U.S., is thought to be the result of reactivation of pre-existing faults formed earlier in times of crustal extension. One such fault system may be the northeast-trending Eastern Piedmont fault system in South Carolina. Although no historical earthquakes can be definitively associated with this fault system, diffuse historical seismicity within the Piedmont (Figure 4-1) suggests that pre-existing zones of weakness such as the Eastern Piedmont fault system could be the source of moderate-sized earthquakes as observed elsewhere throughout the eastern U.S.

4.2 APPROACH

This section provides a brief overview of the approach to modeling ground motion and creating scenario hazard maps. The process is divided into three main steps: 1) generation of ground motions for rock, 2) application of soil amplification factors, and 3) development of ground motion hazard maps. Because of the highly technical nature of the following sections, please refer to the glossary for the definition of unfamiliar terms.

Based on the locations and magnitudes of the earthquake scenarios, ground motions are first modeled for a uniform rock outcrop for a grid of points distributed over the State. Rock motions are generated in terms of 5%-damped acceleration response spectra at a suite of three periods: peak horizontal acceleration (PGA) defined at a period of 0 sec, 0.3 sec, and 1.0 sec (100, 3.33, and 1.00 Hz, respectively) as well as peak horizontal particle velocity (PGV). Two different numerical modeling approaches were used to generate the rock motions. In the first approach, a finite-fault simulation model is used to capture the effects of the propagating rupture of the earthquake source (Silva *et al.*, 1990). This is currently the most thoroughly validated finite fault

model available, having compared recorded and simulated motions for 19 earthquakes at about 600 sites (Silva and Costantino, 1999; Silva *et al.*, 1997).

In the second approach, a simple point-source model, which does not accommodate the effects of rupture directivity as well as spatial variability in near-source ground motions, was used to generate estimates of strong ground motions. This model has been widely accepted for characterizing strong ground motions, particularly in the CEUS, and forms the basis for the two most popular attenuation relations used in the CEUS: the Toro *et al.* (1997; EPRI, 1993) and the Atkinson and Boore (1997) relations. The simple point-source model implemented in this project has also recently been used to form the basis for revising the U.S. Nuclear Regulatory Commission design spectra for the CEUS (Silva *et al.*, 2000) as well as to develop design ground motions for a number of Department of Energy facilities such as the Savannah River National Laboratory, Idaho National Engineering and Environmental Laboratory, Rocky Flats, Colorado, and the Los Alamos National Laboratory, New Mexico.

To accommodate epistemic uncertainty in CEUS source processes, three different implementations of the point-source model were used: a single-corner frequency model with both a constant stress drop (stress parameter, Boore, 1983) as well as a magnitude-dependent stress drop (Silva and Darragh, 1995; Atkinson and Silva, 1997; 2000), and the double-corner frequency model of Atkinson and Boore (1995). The use of the single-corner frequency model with constant stress drop is intended to reflect the Toro *et al.* (1997) relation but with regional specific parameters (Appendix A). Also, to accommodate the effects of regional-specific parameters for South Carolina, Q[f], crustal damping, crustal model, and source depths, were incorporated into the three attenuation relations. An important aspect in the development of the region-specific attenuation relations is an attempt to incorporate appropriate parametric uncertainty, based on observed variations in model parameters, as well as modeling uncertainty, through an extensive validation effort in modeling strong ground motions from over 15 earthquakes at about 500 sites (Silva *et al.,* 1997). Development of the point-source attenuation relations including region-specific parameters, parametric uncertainty, incorporation of total uncertainty, and functional form for the regression equation are presented in Appendix A.

For the finite-fault ground motions, the well-validated stochastic numerical modeling approach was used with two rupture areas for each scenario earthquake: one reflecting empirical observations in seismically active areas (Wells and Coppersmith, 1994) and the other based on assumptions in CEUS crustal processes, e.g., crustal and lithospheric temperatures (Johnston, 1996). The use of two rupture areas is intended to capture epistemic uncertainty associated with static stress drops in the CEUS. As with the point-source model, care has been taken to accommodate appropriate parametric uncertainty as well as modeling uncertainty into the expected ground motions (Silva *et al.*, 1997). The stochastic finite-fault and point-source model descriptions are given in Appendix C.

For each scenario event, expected rock outcrop ground motions are expressed across a spatial grid of points in terms of the mean and standard deviation of the natural log of spectral acceleration and peak particle velocity for each of the five models (two finite-fault and three point-source) for the four ground motion parameters of interest.

Amplification factors were developed to accommodate the effects of near-surface variability in the dynamic material properties of the regional soils, and for their depths to bedrock (Section 4.4). The amplification factors are then applied to each set of rock motions based on the

appropriate combination of surface geology, depth to bedrock, period of motion, and expected rock peak ground acceleration input level.

Ground motions are expressed in terms of the mean and standard deviation of 5%-damped spectral acceleration (Sa) and peak particle velocity for each scenario earthquake and for each model. To properly accommodate material nonlinearity in site response for each ground motion model, soil motions are produced separately for the high and low stress drop finite-source rock motions as well as the three sets of point-source rock motions. The resulting ground motions are combined in Section 4.6 to generate dense spatial grids of ground motions for each scenario. To produce the final maps, the soil motions for each model along with their associated variances are weighted to produce final estimates of median and + 1 standard deviation (84^{th} percentile) ground motions and liquefaction probability.

4.3 SEISMIC SOURCE CHARACTERIZATION

To compute the scenario earthquake ground motions, the location, orientation, and rupture dimensions of the modeled fault and its rupture process need to be defined. These parameters are described in the following sections for the four scenario events.

4.3.1 M 7.3 Charleston Earthquake

In consultation with Drs. Pradeep Talwani and Richard Lee as well as information from recently completed studies for the Savannah River National Laboratory, the source of the 1886 Charleston earthquake was modeled as a north-northeast-trending, predominantly right-lateral, strike-slip fault that coincided with the location, strike, and dip of the Woodstock fault. The center of the fault was placed at the approximate center of the 1886 meizoseismal area as defined by the MMX intensity contour (Bollinger, 1977) (Figure 4-7). This model is consistent with the range of models suggested by Johnston (1996).

To accommodate the uncertainty which exists in the appropriate rupture area for a given earthquake size (magnitude) in the CEUS (Johnston, 1996), two rupture models are used. These two models are taken to express the range in realistic median static stress drops for large earthquakes occurring in the Charleston source zone. The first rupture area (RA) is based on the Wells and Coppersmith (1994) empirical relation from WUS earthquakes (tectonically active regions) which predict an area of about 2,000 km^2 for **M** 7.3, using their magnitude-rupture area relation of log RA = - 3.49 + 0.91 M. To determine an appropriate rupture length, the rupture width was set at 20 km, based on local seismicity (P. Talwani, USC, personal communication, 2001). The resulting rupture length is 100 km, in general agreement with Wells and Coppersmith (1994). This rupture scenario reflects the assumption of WUS rupture areas for CEUS earthquakes, a constant static stress drop of about 30 bars

For the other model, which assumes static stress drops are higher in the CEUS than WUS (Johnston, 1996; Kanamori and Allen, 1986), the preferred rupture model of Johnston (1996) is used. In this model for **M** 7.3, the rupture length is 50 km and the width is 16 km, resulting in a static stress drop of about 100 bars, about a factor of three above the 30 bar stress drop for WUS sources. Relative weighting between the two rupture models is discussed in Section 4.5.1.2.

4.3.2 M 6.3 Charleston Earthquake

To be consistent with the **M** 7.3 finite-fault ground motion simulations, both assumptions in rupture areas (static stress drops) are used for the **M** 6.3 scenario earthquake. This results in an area of about 200 km^2 (≈ 30 bars) and 78 km^2 (≈ 100 bars) for the low and high stress drop models, respectively. For **M** 6.3, Wells and Coppersmith (1994) estimate a subsurface rupture length of 19 km. Assuming a length of 20 km results in a rupture width of 10 km. Maintaining the same aspect ratio (L/W = 2) for the high stress drop rupture area gives a length of 13 km and a width of about 6 km.

4.3.3 M 5.3 Charleston Earthquake

For both the **M** 5.3 and **M** 5.0 earthquakes, due to the small rupture areas, only the point-source ground motion models are used. Neglecting finite-fault effects is a reasonable approach, consistent with assessing strong ground motion in the western United States where earthquakes of magnitudes less than about **M** 6 are generally treated as point-sources in developing empirical attenuation relations. To compute distances from the point-sources to the sites, a rupture length is required as the point-source distance metric used is the closest distance to the surface projection of the rupture (Appendix A).

The rupture surface of the **M** 5.3 Charleston scenario earthquake was centered on the **M** 7.3 and 6.3 rupture areas. To model the **M** 5.3 scenario based on the empirical relationship between magnitude and rupture area of log RA = - 3.49 + 0.91 **M** developed by Wells and Coppersmith (1994), an area of 21.5 km^2 is calculated. The relationship for all fault types was used because of the uncertainty of the rupture mode of a future smaller Charleston earthquake and because of the smaller standard deviation in this relationship compared to that for strike-slip faulting. Simply assuming that the aspect ratio is 1 (length = width), the length and width of the **M** 5.3 scenario event are 4.6 km.

4.3.4 M 5.0 Columbia Earthquake

For the earthquake scenario outside of the Charleston seismic source, a **M** 5.0 earthquake near Columbia was selected by consensus by Dr. Pradeep Talwani, Dr. Richard Lee, Dr. Walter Silva, Dr. Bill Clendenin, and Ivan Wong. It was the group's consensus that a **M** 5.0 earthquake could occur anywhere within the Piedmont of South Carolina and so a location was selected where the infrastructure would be tested by such an event and where useful and valuable loss results could be obtained. Because Columbia is located within the Eastern Piedmont fault system, a location on one of the segments was chosen (Figure 4-12). Using the Wells and Coppersmith (1994) relationship between magnitude and rupture area and assuming all fault types yields a value of 12.0 km^2 for a **M** 5.0 earthquake. Hence, the rupture model used in the scenario calculations was an area about 3.4 km by 3.4 km in size.

4.4 DEVELOPMENT OF AMPLIFICATION FACTORS

In the following section, the development of amplification factors to incorporate the site effects of soils and unconsolidated sediments on rock ground motions is presented.

4.4.1 Methodology

The conventional computational approach in developing spectral amplification factors appropriate for specific profiles would involve selection of suitable time histories to serve as control or rock outcrop motions and a suitable nonlinear computational formulation to transmit the motion through the profile. The computational scheme complemented in this project uses the equivalent-linear approach (Schnabel *et al.*, 1972), an approximation to fully nonlinear site response analyses. While an approximation, the equivalent-linear approach is by far the most widely used method to evaluate site effects. Careful comparisons between equivalent-linear and fully nonlinear analyses as well as recorded motions has demonstrated the validity of the equivalent-linear approach over a wide range in loading levels and site conditions (Silva *et al.*, 1988; EPRI, 1993; Silva *et al.*, 1997; Silva and Costantino, 1998; Silva *et al.*, 2000). To provide more rapid and cost effective computation of amplification factors, the current computational scheme also uses a random vibration theory (RVT) implementation of the equivalent-linear approach. As a result, development and use of time histories is not required. The RVT equivalent-linear approach is discussed in Appendix B.

4.4.2 G/Gmax and Hysteretic Damping Curves

To model the nonlinear dynamic behavior of soils under seismic loading, shear modulus reduction (G/Gmax) and damping curves are required. Three sets of curves are used for South Carolina soils: shallow cohesionless soils in the Piedmont site response category, the largely cohesionless soils of the Savannah River category, and the mixture of cohesive and cohesionless soils comprising the Charleston and Myrtle Beach categories.

4.4.2.1 Piedmont/Blue Ridge Category

The Piedmont/Blue Ridge category consists largely of shallow residual soils over weathered rock, grading into hard crystalline rock (Section 3). Laboratory testing of dynamic material properties has been performed for these soils (Borden *et al.*, 1996; Hoyos and Macari, 1999; Schneider *et al.*, 1999). Although the soil samples for these tests are from residual soils at the NGES site in Opelika, Alabama, they are Piedmont residual soils, and are the only appropriate test data of which we are aware. Although samples extended in depth to only 30 ft (9.1 m), these tests showed results very similar to the EPRI (1993) cohesionless soil G/Gmax and hysteretic damping curves for depth ranges 0 to 20 ft (0 to 6.1 m) and 21 to 50 ft (6.4 to 15.2 m) (Figure 4-13a). Based on this comparison, the EPRI curves are considered appropriate for the shallow soils in the top 50 ft (15.2 m) of the Piedmont site response category. For the deeper portion of the profile, to a depth of 100 ft (30.5 m) where the shear-wave velocity reaches about 3,500 ft/sec (1067 m/sec), a recently developed set of rock curves is used. These curves are shown in Figure 4-13b and were developed by modeling the soft rock ground motions computed using the Abrahamson and Silva (1997) WUS empirical attenuation relation (Silva *et al.*, 1997). Below a depth of 100 ft (30.5 m) (shear-wave velocity exceeds about 3,500 ft/sec [1067 m/sec]), the profile is assumed to have linear response (Silva *et al.*, 1997).

Based on the assumption of 100 ft (30.5 m) of soil grading into weathered rock and finally hard crystalline rock, the total kappa (near-surface attenuation factor; Appendix C) value was taken as 0.015 sec (Silva and Darragh, 1995). The total kappa reflects the sum of low-strain damping over the top 100 ft (30.5 m) (Figures 4-13a and b) as well as the weathered zone and hard

crystalline rock. To accommodate uncertainty in nonlinear dynamic material properties, the curves are randomized about the base case values (Figures 4-13a and b) and amplification factors computed for each realization (Appendix B).

4.4.2.2 Savannah River Category

For the Savannah River site response category, a recently developed set of generic curves for cohesionless soils was used. This set of curves (Peninsular Range) was developed by modeling the ground motions recorded at about 80 strong motion sites from the 1994 **M** 6.7 Northridge, California earthquake (Silva *et al.*, 1997). Since many of the recording sites at close distances to the Northridge earthquake are of Pleistocene age and relatively stiff, these curves were considered appropriate for the Pliocene, Miocene, and Eocene soils comprising the Savannah River category (Figures 3-3 and 3-4). The curves are shown in Figure 4-14. The Savannah River soils, as well as those of the Charleston and Myrtle Beach categories, all of which extend to 4,000 ft (1219 m) (Section 4) are considered to behave linearly below 500 ft (152 m). This depth range for nonlinearity (surface to 500 ft [152 m]) is based on modeling strong ground motions at several hundred sites from a number of earthquakes (Silva *et al.*, 1997). Allowing nonlinearity to occur at deeper depths produces results that are inconsistent with recorded motions. Although laboratory test results for dynamic material properties on samples taken from depths exceeding 500 ft (152 m) (as in the recent Rosrine Project in California) show considerable nonlinearity, even at in-situ confining pressure and above, these trends are attributed to sample disturbance.

The total kappa value for the Savannah River profile, extending to a depth to basement rock of 4,000 ft (1219 m) is taken as 0.03 sec. This includes the small strain damping in the nonlinear zone (top 500 ft [152 m]). This value is based on approximately 0.01 to 0.02 sec for 1,000 ft (305 m) of soil estimated from analyses of blast recordings at a downhole array located at on the Savannah River National Laboratory and adding the effects of the additional soil column as well as crystalline basement rock. An additional constraint in assessing an appropriate total kappa are the values of low-strain kappa at very deep soil sites in California, which are based on recorded ground motions. These values average about 0.04 sec (Anderson and Hough, 1984; Silva and Darragh, 1995; Silva *et al.*, 1997) and include the effects of soft rock damping beneath the soils. It is doubtful that 4,000 ft (1219 m) of Savannah River soil in addition to the very low kappa values for hard crystalline rock (Silva and Darragh, 1995) would exceed deep soil in California. The value of 0.03 sec for total kappa is taken as a reasonable estimate and shallower profile depths (Section 4.4.4) will have correspondingly lower values. It should also be pointed out that the total small strain kappa, due to material nonlinearity is an important factor in high-frequency ($\geq$ 5 Hz) ground motions principally at low loading levels (expected rock peak accelerations of $\leq$ 0.2 g).

4.4.2.3 Charleston and Myrtle Beach Categories

As a result of a project-specific laboratory dynamic testing by Project Team members, region-specific G/Gmax and hysteretic damping curves are available for the Charleston site response category. Three sets of curves are available from test results on samples taken over the top 120 ft (36.6m), just above the steep gradient in the shear-wave velocity profile (Figure 3-8). These shallow materials consist of clayey soil, poorly graded sand and silt, and sandy silts (Figure

4-15). For depths below 120 ft (36.6 m), the Peninsular Range curves are assumed to be appropriate for these relatively stiff Pleistocene materials.

For the Myrtle Beach site response unit, which is the Charleston profile with the top 30 ft (9.1 m) removed, the same curves are applied to the appropriate depth ranges (Figure 4-15).

Based on recent analyses of recordings of local earthquakes within the Charleston category area, the total kappa value for 4,000 ft (1219 m) of soil is taken as 0.05 sec (M. Chapman, VPI, personal communication, 2001). Although Chapman's preliminary analyses suggested a total kappa closer to 0.06 sec for about 2,500 ft (762 m) of soil over Triassic basement, a more conservative value of 0.05 sec was used. This value is based on extensive analyses of recordings made in the Mississippi Embayment on very deep (approximately 3,000 ft [914 m]) soft soils (R. Herrmann, St. Louis University, personal communication, 2000) as well as analyses of recorded motions at deep, soft soil sites in the Imperial Valley, California (Silva *et al.*, 1997).

To compare the predominately surface geology-based profiles to current NEHRP categories Table 4-2 shows the NEHRP category criteria using shear-wave velocity and Table 4-3 summarizes the South Carolina site response categories. Interestingly, below the Fall Line, only NEHRP Category D is reflected while the Piedmont/Blue Ridge category is NEHRP C, for either 50 to 100 ft (15.2 to 30.5 m) of soil over hard rock. Significant differences in amplification exist between 50 ft (15.2 m) of soil over hard rock and 100 ft (30.5 m) of soil over hard rock as well as between the Savannah River, Charleston, and Myrtle Beach profiles (Appendix D). Additionally, the NEHRP categories do not consider depth to competent material, except indirectly in averaging shear-wave velocity over the top 100 ft (30.5 m). The use of the current categorization scheme is intended to overcome such shortcomings in the NEHRP approach (Silva *et al.*, 1999, 2000).

Table 4-2
Site Classifications

Average shear-wave velocity to a depth of 30 m is:

NEHRP 1994	UBC 1997
A > 1,500 m/sec	> 5,000 ft/sec
B 760 – 1,500 m/sec	2,500 – 5,000 ft/sec
C 360 – 760 m/sec	1,200 – 2,500 ft/sec
D 180 – 360 m/sec	600 – 1,200 ft/sec
E < 180 m/sec	< 600 ft/sec

4.4.3 Specification of Control Motions

The following describes the computation of input ground motions at the reference site condition, which are multiplied by the amplification factors to arrive at the ground shaking at the ground surface. The crystalline basement profile (Table 4-4) was used as the reference site condition. This crustal model is based on the South Carolina earthquake location model (P. Talwani, USC, personal communication, 2001) modified for hard crystalline rock outcropping.

Table 4-3
Site Response Unit Profiles, Site Classes, and Dynamic Material Properties

Geology	Average Velocity over Top 30m	NEHRP Site Class	Number of Profiles	G/Gmax and Hysteretic Damping
Crystalline	3,400 m/sec	A	1	linear
Piedmont/Blue Ridge	452.90 m/sec*	C	4, 3**	EPRI
Savannah River	355.17 m/sec	D	180	Peninsular Range
Myrtle Beach	328.32 m/sec	D	2	Region-specific, Peninsular Range
Charleston	239.10 m/sec	D	25	Region-specific, Peninsular Range

* The value of 452.90 m/sec is for 100 ft (30.5 m) of soil over hard rock. For 50 ft (15.2 m) of soil over crystalline basement rock, the value is 542.90 m/sec, still NEHRP Category C.

** Three with soil overburden; Monticello profile (Sumer Nuclear Power Plant) has rock at the surface.

Table 4-4
South Carolina Crustal Model

Thickness (km)	V_S (km/sec)*	Density (gm/cm^3)
3.05	3.40	2.70
6.95	3.60	2.80
10.00	3.64	2.80
12.00	3.78	2.85

* Triassic basement replaces top 750 m with shear-wave velocity of 2.54 km/sec and density of 2.55 gm/cm^3.

Since time histories are not required for the RVT-based equivalent-linear site response analyses (Appendix B), the stochastic point-source model (Appendix C) is used to compute the motions at the surface of the base rock or reference rock as well as the other profiles. Both qualitative assessments and quantitative validations of the stochastic point-source model (Hanks and McGuire, 1981; Boore, 1983, 1986; McGuire *et al.*, 1984; Boore and Atkinson, 1987; Silva and Lee, 1987; Toro and McGuire, 1987; Silva *et al.*, 1998; EPRI, 1993; Schneider *et al.*, 1993; Silva and Darragh, 1995; Silva *et al.*, 1997) have demonstrated that it provides accurate ground motion estimates, making it an appropriate choice to produce ground motions representative of the site response unit profiles.

To generate the motions, an **M** 6.5 earthquake is used with the distance (epicentral) varied to produce a suite of distinct median peak acceleration values at the surface of the reference rock unit. The same source and path parameters are then used for the other unit profiles resulting in a suite of amplification factors as a function of reference rock outcrop peak acceleration values

(Silva *et al.*, 1999; 2000; EPRI, 1993; Toro *et al.*, 1992). For the point-source, a stress drop of 110 bars (Appendix A) and a small strain kappa value of 0.006 sec is used for the crystalline rock outcropping (Silva and Darragh, 1995). The profile is randomized over the top 100 ft (30.5 m) (Appendix B) along with the other source and path parameters (Table 4-5, see also Appendix A) to produce a stable smooth estimate of median 5% damped response spectra, the denominator in the site amplification factors.

The Q(f) model (Appendices A and C) is based on inversions of regional earthquakes occurring in the Appalachian region and recorded at hard rock sites (Chapman, 1990). The frequency-dependent is $Q(f) = 811\ f^{0.42}$ based on regional inversions (Martin Chapman, VPI, personal communication, 2001).

Table 4-5
Control Motion Randomization

Parameter	Base Case Value	σ_{ln}
Stress Drop	110 bars	0.7
Q_o	811	0.4
Kappa	0.006 sec (rock)	0.3
Source Depth	8 km	0.6 (2 to 15 km range)

To generate motions which cover the range from linear response to the potentially largest horizontal motions to be expected, six distances are run with reference rock outcrop peak accelerations ranging from 0.05 to 1.00 g (Table 4-6). The magnitude is fixed at **M** 6.5 with the assumption that the amplification factors (ratios) are not highly sensitive to magnitude (EPRI, 1993). Since the profiles are randomized in velocity and layer thickness, the median peak acceleration (taken as the 100 Hz 5%-damped response spectral values) may not exactly correspond to the target peak acceleration. In general, the median values are very close, within about 1% of the target which is considered acceptable since the amplifications vary little for a 10% change in input motions.

Table 4-6
Crystalline Rock Reference Site Ground Motion Parameters
Single Corner Frequency Point Source Model

Target Outcrop* PGA(g)	Median Outcrop* PGA(g)	Median Outcrop* PGV(cm/sec)	Median Outcrop* PGD(cm)	Median Outcrop* V/A (cm/sec/g)	Median Outcrop* AD/V^2 (gcm/cm^2/sec^2)	Dist. (km)	Depth (km)	M	Δσ (bars)
0.05	0.05	3.18	1.48	67.14	6.77	90.88	8.00	6.5	110
0.10	0.10	5.33	2.29	57.47	7.34	51.17	8.00	6.5	110
0.20	0.20	9.64	4.06	52.64	7.84	28.47	8.00	6.5	110
0.40	0.40	17.95	7.46	49.78	8.19	14.15	8.00	6.5	110
0.75	0.75	32.60	13.45	48.29	8.38	5.00	8.00	6.5	110
1.00	1.00	43.08	17.76	47.92	8.44	0.00	7.70	6.5	110

*Top of crystalline crust

Figure 4-16 shows the crystalline outcrop 5% damped pseudo acceleration spectra (median and ± 1 σ) for the lowest level of motion, 0.05g. The parametric variation, reflected in the sigma (σ_{ln} = 0.6 for PGA), includes profile velocity and layer thickness variation (top 100 ft [30.5 m]) in addition to variability in the source and path parameters (Table 4-5).

The remaining reference rock outcrop median spectra are shown in Figure 4-16. These median spectra then represent the denominator or reference geologic unit in computing the amplification factors.

4.4.4 Development of Site Amplification Factors

Site amplification factors are computed as the ratio of 5%-damped response spectral acceleration (Sa) computed at the surface of each site for each randomized profile to the median 5%-damped response spectral acceleration (Sa) computed for the reference rock outcrop motion (Figure 4-17). In addition, peak acceleration, peak particle velocity, and peak particle displacement were computed for the site and reference outcrop as well. Levels of reference rock outcrop peak acceleration values of 0.05, 0.1, 0.2, 0.4, 0.75, and 1.00 g were used to accommodate the effects of material nonlinearity upon site response. Table 4-6 shows the magnitude (**M**), distance (R), peak acceleration, peak particle velocity, and peak particle displacement computed for the outcrop motions.

To accommodate likely profile depth ranges appropriate for the four site response areas (Figures 3-4 and 3-5), categories based upon depth to basement (taken here as top of crystalline or Triassic basement; Table 4-4) were developed. The categories reflect a mean depth and a range over which the amplification factors are considered applicable. Table 4-7 lists the categories, depth ranges, and the corresponding site response units which are considered to have underlying crystalline or Triassic basement material. The range in depth to basement material over which the amplification factors for each depth category are considered applicable are based on the randomization (uniform distribution) depth range.

The amplification factors, 5%-damped Sa/Sa(reference basement rock), were computed at approximately 90 frequencies from approximately 0.10 to 100 Hz. As an example of the general shape of the amplification factors, Figure 4-18 shows the median factors and ± 1 σ sigma values computed for the Charleston category 7 (2,000 to 4,000 ft [610 to 1219 m], Table 4-7) for crystalline outcrop peak acceleration values of 0.05 and 0.50 g (solid and dashed lines, respectively). Due to the randomizing over depth, only a minor contribution of the fundamental resonance is present. The variability reflects parametric uncertainty in the profile, and includes profile layer thickness, shear-wave velocity, profile depth (2,000 to 4,000 ft [610 to 1219 m]), and G/Gmax and hysteretic damping curves (Appendix B). The first layer of the crust (base of the profiles) is also randomly varied assuming a lognormal distribution with a σ_{ln} of 0.3 (EPRI, 1993). The depth variation assumes a uniform distribution resulting in a mean profile depth (depth to first layer of the crystalline) of 3,000 ft (914 m) (Table 4-7).

The effects of nonlinearity are seen in the reduction of amplification at high frequency and the increase in amplification at lower frequency for the 0.5 g crystalline outcrop motions. The increase in variability apparent in the higher motions is likely due to the effects of variability in the G/Gmax and hysteretic damping curves as they influence the motions more at higher loading levels.

Table 4-7
Depth Categories and Depth Ranges

Category	Mean Depth (ft)	Range* (ft)
1	30 (9.1 m)	10 - 50 (3.0 - 15 m)
2	75 (22.9 m)	50 - 100 (15 - 30 m)
3	150 (45.7 m)	100 - 200 (30 - 61 m)
4	350 (106.7 m)	200 - 500 (61 - 152 m)
5	750 (228.6 m)	500 - 1000 (152 - 305 m)
6	1500 (457.2 m)	1000 - 2000 (305 - 610 m)
7	3000 (914.4 m)	2000 - 4000 (610 - 1219 m)

Site Response Units and Depth Categories	
Site Response Unit	**Depth Categories**
Charleston	1, 2, 3, 4, 5, 6, 7
Myrtle Beach	1, 2, 3, 4, 5, 6, 7
Savannah River	1, 2, 3, 4, 5, 6, 7
Piedmont/Blue Ridge	1, 2

* Range of profile depth over which category applies as well as range of depth randomization for each category. Profile depth is defined as depth to basement material: top of (South Carolina crust) (Table 4-4).

4.4.4.1 Effects of Depth to Basement

To assess the effect of soil depth (depth to basement material) as well as the appropriateness of the depth bins in terms of mean depth and depth ranges (Table 4-7), Figure 4-19 shows median amplification factors computed for the Charleston site response category for all seven depth bins and an expected crystalline rock peak acceleration of 0.30 g. Because of this high motion, considerable nonlinearity exists in the shallow portion of the profile (Figure 3-8). The depth effect is apparent at both high frequency ($\geq$ 3 Hz) and low frequency. High-frequency amplification decreases with increasing depth with a crossover in the 2 to 3 Hz range. Below the crossover, the amplification increases strongly as depth increases. In general, the median factors are sufficiently well separated to justify distinct depth bins that have a factor of two between mean depths. To produce depth-independent categories, results should be enveloped, which would produce unnecessary overconservatism, provided depth to basement material is known with a resolution that does not exceed the category depth range (Silva *et al.*, 2000).

4.4.4.2 Effects of Pre-Cretaceous Basement Material

The Savannah River, Charleston, and Myrtle Beach zones include areas within Triassic basins which have the top 750 m of crystalline crust replaced with sedimentary rock of lower shear-wave velocity (2.54 km/sec instead of 3.40 km/sec, Table 4-4). To accommodate any resulting

differences in amplification this may have, a separate suite of amplification factors was computed for all the profiles placed on top of the Triassic crustal model.

Figure 4-20 compares results for the two crustal models using the Charleston site response category 7 (2,000 to 4,000 ft [610 to 1219 m]). As expected the effects of Triassic material below the soils increases the amplification slightly, about 10%. Similar results are shown for the remaining suites of amplification factors (Appendix D). While the difference in amplification between a basement of crystalline or Triassic materials is small, it does reflect a bias and should be accommodated, as we have done.

4.4.4.3 Comparison of Amplification Factors for the Different Site Response Categories

For the shallow depth category 2 (50 to 100 ft [15.2 to 30.5 m]) and crystalline rock peak acceleration of 0.30 g, Figure 4-21 compares median amplification factors computed for the Piedmont, Savannah River, Myrtle Beach, and Charleston site response categories. For frequencies below about 3 to 4 Hz and as low as about 0.3 Hz, the Piedmont amplification is approximately 30 to 40% below the others. At higher frequency, the Piedmont and Myrtle Beach have about the same amplification, with Charleston the lowest, particularly above 10 Hz.

To compare deeper soils, Figure 4-22 shows Savannah River, Myrtle Beach, and Charleston amplification factors for the depth range of 1,000 to 2,000 ft (305 to 610 m), also for expected crystalline outcrop peak acceleration of 0.30 g. For this depth range the Savannah River site response category is even farther above the Myrtle Beach and Charleston amplification levels at low frequency (0.3 to 1.0 Hz) and comparable at high frequency. Interestingly the Myrtle Beach and Charleston reflect similar levels of amplification for this depth range (1,000 to 2,000 ft [305 to 610 m]) at high frequency (above about 3 Hz) but showed about a 30% difference for the 50 to 100 ft [15 to 30 m] depth category (Figure 4-22).

The complete suite of amplification factors is included in Appendix D. These amplification factors are designed to serve as a means of approximately accounting for the effects of surficial soil conditions and depth to basement rock for seismic hazard estimation. Although detailed site-specific results could produce results different from those predicted for these generalized categories, we believe that the amplification factors accommodate appropriate degrees of uncertainty and randomness in dynamic material properties and represent a useful tool for seismic hazard estimation in South Carolina. Linear interpolation is used to provide amplifications between discrete frequency as well as reference rock peak acceleration values.

4.4.4.4 Assessment of Two-Dimensional Effects

The amplification factors assume vertically-propagating shear-waves dominate soil ground motions over the frequency range of interest (1 Hz to peak acceleration, Appendix B1) and neglect surface wave contributions due to potential basin effects (Silva, 1991). The major source of the surface wave contribution to strong ground motions in South Carolina is due to the eastward-dipping interface between the Coastal Plain and underlying hard crustal rocks (Figure 3-4). Appendix B.3 assesses potential impacts of this two-dimensional structure, finding the effects of the Coastal Plain sedimentary wedge to be controlled by vertically propagating shear-waves with little surface wave contribution.

Additional potential basin effects localized to the Triassic basins, South Georgia, Dumbarton, and Florence Basins, are also considered not to be dominated by surface waves. These basins are differentiated from the remaining Coastal Plain only by a layer of soft rock of varying thickness overlying the hard crystalline basement rock. These Triassic units are absent throughout the remaining Coastal Plain, likely thinning towards the basin boundaries, which are not well defined. The difference in impedance between the Triassic units and Paleozoic basement, shear-wave velocities of 2.54 and 3.40 km/sec, respectively (Table 4-4), is not considered large enough to generate significant surface waves (Hartzell *et al.*, 1999; Silva, 1991). The presence of the Triassic units beneath the soils has been accommodated in the amplification factors (Section 3).

4.5 SCENARIO EARTHQUAKE GROUND MOTIONS

Ground motions for the four earthquake scenarios were estimated using a numerical modeling approach. The methodology was developed to incorporate seismic source, path, and site effect uncertainties into hazard assessments to provide statistical stability as well as accuracy in median and fractile estimates of both ground motions and liquefaction potential. This approach maintains the same hazard level in both ground shaking and deformation, providing consistent input to the HAZUS loss estimation model. Expected (median) ground motions (peak acceleration, peak particle velocity, and 5%-damped response spectra at 0.3 and 1.0 sec) for the four scenario earthquakes were developed by first generating rock (Paleozoic basement) motions over a 5 x 5 km grid throughout the State. For the large magnitude scenario earthquakes (**M** 7.3 and 6.3), the grid was significantly increased in density within about 10 km of the rupture to accommodate potential spatial variation due to source finiteness. This resulted in about 3,000 rock motion sites throughout the State. To provide for greater resolution in applying the site amplification factors, the rock motions were interpolated to a 2 x 2 km grid, which provided the base grid for input to HAZUS.

For the large scenario earthquakes, **M** 7.3 and **M** 6.3, the effects of source finiteness are included through finite rupture simulations. For earthquakes with magnitudes less than ~**M** 6, source dimensions are typically very limited in areal extent and the corresponding effects of an extended source are quite small, when averaged over multiple slip models and nucleation points.

To accommodate variability in strong ground motions due to unknown slip distributions and nucleation points for future earthquakes, we developed a methodology which generates random slip distributions as well as random nucleation points (Silva, 1992). To generate random nucleation points, a nucleation zone is defined as the lower half and within 10% of the ends of the rupture surface, based on data from past large earthquakes. Using a uniform distribution, random nucleation points are generated to accommodate the effects of rupture directivity. Figure 4-23 shows the rupture area for the low stress drop **M** 7.3 simulation (Section 4.3.1). The rupture length and width are 100 km and 20 km, respectively, and the nucleation zone is 80 km long, running down dip from 10 to 20 km. The 30 random nucleation points are shown and accommodate the range in expected effects on strong ground motions due to rupture directivity.

To accommodate the range in effects that different possible slip models (distribution of displacement along the fault rupture) may have on strong ground motions, 30 random slip models are used in generating the rock motions. The random slip models are generated using a statistical model based on analyses of variance of slip models of past large earthquakes (Silva, 1992). Four realizations from the suite of 30 are shown in Figure 4-24. The areas of large slip

are termed asperities and sites located at close horizontal distances (≤ 20 km) above these regions experience larger than average motions. Motions at sites located near low slip zones have lower than average motions. This variability in slip allows a realistic accommodation of the increased variability observed in strong ground motions at close distances to large earthquakes (most notably in the recent **M** 7.7 Chi-Chi, Taiwan earthquake).

4.5.1 Weighting of Models

As discussed in Section 4.2, a total of five models, two finite-fault and three point-source, are used to estimate ground motions and liquefaction potentials for the **M** 7.3 and **M** 6.3 scenario earthquakes. Because the finite-fault model implemented in this project has been extensively validated (Appendix C) and provides more accurate estimates of motions at close rupture distances, e.g., near the Charleston source zone where a significant density of infrastructure is located, the finite-fault simulations are given a significantly higher relative weight (0.8) than the point-source (0.2). Weighting between the high and low stress drop finite-fault simulations is based on assessment of liquefaction prediction (Section 4.5.1.2). The areal extent of predicted onset of liquefaction for both rupture models is compared to mapped relic features associated with the 1886 earthquake. Based on qualitative judgment of the most favorable comparison, weights are assigned to the high and low stress drop rupture models. For the smaller scenario earthquakes, **M** 5.3 and **M** 5.0, where the effects of extended rupture are not significant, only the point-source motions are used.

4.5.1.1 Point-Source Model Weights

Attenuation relations have been developed for three point-source models using South Carolina regional parameters (Section 4.2 and Appendix A): the single-corner frequency constant stress drop, variable stress drop, and the double-corner frequency model. Comparisons of peak acceleration versus distance computed for an **M** 7.3 earthquake using the three models are shown in Figure 4-25. Also shown are the values computed from the generic hard rock CEUS models of Atkinson and Boore (1997) and Toro *et al.*, (1997). In general, there is about a 10 to 30% difference between the models, with the variable stress drop the lowest. For the single-corner frequency point-source model, the variable stress drop model is considered to be more appropriate, based on analyses of WUS earthquakes where sufficient strong motion data exist to clearly show a reduction of stress drop with increasing magnitude (Atkinson and Silva, 2000; Silva *et al.*, 1997). With stress drop decreasing with increasing magnitude, a concern with the constant stress drop model involves potentially over-conservative motions at large magnitude and possible under-conservatism at low magnitudes (**M** < 6).

While the differences in peak acceleration between the three region-specific relationships and the generic models for **M** 7.3 is not large, a large difference exists at low frequency. The double-corner frequency model shows significantly lower motions for frequencies near 1 Hz and below, compared to the single-corner frequency models (Figure 4-26). The only close-in data for a large magnitude CEUS earthquake is the 1985 **M** 6.8 Nahanni, Canada, earthquake and comparisons of response spectral shapes with those of the double-corner model show that the predicted spectral sag may be too pronounced (Silva *et al.*, 1999). As a result of these qualitative considerations, the adopted point-source relative weights are as follows: variable stress drop, 0.6; constant stress drop, 0.2; and double-corner, 0.2, for a total relative weight of 1.0.

4.5.1.2 Finite-Source Model Weights

To develop the relative weighting between the low and high stress drop finite-source simulations for the **M** 7.3 and **M** 6.3 earthquake scenarios, predicted and observed areas of liquefaction from the 1886 earthquake were compared. Figure 4-8 shows the area of greatest liquefaction features attributable to the 1886 earthquake (Talwani and Schaeffer, 2001). This northeast-southwest-trending feature, along with the identification of liquefaction-associated sand craters which extend south of Charleston about 40 km near the coast (Obermeier *et al.*, 1987), suggest that a high likelihood of liquefaction should be predicted for an area roughly elliptical extending about 40 km northwest of Charleston and some 50 km south, as well as about 20 to 30 km north, and to the coast.

For comparison, Figures 5-6 and 5-7 show probability of liquefaction based on median factors of safety (Equation 5-4) computed for the low and high stress drop rupture models. The low stress drop model shows 30 to 40% probability contours (factor of safety ≈ 1 for 30% probability) extending northeast-southwest just over about 100 km and about 50 km inland from the coast near Charleston. The high stress drop model (Figure 5-7) predicts a much larger area for the 30 to 40% probability contour, nearly 150 km long, extending south to within 20 km of the South Carolina-Georgia border as well as a 70 to 80% probability of liquefaction for Charleston. This would likely correspond to extensive liquefaction, not observed for the 1886 earthquake. Northwest of Charleston, the 30 to 40% probability contour extends about 80 km, clearly too far inland. While the selection of a factor of safety of 0.9 to1.0 as a criterion for assessing relative weights is not definitive, the high stress drop results clearly overestimates the extent of currently identified paleoliquefaction features. As a result, a relative weight of 0.8 was selected for the low stress drop rupture, leaving a weight of 0.2 for the high stress drop rupture scenario.

Median peak hard rock accelerations near the rupture (0 to 2 km rupture distance) were near 3 g for the high stress drop rupture scenario (Figure 4-27a). At similar distances, the low stress drop peak accelerations were about 1 g (Figure 4-27b), in general agreement with the point-source models (Figure 4-25). The relative and combined weights are listed in Table 4-8.

Based on recommendations from Professor Arch Johnston (University of Memphis, personal communication, 2001), hard rock motions for a medium stress drop scenario were also considered. This scenario was motivated by the apparently deep rupture associated with the recent **M** 7.6 Bhuj, India earthquake. For this deep rupture scenario, the width of the high-stress drop scenario (16 km, Table 4-8) was increased to 25 km, 10 km below the maximum depths of contemporary seismicity, resulting in a static stress drop of about 55 bars. The resulting hard rock motions were about 40% lower than those of the high-stress drop scenario, about 2 g at very close rupture distances (0 to 2 km) (Figure 4-27c). These rock motions would likely result in too large a high probability liquefaction zone, more similar to the high-stress drop results (Figure 5-7). As a result, the relative weights of 0.8 and 0.2 for the low-and high-stress drop scenarios were maintained. For this suite of rupture areas associated with the **M** 7.3 scenario earthquake and static stress drops of 27, 55, and 108 bars, we believe the realistic range in rupture lengths and widths as well as static stress drops (Johnston, 1996; personal communication, 2001) has been reasonably well evaluated.

Table 4-8
Ground Motion Models and Weights

Finite-Source Models	Relative Weight	Combined Weight*
Low Stress Drop (27 bars, 100 x 20 km^2)	0.8	0.64
High Stress Drop (108 bars, 50 x 16 km^2)	0.2	0.16
	Sum = 1.0	Sum = 0.80
Point-Source Models	**Relative Weight**	**Combined Weight***
Variable Stress Drop	0.6	0.12
Constant Stress Drop	0.2	0.04
Double Corner	0.2	0.04
	Sum = 1.0	Sum = 1.00

*__M__ 7.3 and 6.3 scenarios only

The final **M** 7.3 liquefaction map, using the weighted finite- and point-source models is shown in Figure 5-8. The 80 to 90% liquefaction probability contours (factor of safety ≈ 0.5, Figure 5-12) enclose an elliptical area roughly 55 km long and 25 km wide, in general agreement with the area of pronounced craterlet activity (Figures 4-7 and 4-8). Although uncertainties are large, this comparison suggests that our final weighted ground motions are likely not unconservative as a 80 to 90% probability would be expected to result in pronounced liquefaction features (Ron Andrus, Clemson University, personal communication, 2001).

4.5.2 Hazard Maps

The scenario ground motions incorporating site response effects are shown on Figures 4-27d to 4-42. The ground shaking maps were produced using a vector- and raster-based GIS. Each 2 × 2 km grid point was assigned to a site response category. The thickness of unconsolidated sediments was estimated for each grid point based on the contour map shown in Figure 3-5. Surface ground motions were calculated by multiplying the scenario rock ground motions by the appropriate amplification factors. The amplification factors for each grid point were selected based on the site response unit, the thickness of the unconsolidated sediments, and the input rock peak acceleration as described above. For each map, the peak or spectral acceleration values were color-contoured by interpolation generally in intervals of 0.10 g. The ground motion values were then spatially smoothed with a circular window of 15-km-radius so that no features smaller than this size were present on the maps. The intent was to avoid implying a greater level of resolution and/or accuracy than was possible given the limitations of the available geologic data.

The ground motion parameters plotted are median estimates of PGA, 0.3 and 1.0 sec horizontal spectral acceleration, and PGV. Also shown on the maps are the modeled rupture planes. In the case of the **M** 7.3 and **M** 6.3 Charleston earthquakes, the low stress drop rupture lengths are shown.

Figure 4-27d shows that the expected median PGA in a **M** 7.3 Charleston earthquake could be as high as 0.6 to 0.7 g. Although these values might seem relatively low close in to a large event, high-frequency ground shaking as typified by PGA is probably being subjected to some deamplification due to the damping and nonlinearity of the thick Coastal Plain sediments. Because the use of median estimates reflects conventional practice in scenario earthquake

shaking maps, it is important to emphasize these values have a 50% (1 in 2) chance of being exceeded. To provide reliable estimates of the upper range in expected motions, the methodology implemented in developing the ground motion maps (HAZUS inputs) has taken careful account of all potential sources of uncertainty (Section 4.7 and Appendix A). An illustration of expected 84th percentile soil peak acceleration values for the **M** 7.3 scenario is shown in Figure 4-27e. In general, the plus 1-sigma (84th percentile) motions exceed the median by about 50 to 100%. This range is large, but consistent with the total uncertainty in the hard rock attenuation relations of about 0.8 (natural log, Appendix A) for peak acceleration. Although nearly 1 g soil site recordings have been made, the +1 g values near the rupture may not be sustainable for the soft surficial soils. We are likely overestimating the total uncertainty (Section 4.7) as no provision has been made in our variance structure to accommodate a soil's tendency to saturate in high-frequency motions due to nonlinearity. This is currently a research topic with, as yet, no unambiguous resolution, resulting in somewhat conservative 84th percentile high-frequency ground motion estimates.

PGV, a better ground motion parameter for gauging structural damage, could exceed 100 cm/sec close into the rupture (Figure 4-30). Significant ground shaking PGA > 0.2 g and PGV > 20 cm/sec, extends out to distances of about 75 to 100 km from the rupture plane. Damaging ground shaking, PGA > 0.1 g and PGV > 15 cm/sec, will occur in more than half of the State. Strong long-period ground shaking as shown by 1.0 sec spectral acceleration, will occur throughout the State (Figure 4-29).

In the **M** 6.3 Charleston scenario earthquake, PGA could exceed 0.3 g and PGV more than 50 cm/sec (Figures 4-31 and 4-34). Strong shaking will generally be within distances of about 60 km. PGA values between 0.20 to 0.25 g could result from a **M** 5.3 earthquake in Charleston and PGVs greater than 15 cm/sec (Figures 4-35 and 4-38).

Strong ground motions from a **M** 5.0 earthquake in Columbia will be localized around the city although it will be felt throughout the State and possibly beyond. A small localized area could have PGA values that exceed 0.2 g and PGVs of more than 5 cm/sec (Figures 4-39 and 4-42).

To assist the public in relating the ground motion parameters and their values to ground shaking intensities, we have developed an isoseismal map for each scenario earthquake. The maps for each of the four scenarios (Figures 4-43 to 4-46) were produced by converting the PGV values to intensities (Table 4-1) using the relationship developed by Trifunac and Brady (1975):

$$\text{MM I} = \frac{\log \nu_{\text{H}} + 0.63}{0.25} \qquad \text{for IV} \le \text{MM I} \le \text{X} \tag{4-1}$$

where the subscript "H" designates the horizontal component of velocity. As evidenced in the regressions of Trifunac and Brady (1975), the uncertainties in the calculated intensities are at least ± one intensity unit.

Similar empirical relations by Wald *et al*. (1999) and Atkinson and Sonley (2000) were tried but resulted in very different intensity patterns for the various ground motion measures. These two relationships are based on relatively recent estimates of intensities which reflect more modern construction practices and thus may not be as appropriate as the relationship of Trifunac and Brady (1975).

For the **M** 7.3 Charleston scenario earthquake, the highest intensity is MM X (Figure 4-43) (see following section). In the **M** 6.3 and 5.3 Charleston events, the predicted maximum intensities

are MM X and VII, respectively (Figures 4-44 and 4-45). MM II intensities and greater will be felt throughout the State in the **M** 6.3 scenario event. In the **M** 5.0 Columbia scenario, a localized area around the city will undergo MM V effects (Figure 4-46).

4.6 COMPARISON WITH 1886 INTENSITIES

In the selection of weights for the high and low stress drop finite fault simulations, some consideration was given to matching the intensities observed in the 1886 Charleston earthquake (Figure 4-4). Thus, it is not surprising that the resulting computed isoseismal map for the **M** 7.3 scenario earthquake (Figure 4-43) compares fairly well to the actual map in terms of general features. In comparing the two maps, several factors need to be recognized. The assignment of intensities based on felt and observed effects is an exercise in judgment. Because of the qualitative nature of intensities there are large uncertainties in these assignments, probably on the order of ± one intensity unit or more. Bollinger (1977) notes in the development of the 1886 isoseismal map that in the case of multiple reports for a given location, the highest intensity was used. As noted earlier, the conversion from ground motion values to intensities as required for our computed isoseismal maps (Figures 4-43 to 4-46) is also extremely uncertain.

Comparing Figures 4-4 and 4-43, the computed maximum intensity in the near-source region was MM X, which is the same as the observed MM X. The computed intensities within about 100 km of the modeled rupture plane decay to MM VIII compared to the observed MM VI, although the observed intensities increase up to MM VII and VIII at greater distances. The latter does not seem to be well constrained by observations. In the Piedmont, our map shows the region to be characterized by MM V to VI, slightly lower than observed intensities (MM VI to VII). This difference is not considered significant given the various sources of uncertainties.

A noticeable difference between the 1886 isoseismal map and our **M** 7.3 isoseismal map is the observed localized areas of postulated higher intensities such as the northeast-southwest elliptical area of MM VIII west and southwest of Columbia (Figure 4-4). These localized areas are difficult to understand because there does not appear to be a geologic basis for the higher intensity areas shown on the 1886 map based on the statewide analyses of site response in this study (Section 3-3). These higher intensities are based on a small number of observations (Figure 4-4) and may reflect very localized areas of greater shaking smaller than the resolution in which we have defined site response units.

In summary, the differences between our computed isoseismal map and the 1886 map are generally on the order of one intensity unit within the uncertainties of this parameter. We believe, on average, that we have captured the distributions and levels of ground motions that would be generated in a future **M** 7.3 Charleston earthquake as well as the other three scenario events.

4.7 TREATMENT OF UNCERTAINTIES IN GROUND MOTIONS

Because of the variations inherent in natural processes such as earthquakes and our current lack of understanding of all the causes and effects associated with ground shaking due to earthquakes, large uncertainty exists in specifying strong ground motions for engineering design. As a result, ground motion parameters are usually expressed in terms of median values. This means there is a 50% probability or likelihood that the actual motions could exceed or be less than the predicted

values. If the uncertainty in the predicted motions is also quantified, accurate estimates can also be made for the range in expected motions. This is generally expressed as the median and median-plus-one standard deviation, or the 50th and 84th percentile ground motion estimates. At the 84th percentile motions, there is only a 16% chance the values will be exceeded and are generally considered upper-range design conditions.

For seismically active regions, such as California, the occurrence rate for large earthquakes is such that a sufficient number and range of recordings of ground shaking exists to define empirical relations for predicting ground motions due to future earthquakes. In this case, both median estimates and their uncertainties (standard errors) are based on observations and prediction of strong ground motion for a given earthquake and source-to-site distance is relatively straightforward.

For the central and eastern U.S., however, recordings of large earthquakes are unavailable and, unfortunately, recordings of small earthquakes (**M** < 6) indicate fundamentally distinct ground motion characteristics from earthquakes occurring in the western U.S. (e.g., California). As a result, estimation of strong ground motions for the central and eastern U.S. relies primarily on models that reflect our current knowledge of earthquake rupture processes and wave propagation. Because there are several plausible models (Section 4.5, Appendix A) and currently available data cannot distinguish between them, uncertainty in estimating strong ground motions is significantly larger in the eastern U.S. compared to the western U.S. Since the uncertainty in estimating strong ground motions results directly in uncertainty in risk (loss), considerable effort has been undertaken in this project to quantify all the components of uncertainty as accurately as possible and, at the same time, avoid unnecessary conservatism by double-counting contributions. The following section details the statistical models used to compute the total uncertainties in the ground motions to provide estimates of 84th percentile ground motion.

4.7.1 Uncertainty Models

Median ground motions are given by exp(mean[Ln(Sa)], where the Ln(Sa) is assumed to be lognormally distributed. The mean [μLn(Sa)] ground motions for each individual model are given by:

$$\mu_{\ln(Sa_i)soil} = \mu_{\ln(Sa_i)rock} + \mu_{Ln[Amp(Sa_i)]} \tag{4-2}$$

The weighted average mean for the combination of all models is given by:

$$\mu_{\ln(Sa)soil} = \sum_{i=1}^{n} W_i \left[\mu_{\ln(Sa_i)rock} + \mu_{Ln[Amp(Sa_i)]}\right] \quad . \tag{4-3}$$

The standard deviation (sigma) for an individual model is calculated as the square root of the sum of the variances from rock and soil uncertainty, as follows:

$$\sigma_{\ln(Sa_i)soil} = \sqrt{\sigma^2_{\ln(Sa_i)rock} + \sigma^2_{\ln[Amp(Sa)]_i}} \tag{4-4}$$

The variance from the weighted combination of different models is computed as:

$$Var[\ln(Sa)_{soil}] = \sum_{i=1}^{n} W_i \left[\sigma^2_{\ln(Sa_i)soil}\right] = \sum_{i=1}^{n} W_i \left[\sigma^2_{\ln(Sa_i)rock} + \sigma^2_{\ln[Amp(Sa)]_i}\right] \quad (4\text{-}5)$$

This formulation of the variance does not include the additional variance contributed by the epistemic uncertainty between models, due to the difference in the mean between ground motion models (for rock). An expression including this additional source of uncertainty is given by:

$$Var[\ln(Sa)_{soil}] = \sum_{i=1}^{n} W_i \left[\mu^2_{\ln(Sa_i)soil} + \sigma^2_{\ln(Sa_i)soil}\right] - \mu^2_{\ln(Sa)soil} \quad (4\text{-}6)$$

For this study, the uncertainty is expressed using Equation 4-5. As discussed in Appendix C, the additional variance associated with Equation (4-6) is not warranted as the variance contributed by the site has been included twice: once in the total variance for the rock motions and again in the variance associated with the amplification factors. Use of Equation 4-6 requires a correct partitioning of variances into source/path and site components, a very desirable objective. However, given the current limitations of data and models, this is not an unambiguous process.

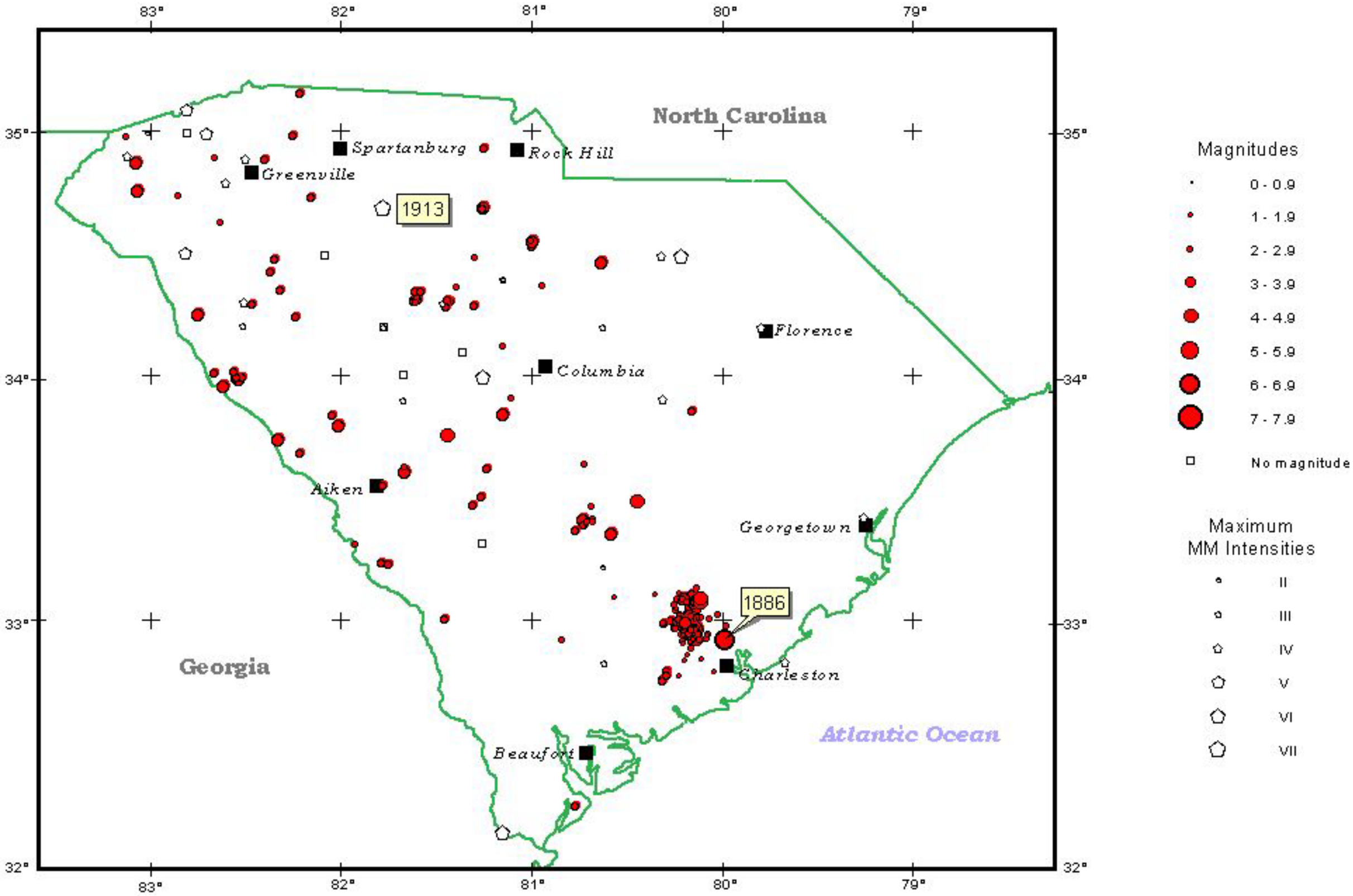

Figure 4-1 Historical Seismicity of South Carolina, 1800 to 1999

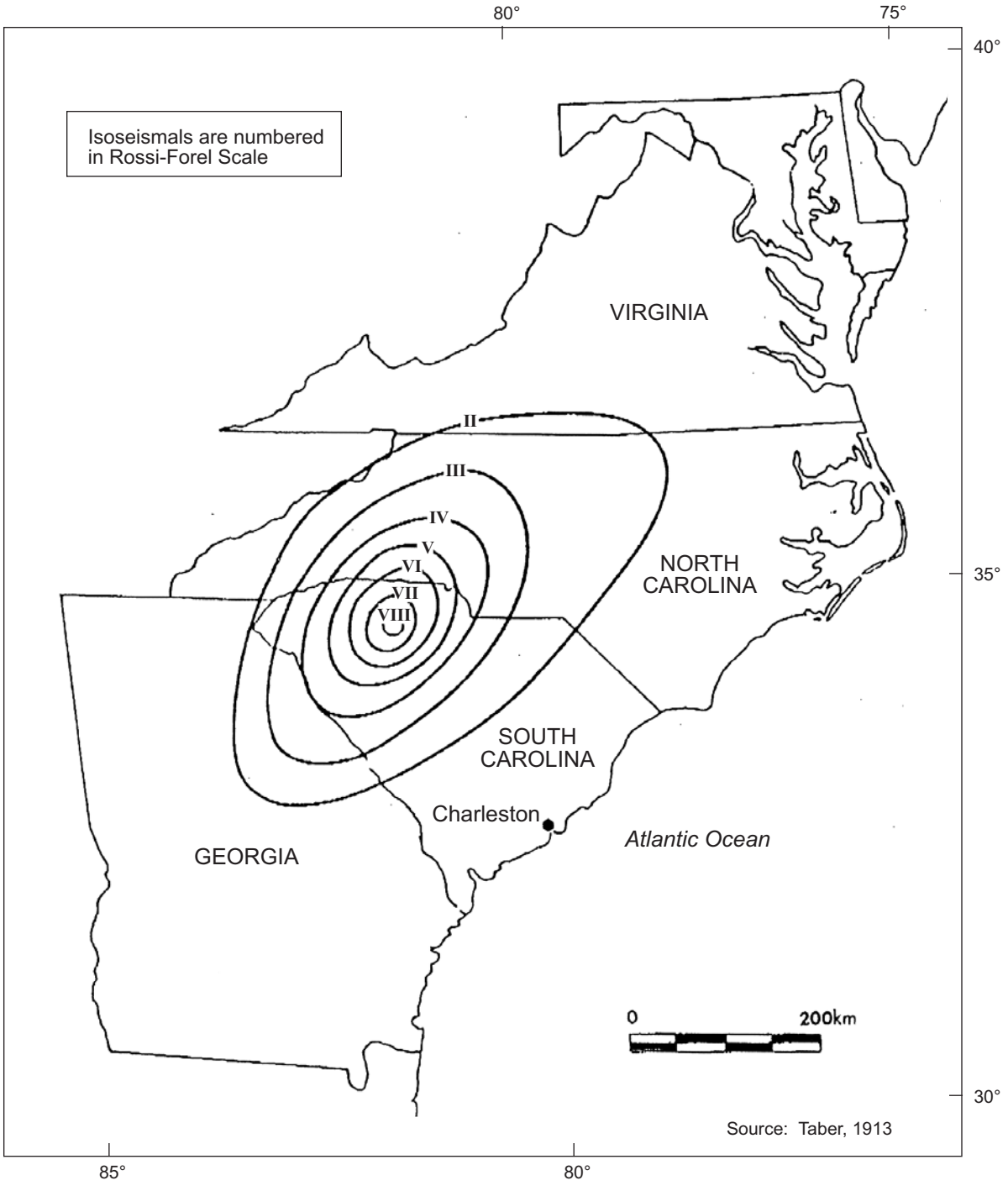

Figure 4-2. Isoseismal Map of the 1 January 1913 Earthquake

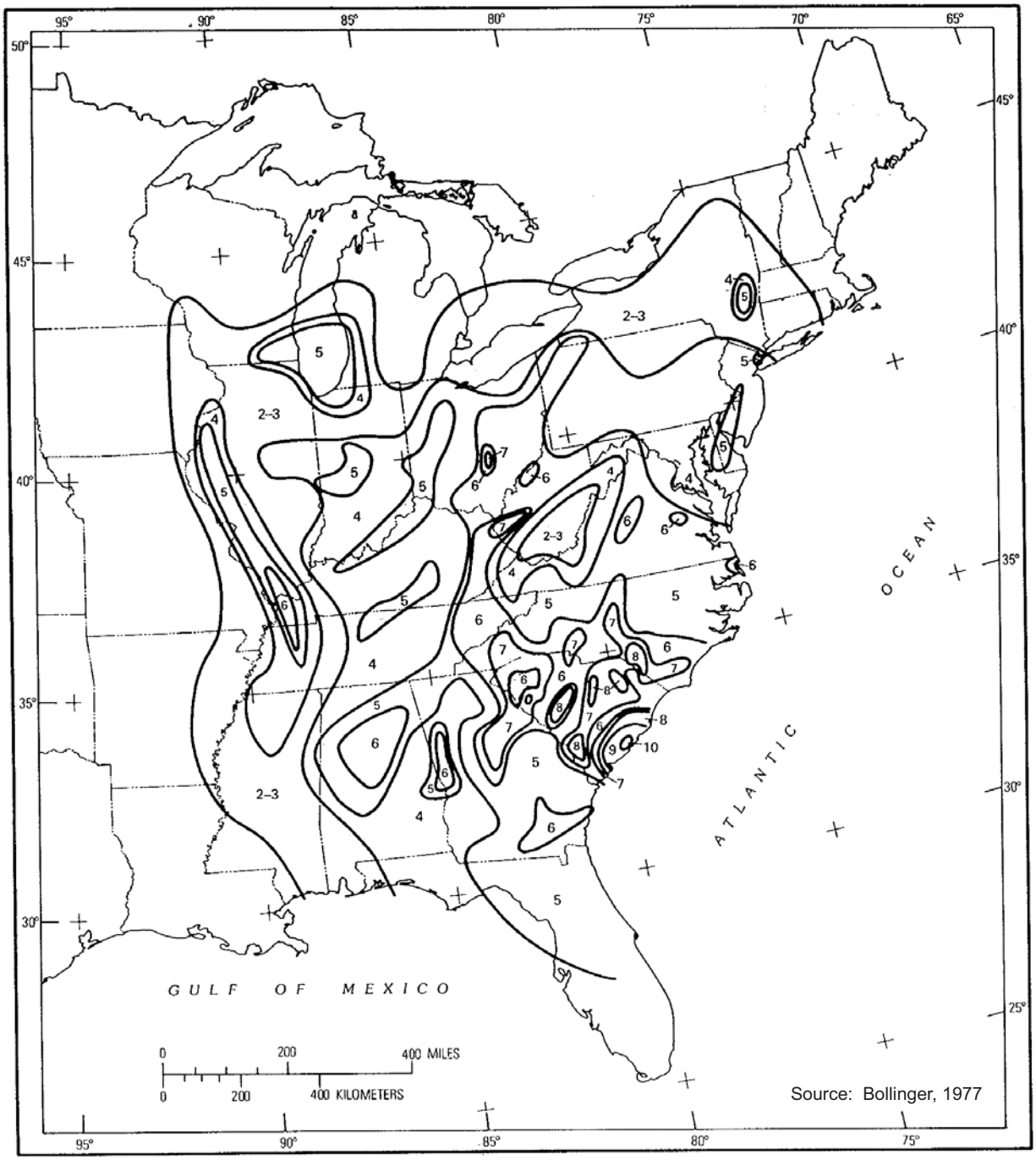

Figure 4-3. Isoseismal map of the 1886 Charleston earthquake.

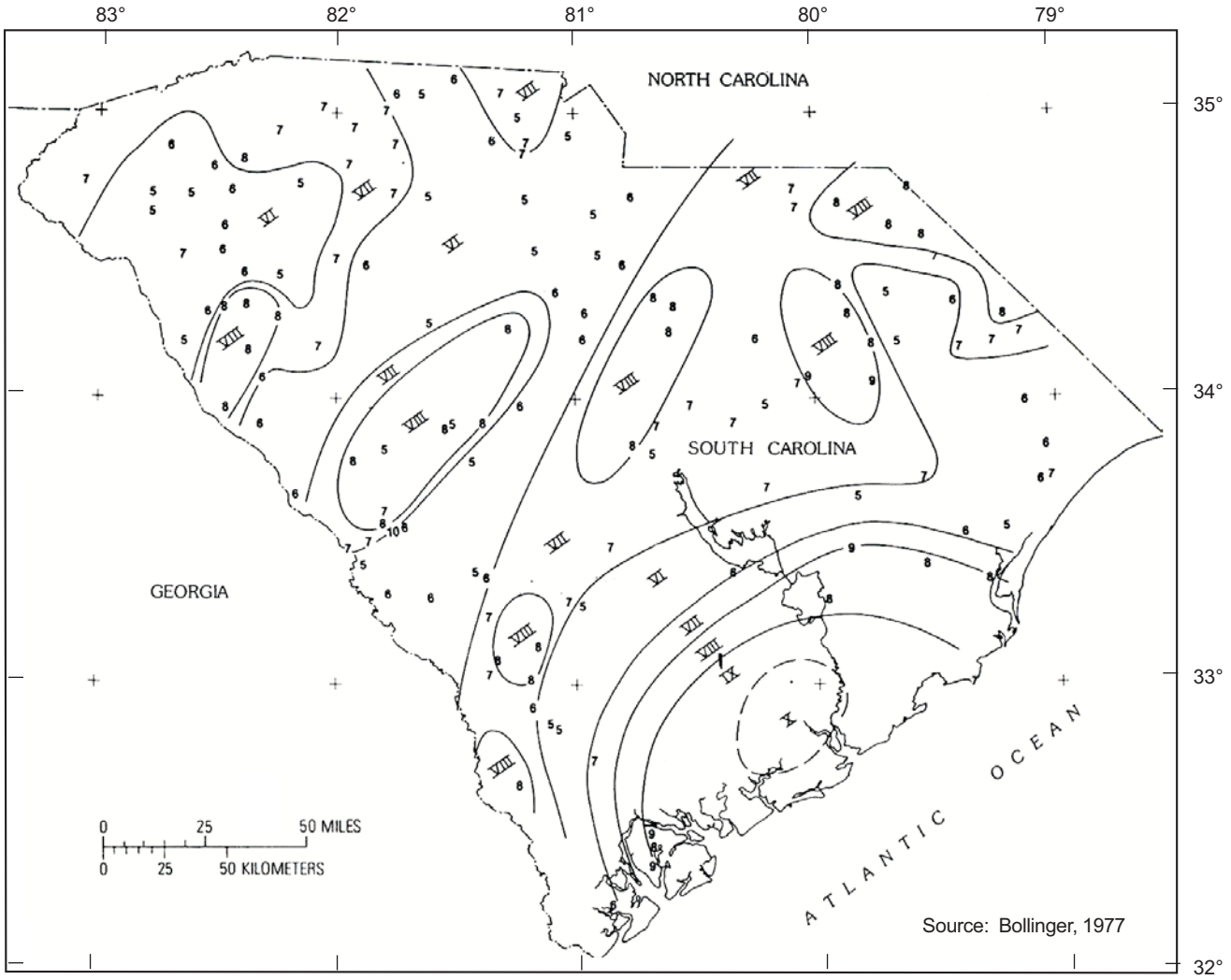

Figure 4-4. Statewide isoseismal map of the 1886 Charleston earthquake.

Source: Stover and Coffman, 1993

Figure 4-5. Damage on East Bay Street, Charleston in 1886.

Source: Stover and Coffman, 1993

Figure 4-6. Brick house at 157 Tradd Street, Charleston in 1886.

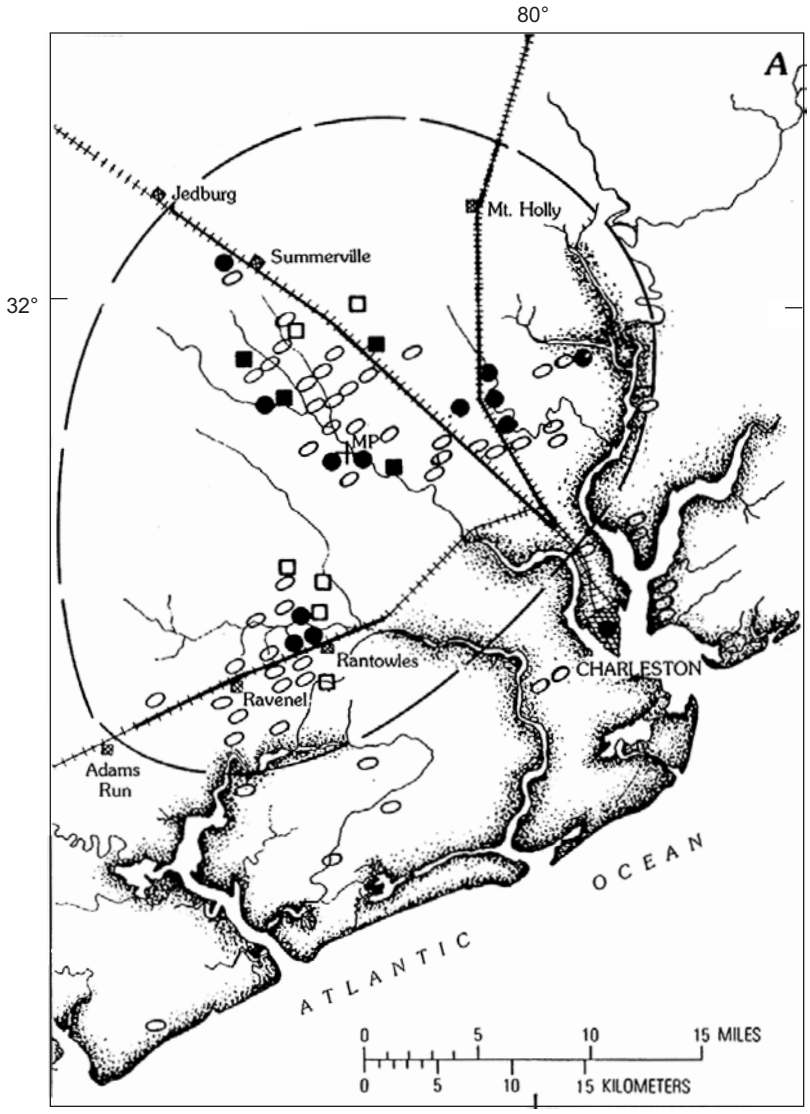

Source: Bollinger, 1977

EXPLANATION

- Railroad track damaged
- Building destroyed
- Marked horizontal displacement
- MP Middleton Place
- Craterlet area
- Chimney destroyed

Figure 4-7. Map of intensity X effects in Charleston in 1886.

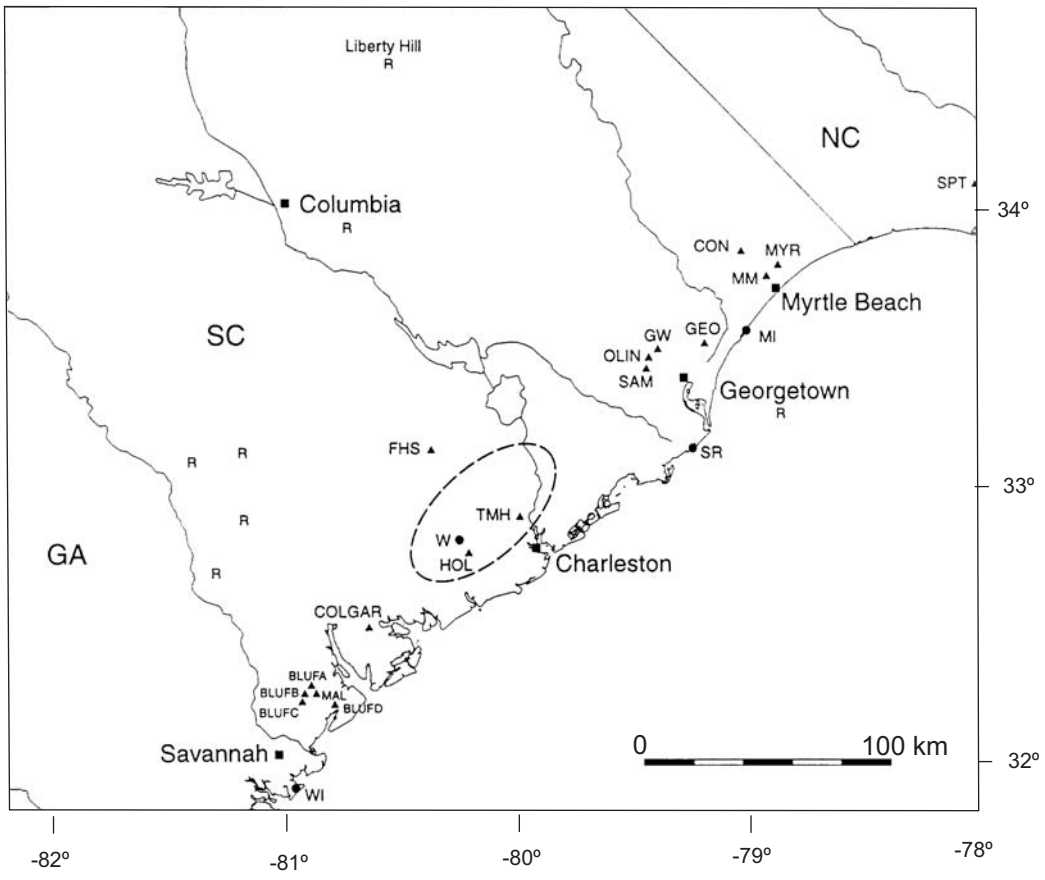

Source: Talwani and Schaeffer, 2001

LEGEND

— — — — Area of pronounced craterlet activity

R Reports of liquefaction features

▲ Location of paleoliquefaction sites with datable material associated with prehistoric earthquakes

Figure 4-8. Extent of pronounced craterlet activity in 1886 and other paleoliquefaction features in South Carolina.

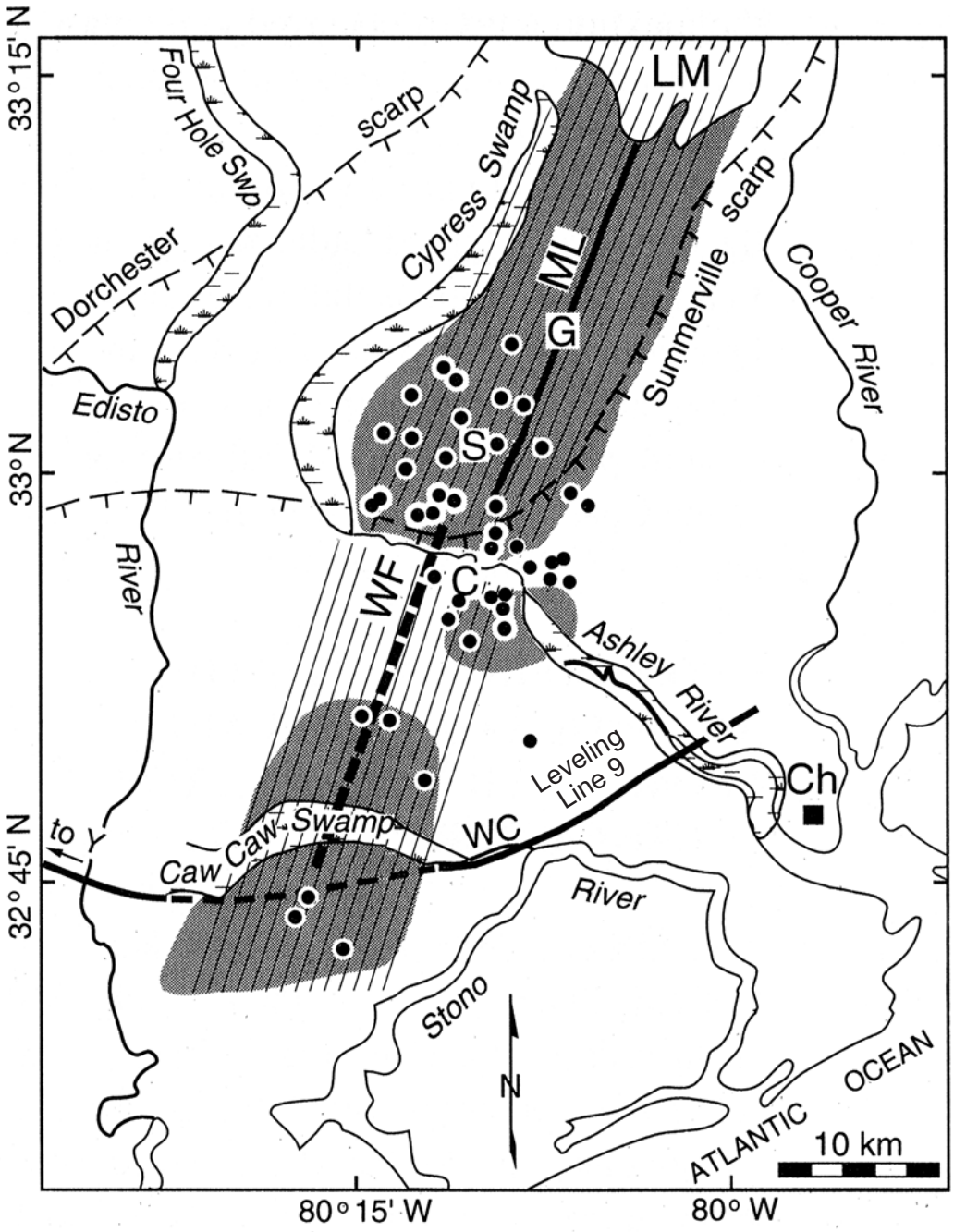

C – Cooke Fault
G – Gants Fault
WF – Woodstock Fault
LM – Lake Moultrie
ML – Linear aeromagnetic anomaly
S – Summerville
WC – Wallace Creek

Source: Marple and Talwani, 2000

Figure 4-9. Map of the Woodstock fault, zone of river anomalies, and seismicity (1974-1996) near Summerville.

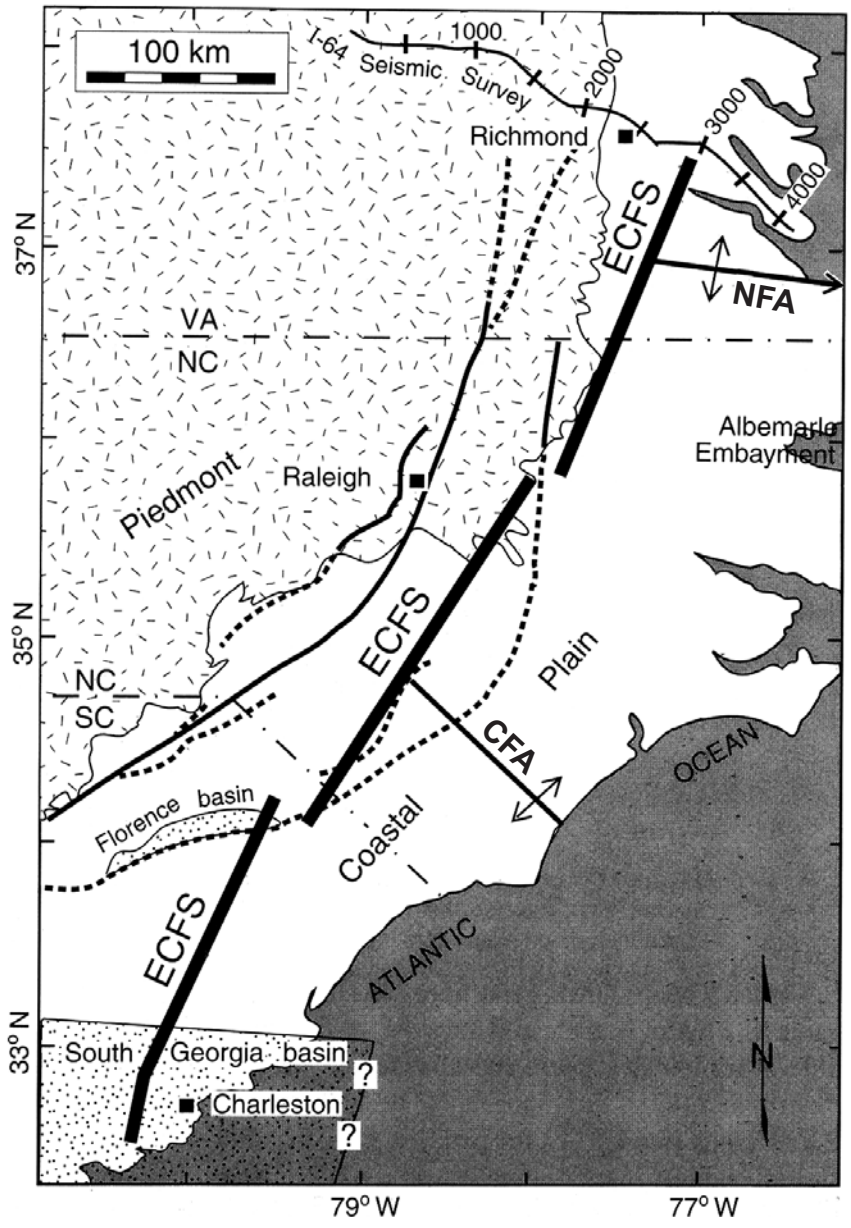

CFA: Cape Fear Arch

NFA: North Fork Arch

Figure 4-10. East Coast fault system as proposed by Marple and Talwani (2000).

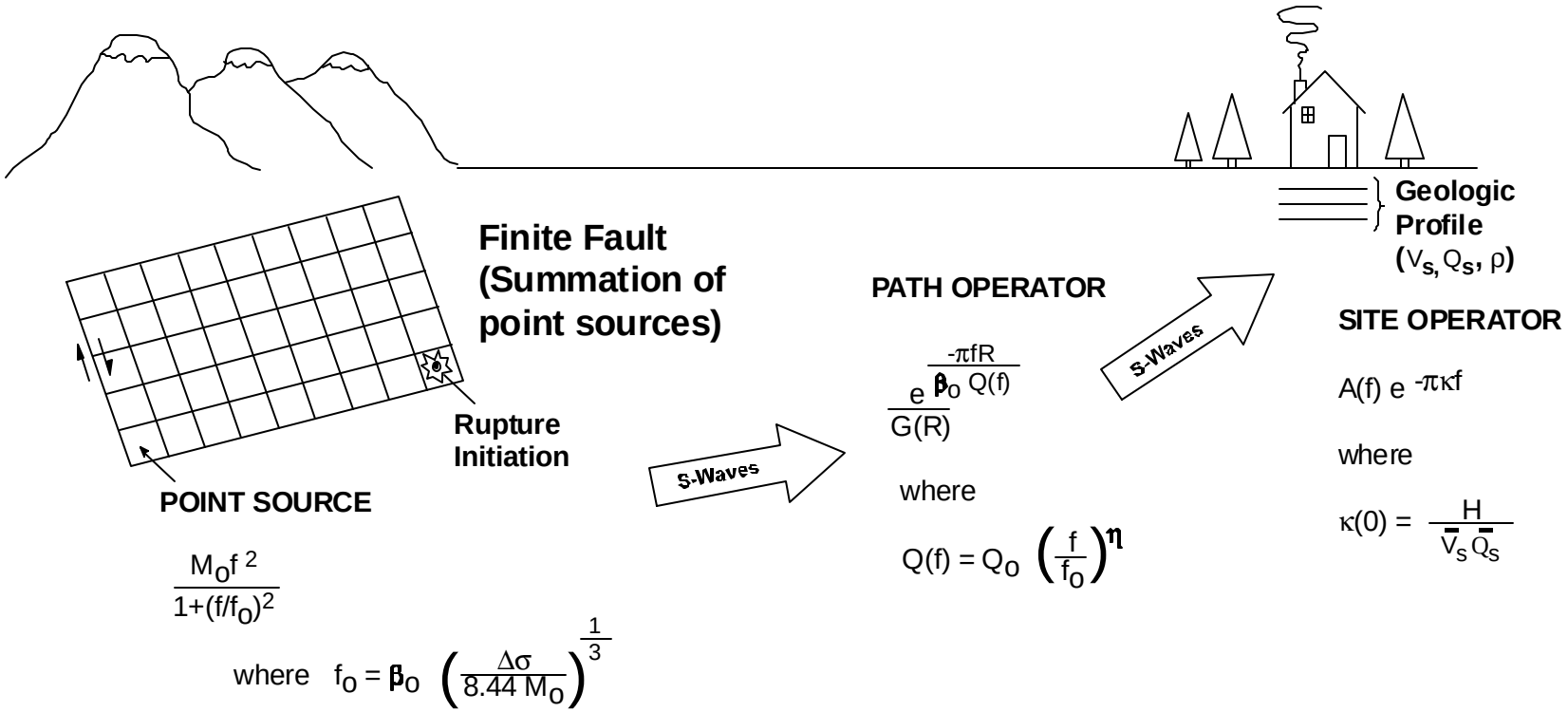

Figure 4-11. Schematic diagram of the stochastic ground motion model.

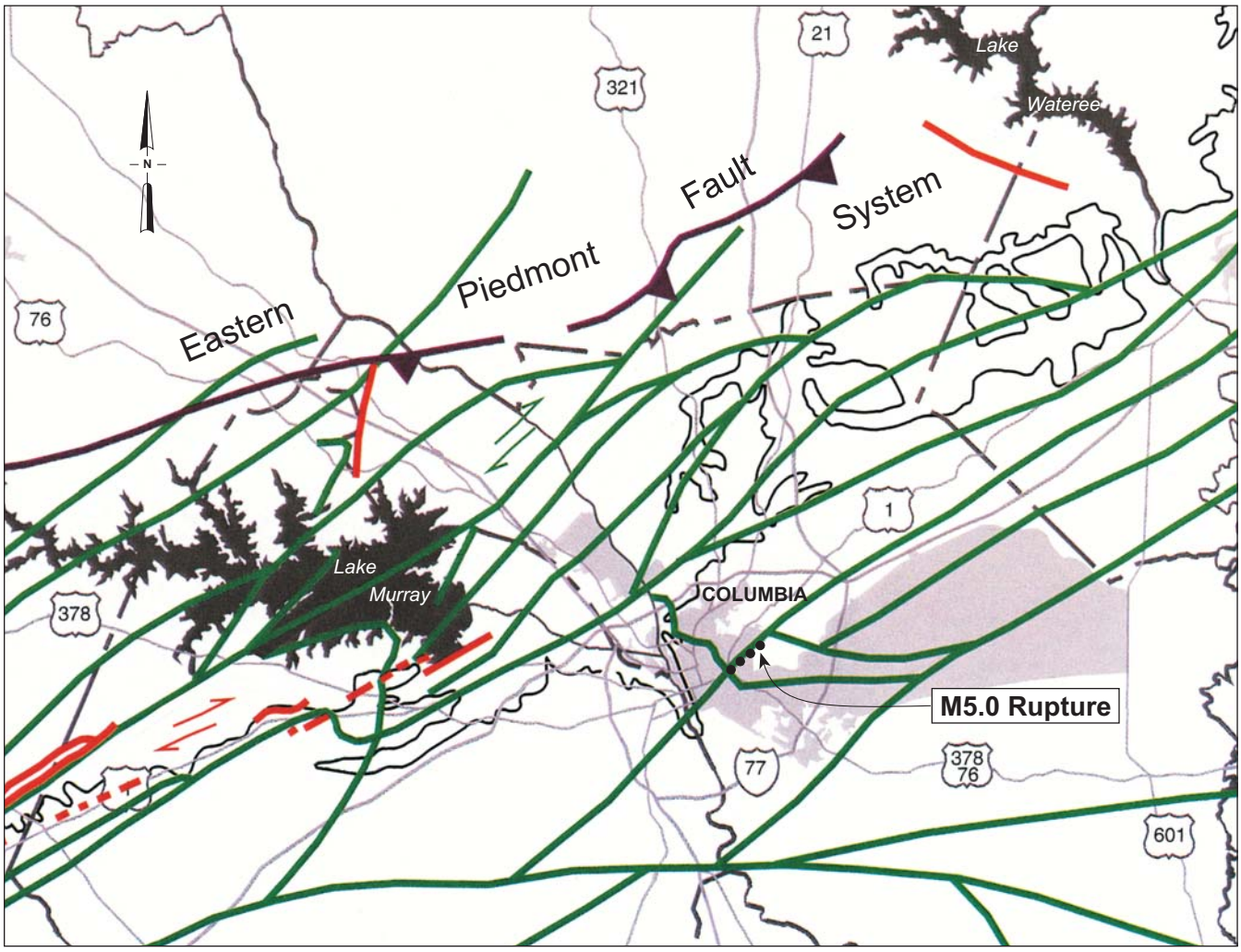

Figure 4-12. Location of the M 5.0 Columbia earthquake along the Eastern Piedmont fault system.

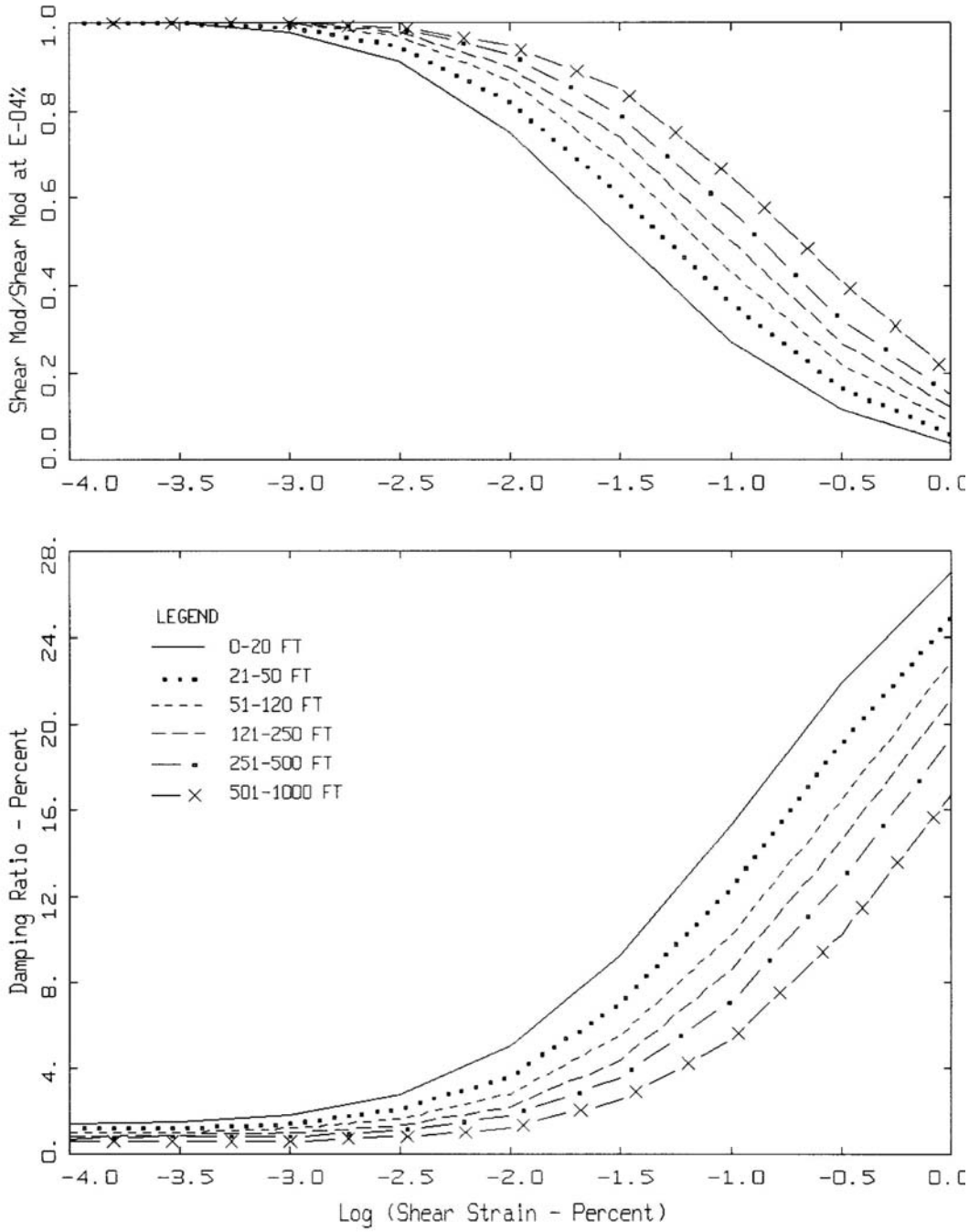

Figure 4-13a. Generic G/Gmax and hysteretic damping curves for cohesionless soil site conditions (EPRI, 1993), used for the top 50 ft (15.2m) of the Piedmont profile.

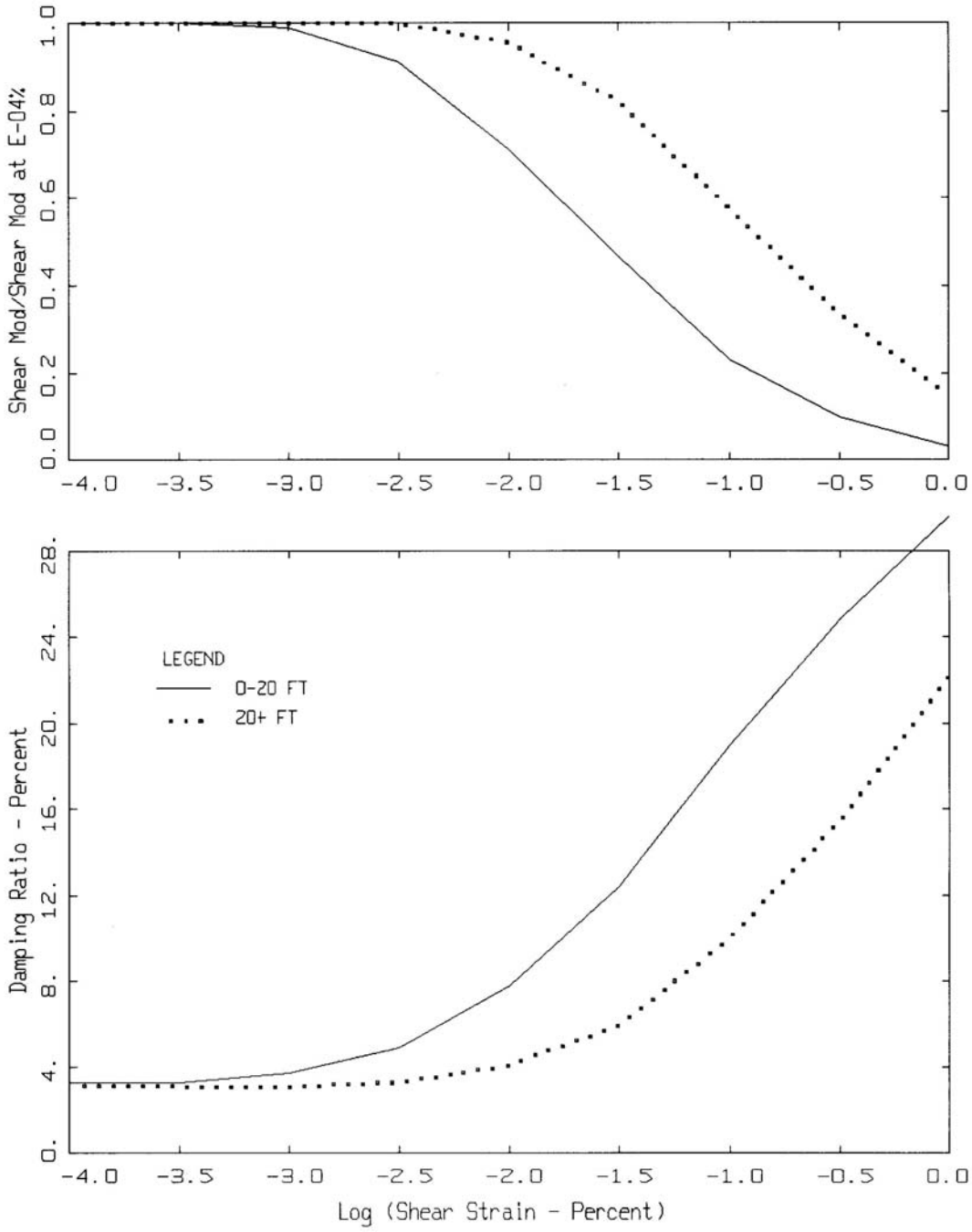

Figure 4-13b. Generic G/Gmax and hysteretic damping curves for soft rock site conditions (EPRI, 1993), used for 50 to 100 ft (15.2 to 30.5 m) in the Piedmont profile.

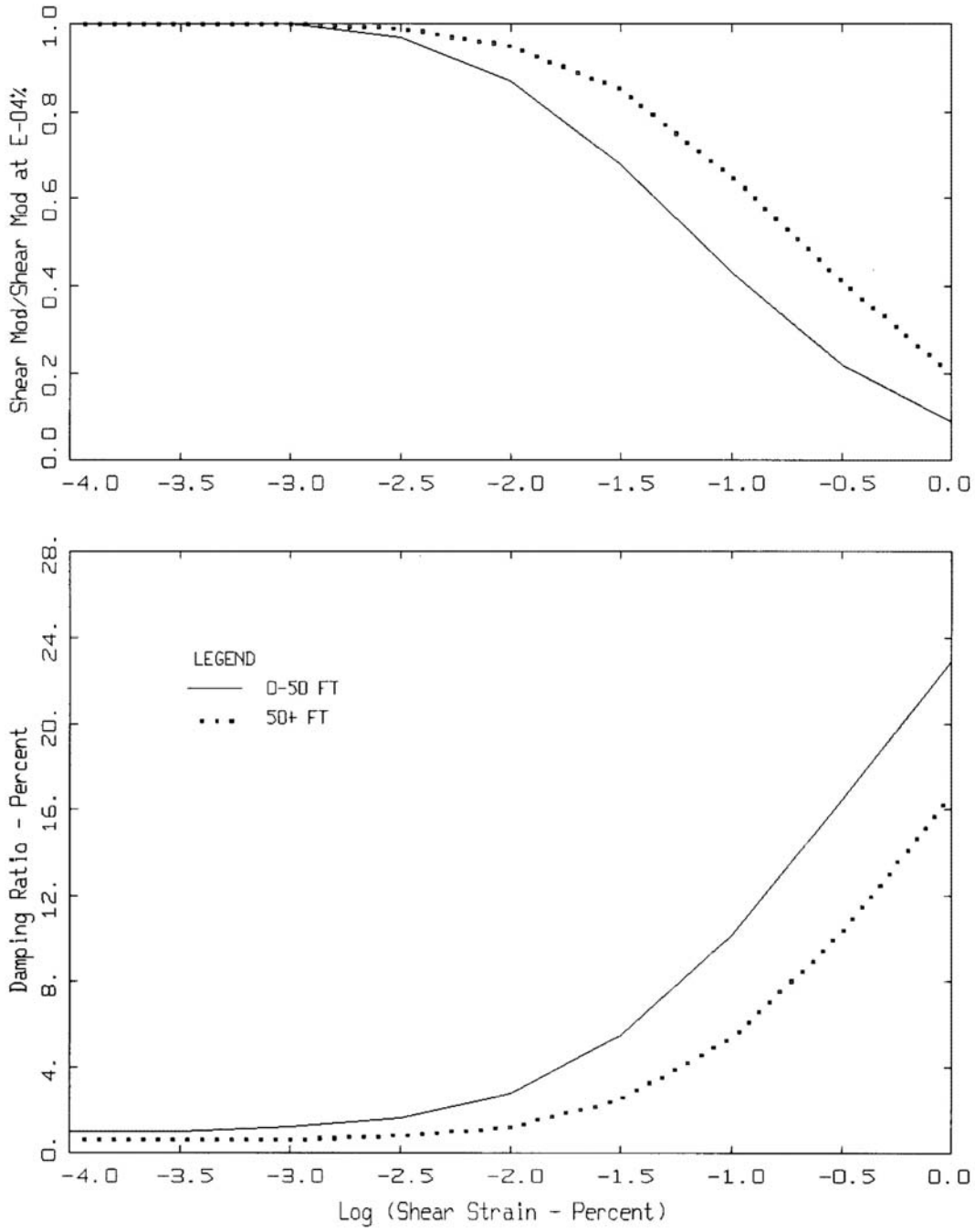

Figure 4-14. Generic G/Gmax and hysteretic damping curves for Peninsular Range cohesionless soil site conditions (Silva et al., 1997), used for the Savannah River profile and deep portions of the Charleston and Myrtle Beach profiles.

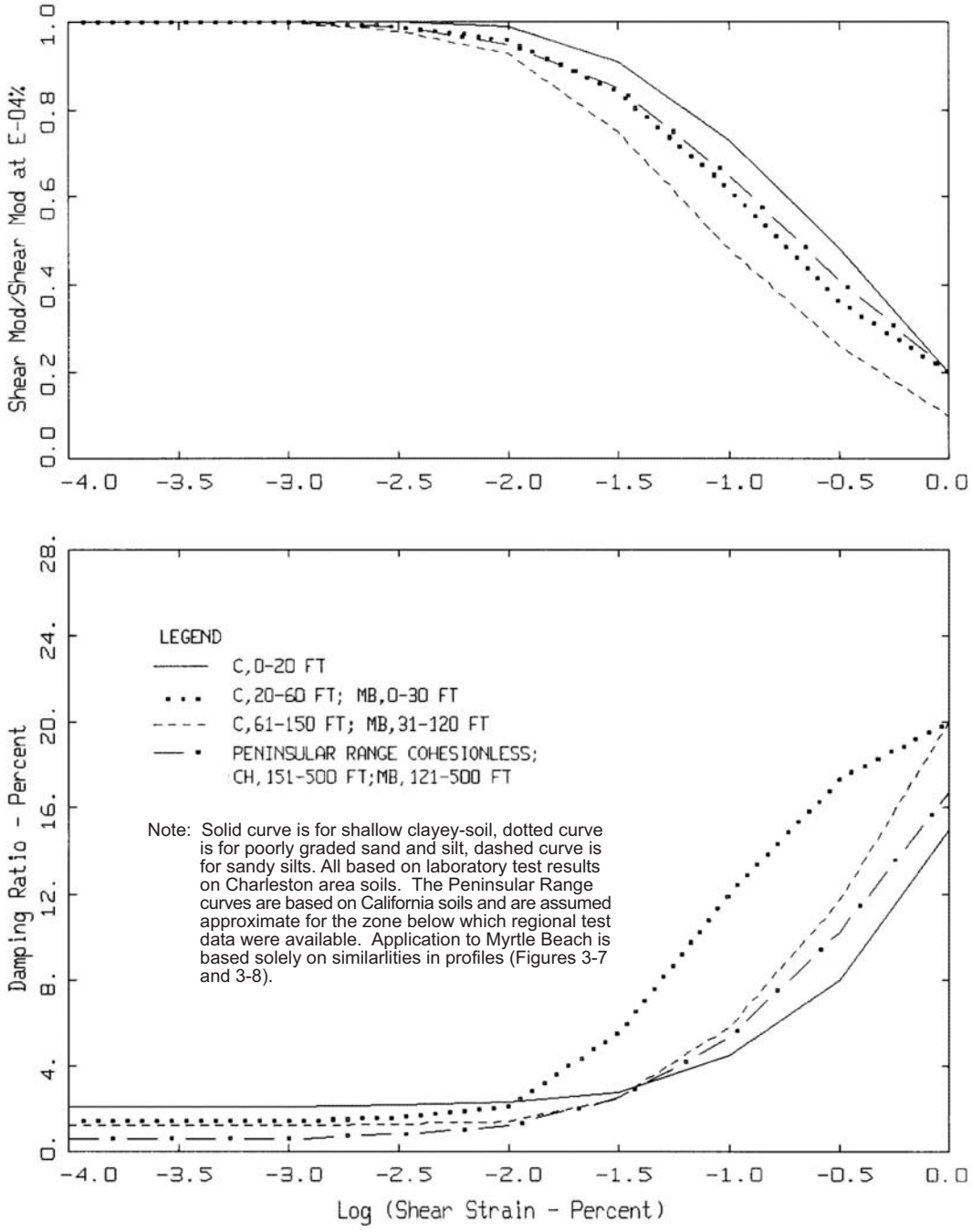

Figure 4-15. Generic G/Gmax and hysteretic damping curves for Myrtle Beach (MB) profile.

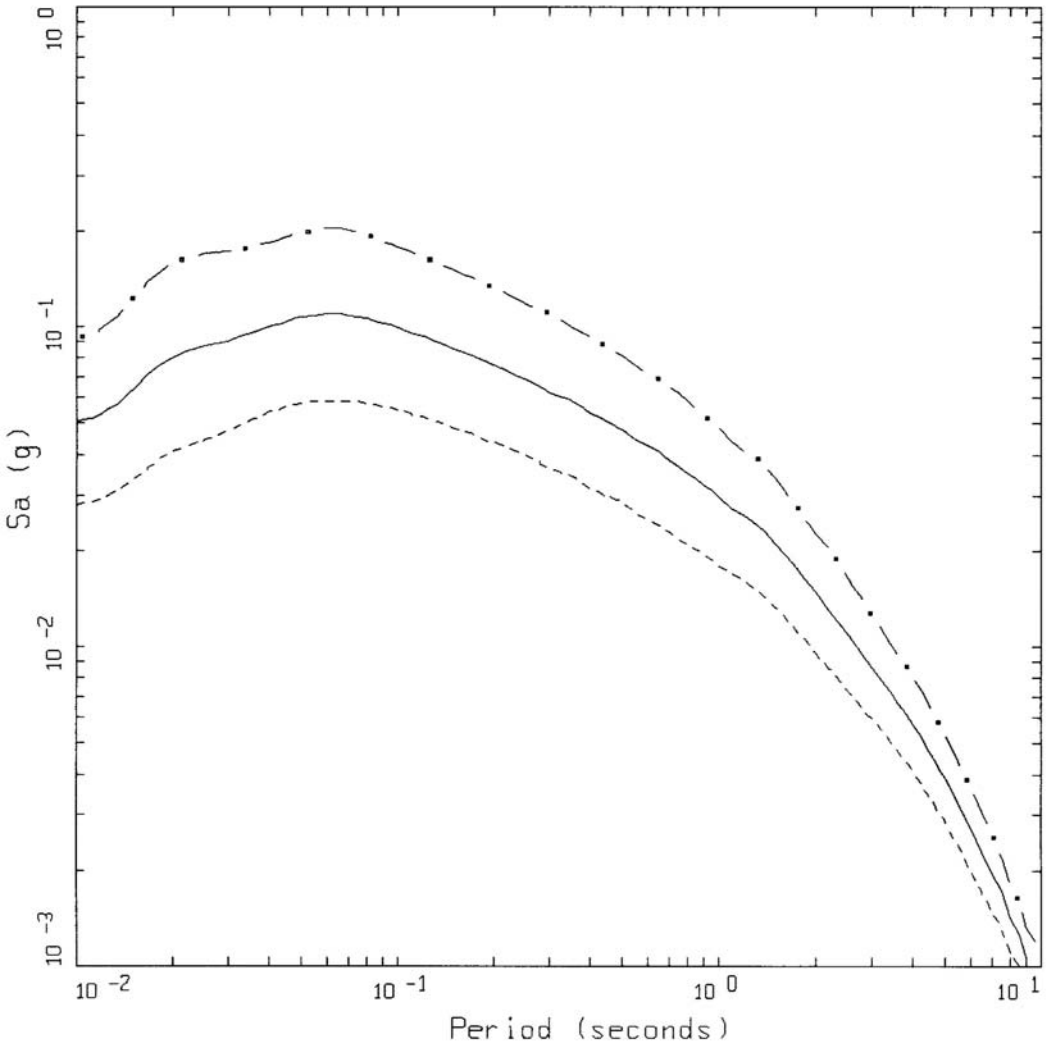

Note: Distance adjusted to give a median outcrop peak acceleration of 0.05g (Table 4-5)

LEGEND

—·— 84th Percentile Parametric Uncertainty; PGA = 0.092 g

——— 50th Percentile Parametric Uncertainty; PGA = 0.051 g

- - - - - - - - 16th Percentile Parametric Uncertainty; PGA = 0.028 g

Figure 4-16. Median and ± 1σ motions (5% damped response spectra) computed for crystalline basement rock outcropping using the point-source model with the South Carolina crustal structure (Table 4-3) and parameters listed in Table 4-4.

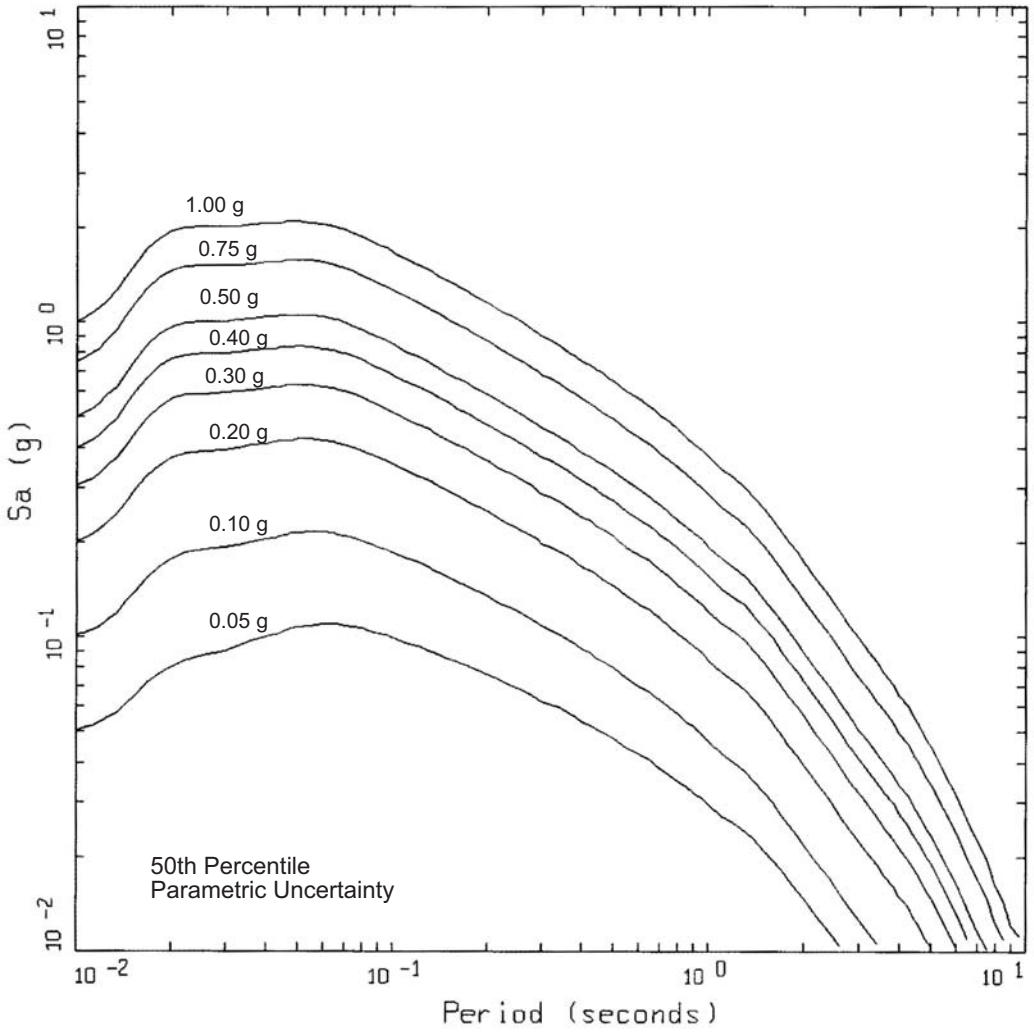

Note: Distance adjusted to give a median outcrop peak acceleration of 0.05g to 1.00g (Table 4-5)

Figure 4-17. Median motions (5% damped response spectra) computed for crystalline basement rock outcropping using the point-source model with the South Carolina crustal structure (Table 4-3) and parameters listed in Table 4-4.

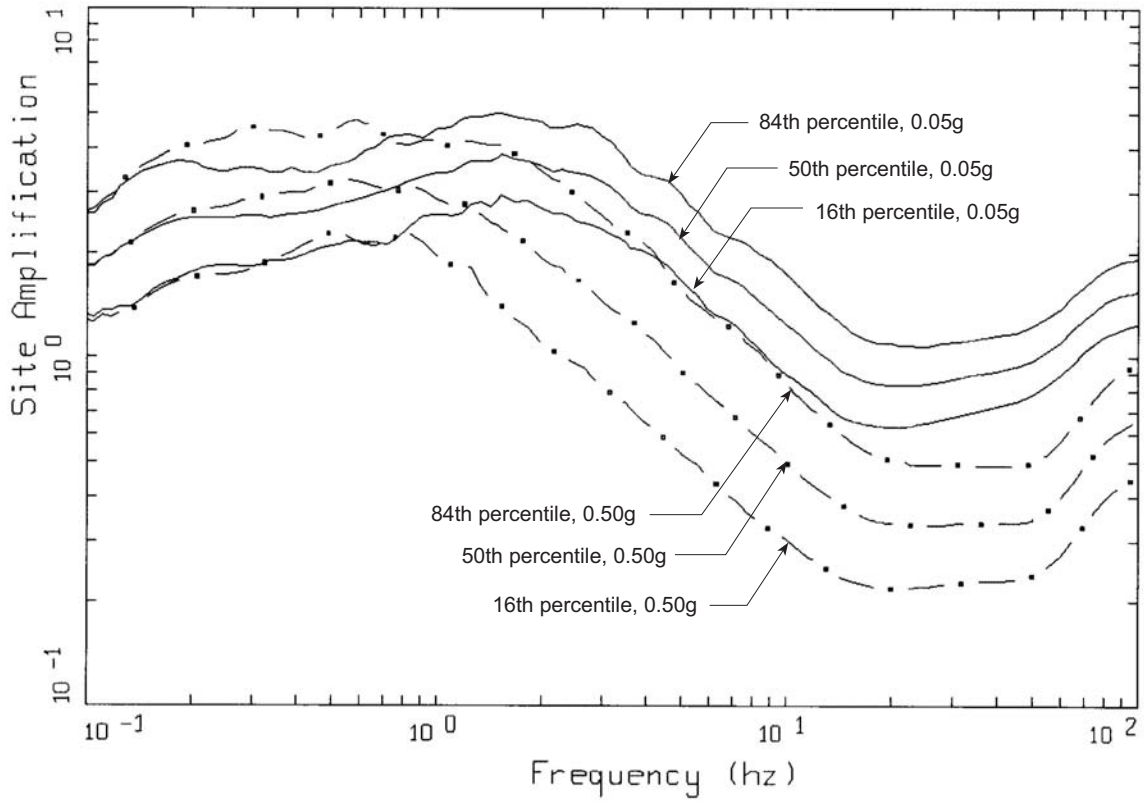

Figure 4-18. Comparison of median and ± 1σ amplification (5% damped response spectra) computed for the Charleston site response category 7, depth 2,000 to 4,000 ft and levels of expected crystalline rock peak accelerations of 0.05 and 0.50 g.

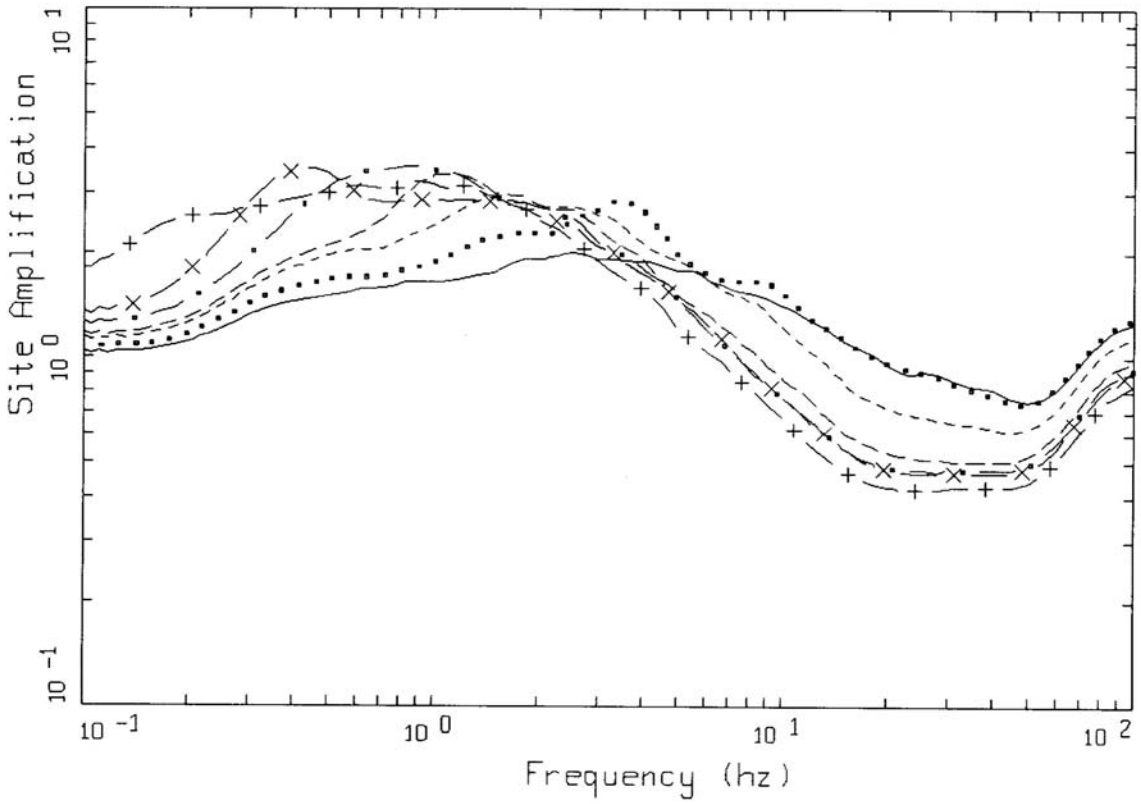

LEGEND

50th Percentile, 10-50 ft, Depth Category 1
50th Percentile, 51-100 ft, Depth Category 2
50th Percentile, 101-200 ft, Depth Category 3
50th Percentile, 201-500 ft, Depth Category 4
50th Percentile, 501-1000 ft, Depth Category 5
50th Percentile, 1001-2000 ft, Depth Category 6
50th Percentile, 2001-4000 ft, Depth Category 7

Figure 4-19. Comparison of median amplification (5% damped response spectra) computed for the Charleston site response category, depth categories 1 to 7 and levels of expected crystalline rock peak acceleration of 0.30 g.

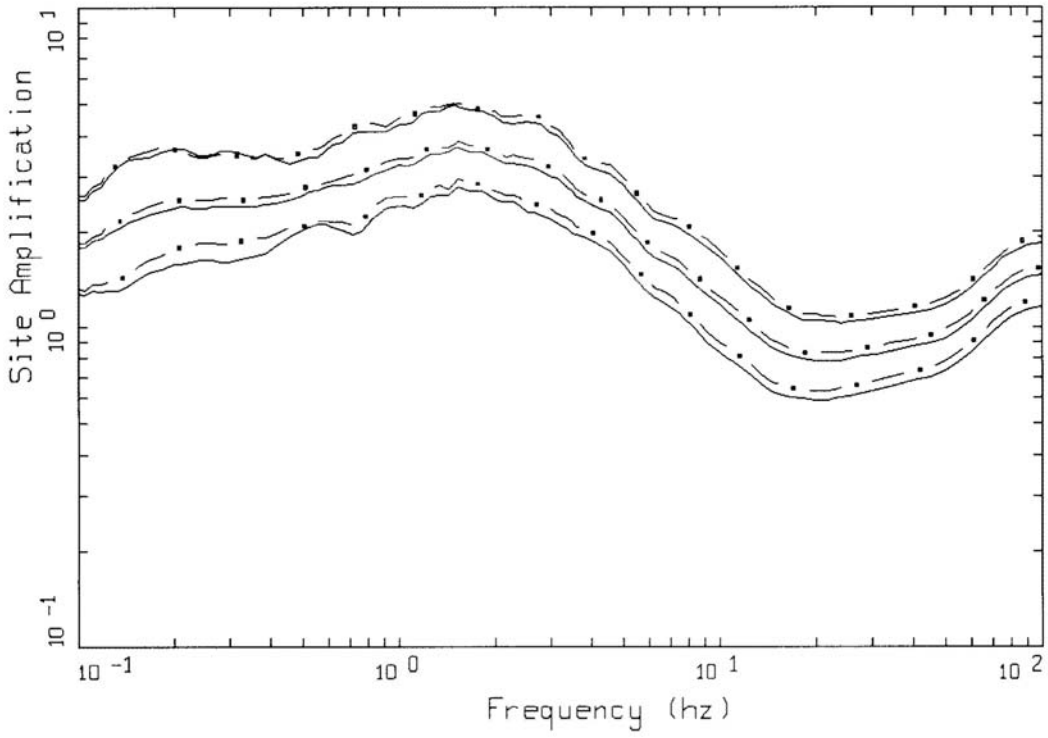

LEGEND

84th Percentile, 0.05 g, Crystalline
50th Percentile, 0.05 g, Crystalline
16th Percentile, 0.05 g, Crystalline
84th Percentile, 0.05 g, Triassic over Crystalline
50th Percentile, 0.05 g, Triassic over Crystalline
16th Percentile, 0.05 g, Triassic over Crystalline

Figure 4-20. Comparison of median amplification (5% damped response spectra) computed for the Charleston site response category 7 with soil over crystalline and Triassic basement material (Table 4-3).

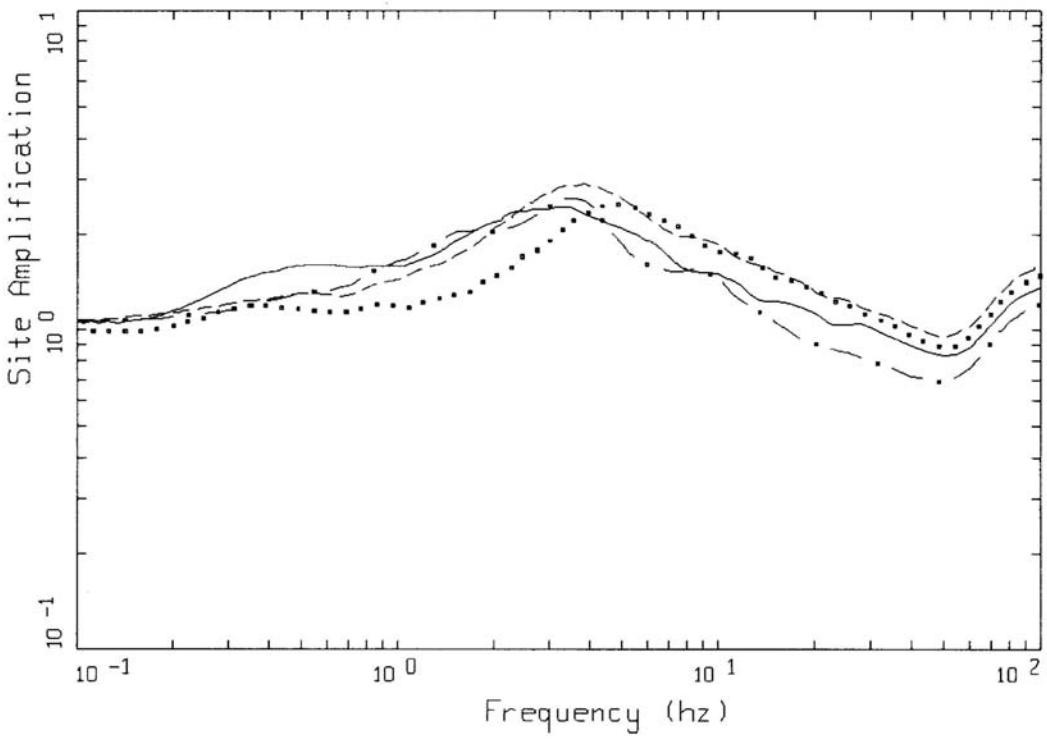

LEGEND

50th Percentile, Piedmont, 51-100 ft, Depth Category 2
50th Percentile, Savannah River, 51-100 ft, Depth Category 2
50th Percentile, Myrtle Beach, 51-100 ft, Depth Category 2
50th Percentile, Charleston, 51-100 ft, Depth Category 2

Figure 4-21. Comparison of median amplification (5% damped response spectra) computed for the Piedmont, Savannah River, Myrtle Beach, and Charleston site response categories: depth 50 to 100 ft; expected crystalline rock outcrop peak acceleration of 0.30 g.

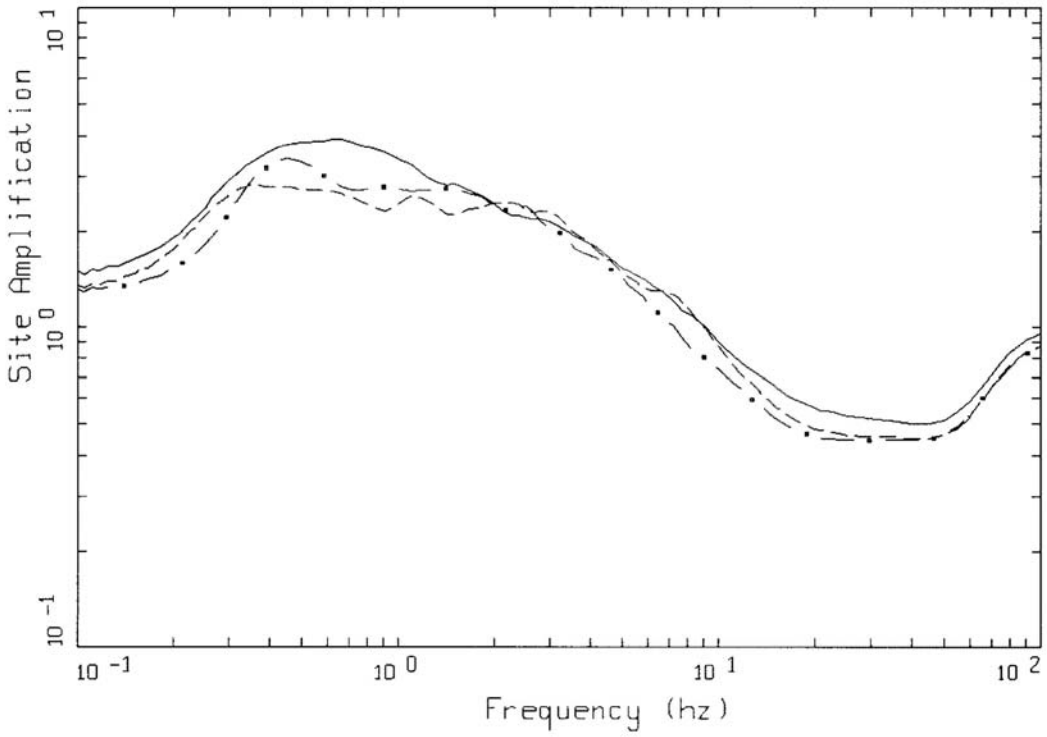

LEGEND

50th Percentile, Savannah River, 1001-2000 ft

50th Percentile, Myrtle Beach, 1001-2000 ft

50th Percentile, Charleston, 1001-2000 ft

Figure 4-22. Comparison of median amplification (5% damped response spectra) computed for the Savannah River, Myrtle Beach, and Charleston site response categories: 1000 to 2000 ft; expected crystalline rock outcrop peak acceleration of 0.30 g.

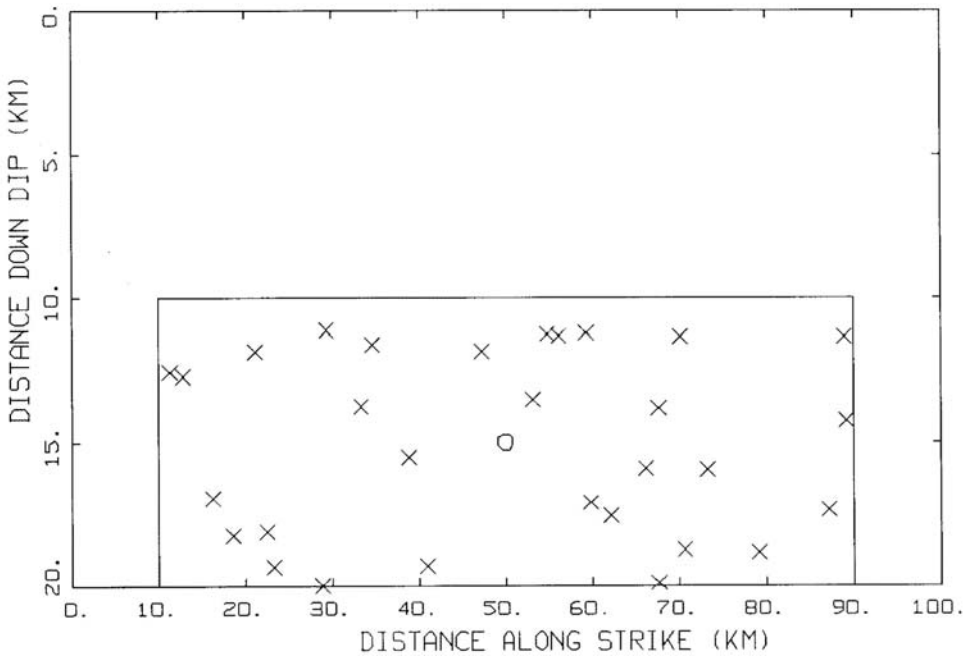

Note: Base-case nucleation point is at the geometrical center of the nucleation zone.

LEGEND

× × Nucleation Points

——— Nucleation Zone

○ ○ Base Case Nucleation Point

Figure 4-23. Rupture surface of the M 7.3 Charleston earthquake (100 km x 20 km) showing nucleation zone and 30 random nucleation points.

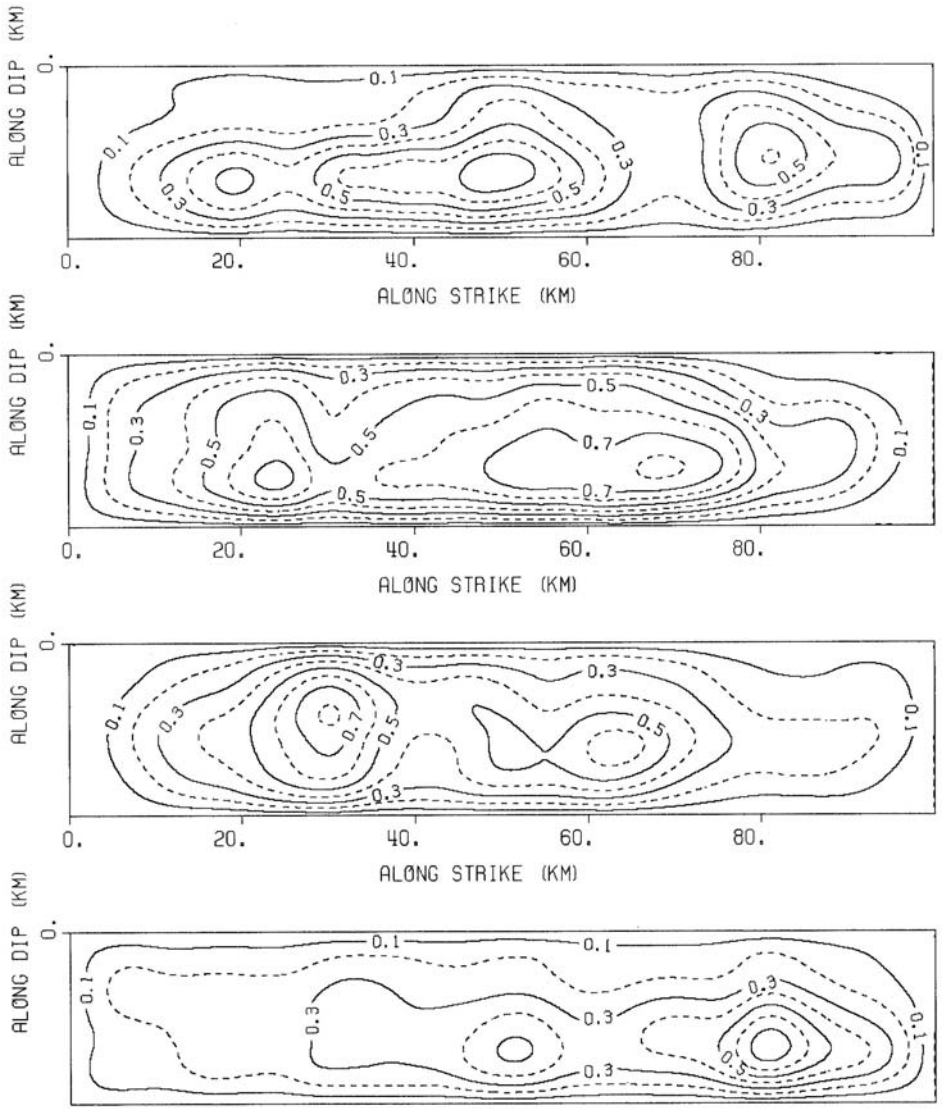

Note: Slip is normalized by the peak with the average slip of about 1.5m.

Figure 4-24. Example suite of four (total of 30) random slip models for the M 7.3 Charleston earthquake scenario.

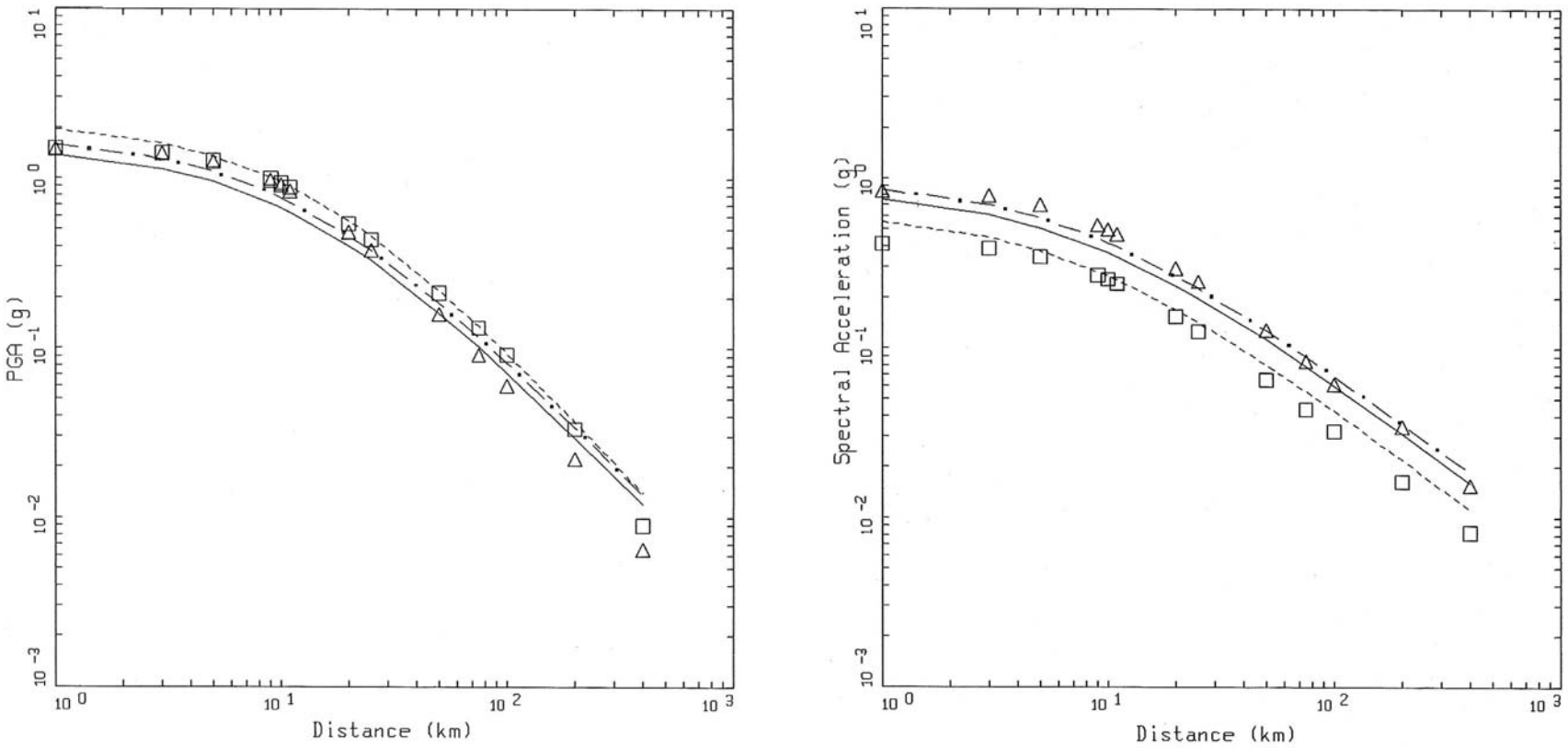

(a) Peak horizontal acceleration

(b) 1.0 sec spectral acceleration

LEGEND

5 % Single-Corner Variable Stress Drop

5 % Single-Corner Constant Stress Drop

5 % Double-Corner Constant Stress Drop

5 % Toro et al. (1997)

5 % Atkinson and Boore (1997)

Figure 4-25. Comparison of single-corner frequency variable and constant stress drop and double-corner frequency attenuation models for peak acceleration and M 7.3 (Appendix A). Also shown are the generic CEUS hard rock relations of Atkinson and Boore (1997) and Toro et al. (1997).

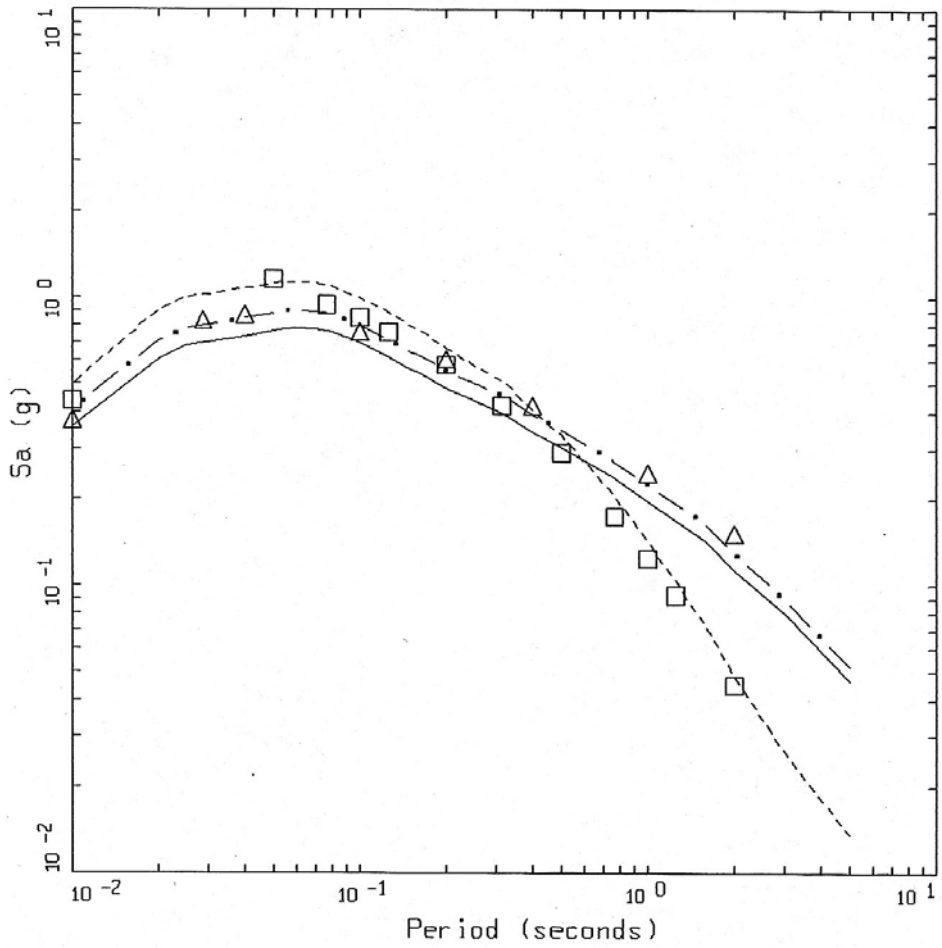

LEGEND

5 % Single-Corner Variable Stress Drop

5 % Single-Corner Constant Stress Drop

5 % Double-Corner Constant Stress Drop

5 % Toro et al. (1997)

5 % Atkinson and Boore (1997)

Figure 4-26. Comparison of single-corner frequency variable and constant stress drop and double-corner frequency attenuation models, 5% damped response spectra at a distance of 25 km for M 7.3 from Figure 4-25 (Appendix A). Also shown are the generic CEUS hard rock relations of Atkinson and Boore (1997) and Toro et al. (1997).

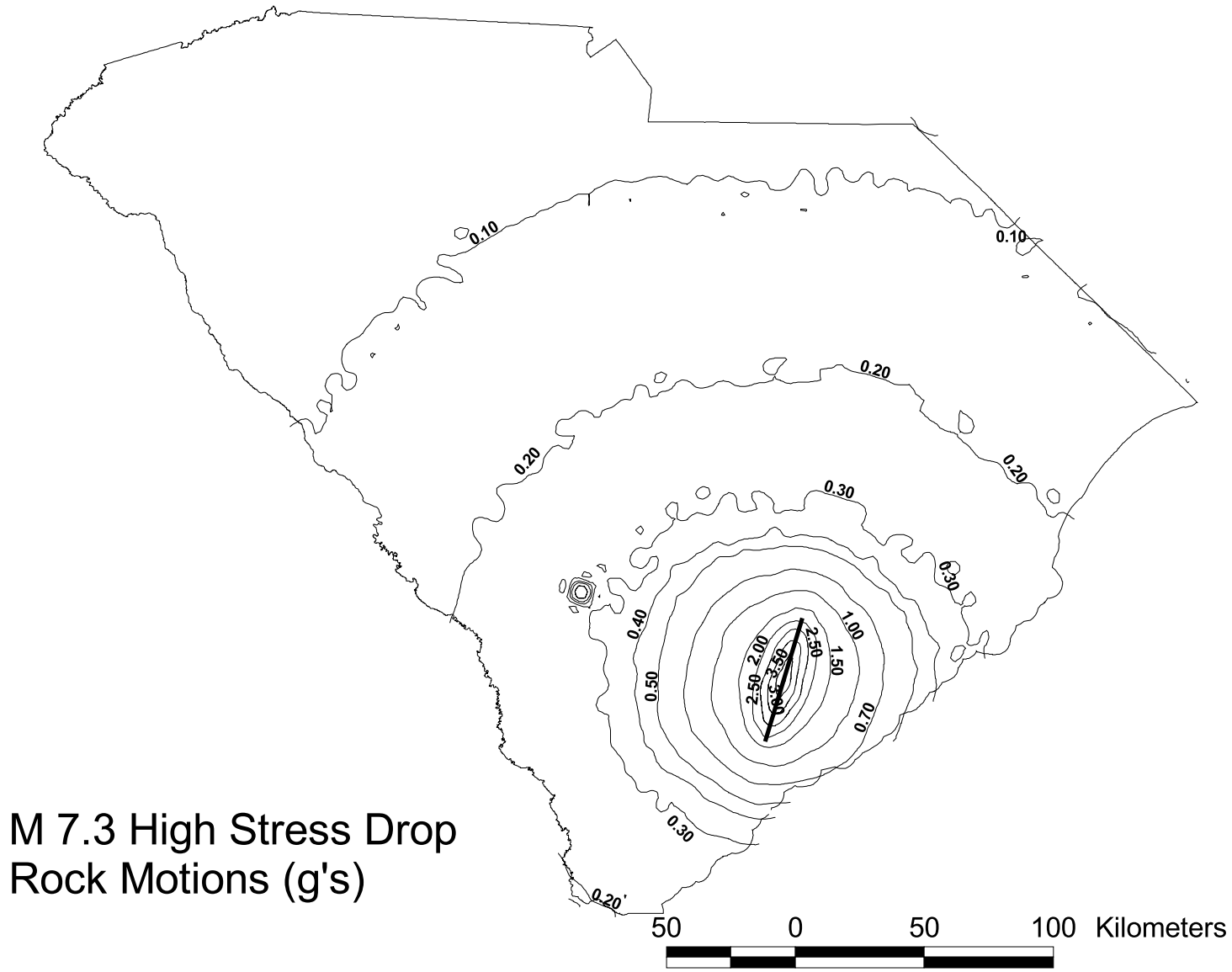

Figure 4-27a. Unsmoothed Scenario Ground Motions on Rock for a M 7.3 Charleston Earthquake, High Stress Drop.

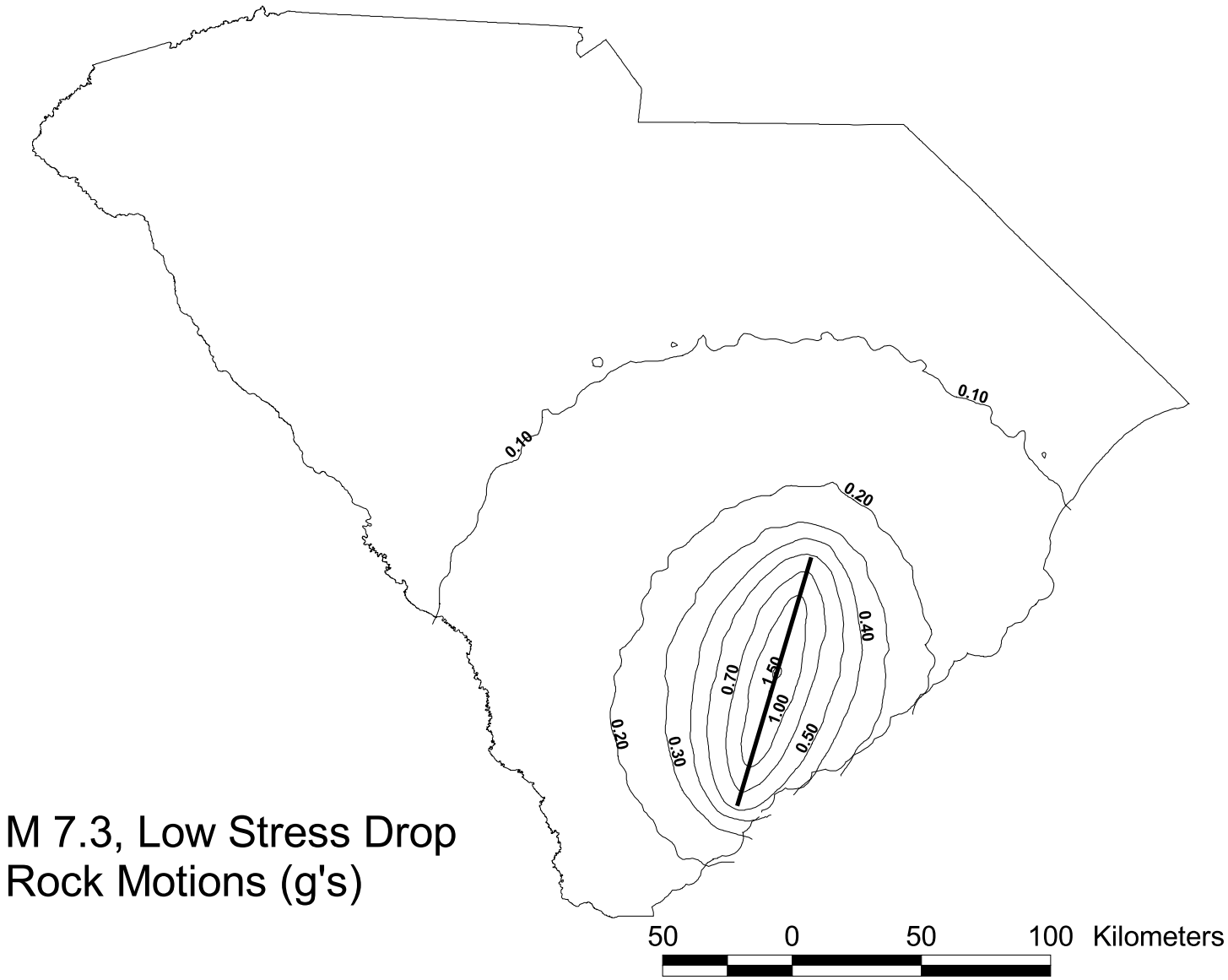

Figure 4-27b. Unsmoothed Scenario Ground Motions on Rock for a M 7.3 Charleston Earthquake, Low Stress Drop.

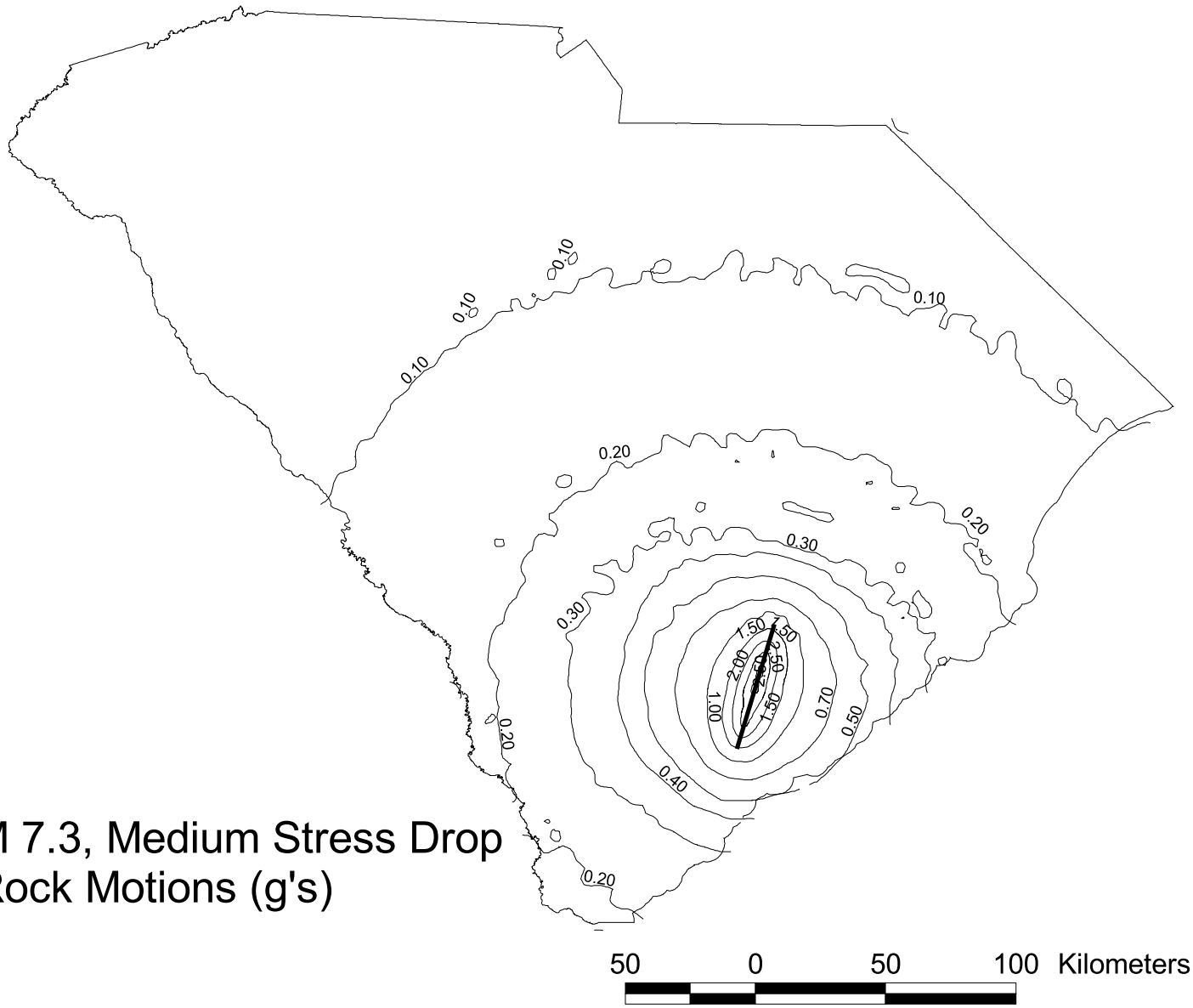

Figure 4-27c. Unsmoothed Scenario Ground Motions on Rock for a M 7.3 Charleston Earthquake, Medium Stress Drop.

Figure 4-27d. Scenario Ground Motions for a M 7.3 Charleston Earthquake, Peak Horizontal Acceleration (g) at the Ground Surface.

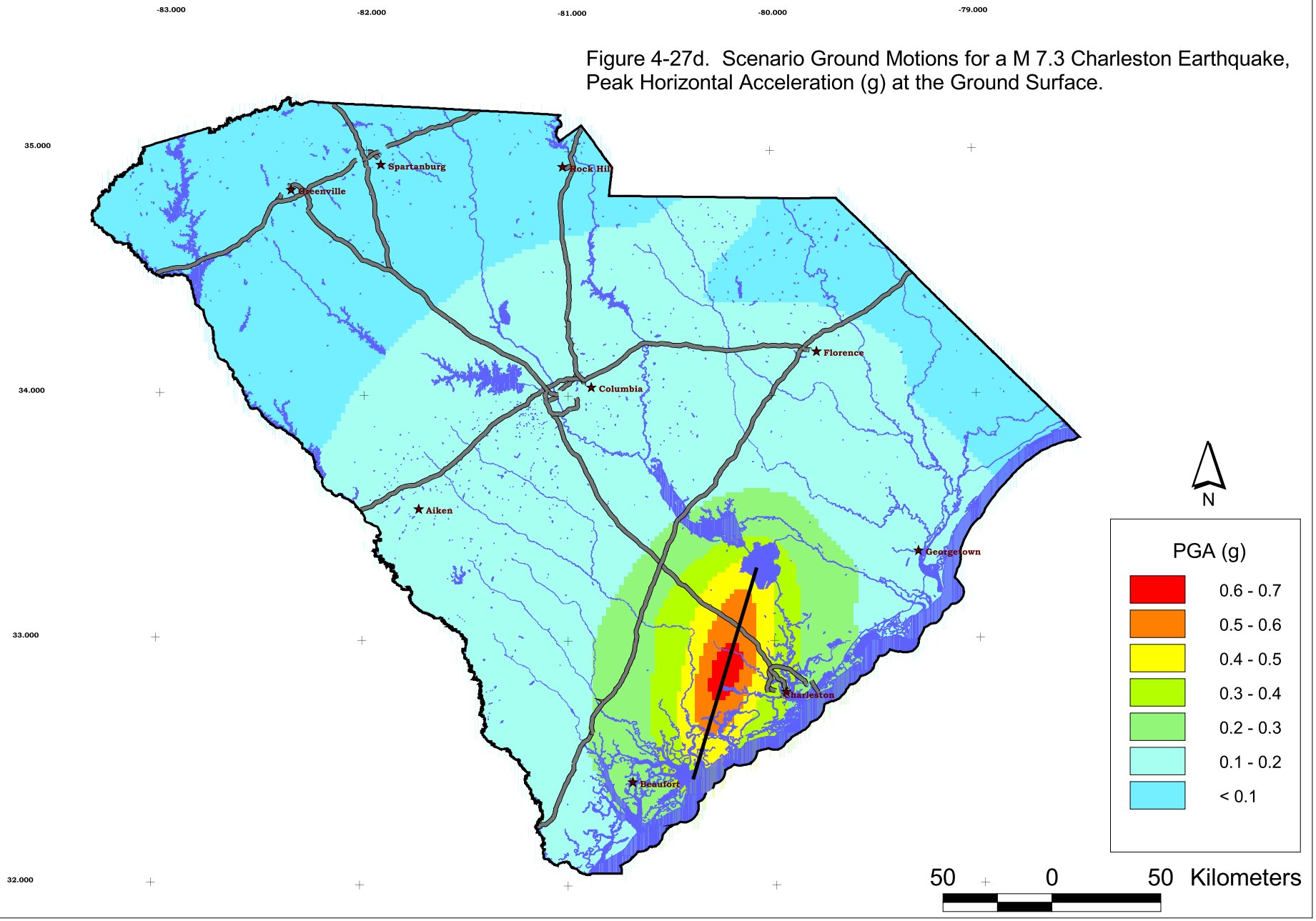

Figure 4-27e. Scenario Ground Motions for a M 7.3 Charleston Earthquake, 84th Percentile Peak Horizontal Acceleration (g) at the Ground Surface.

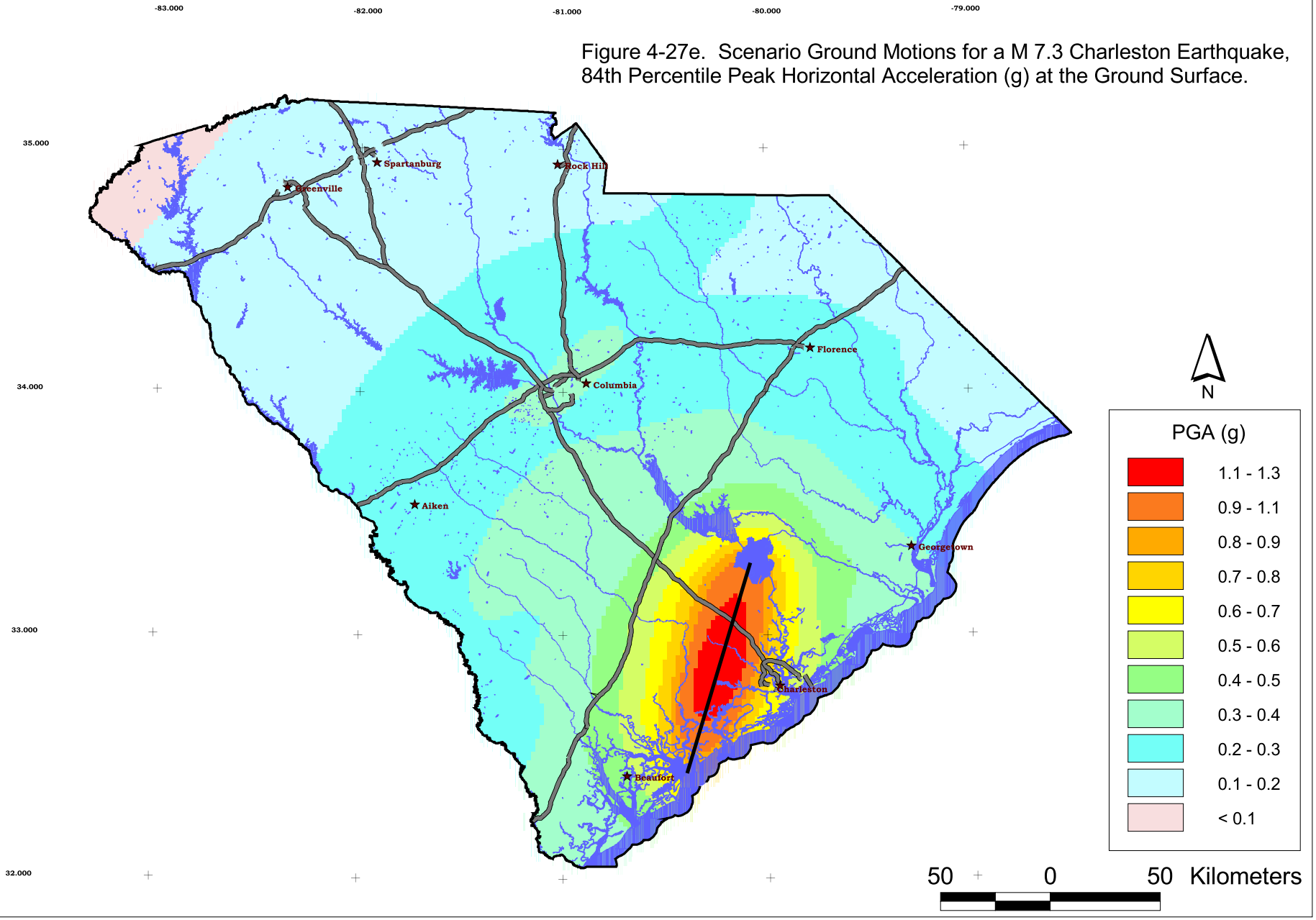

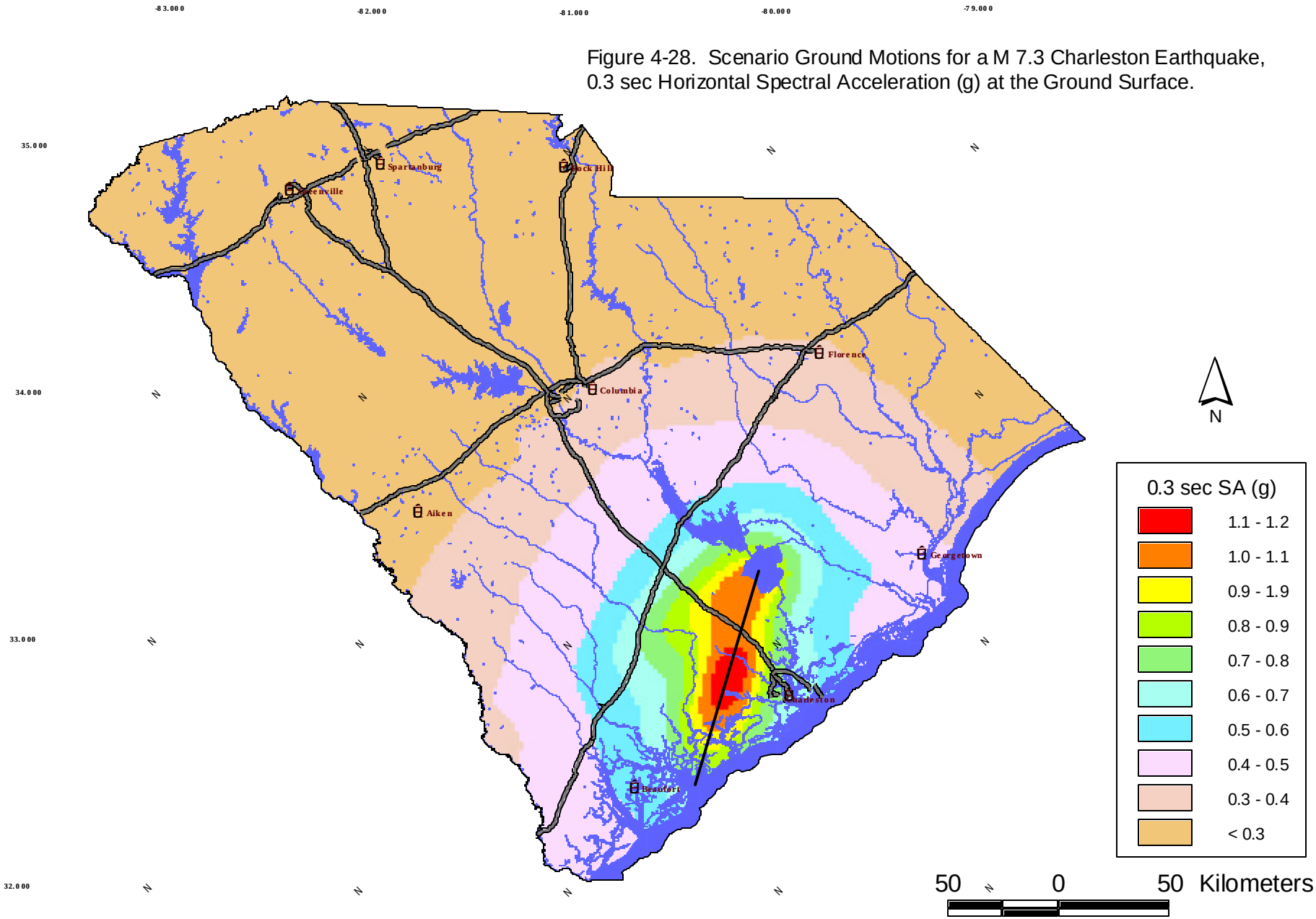

Figure 4-28. Scenario Ground Motions for a M 7.3 Charleston Earthquake, 0.3 sec Horizontal Spectral Acceleration (g) at the Ground Surface.

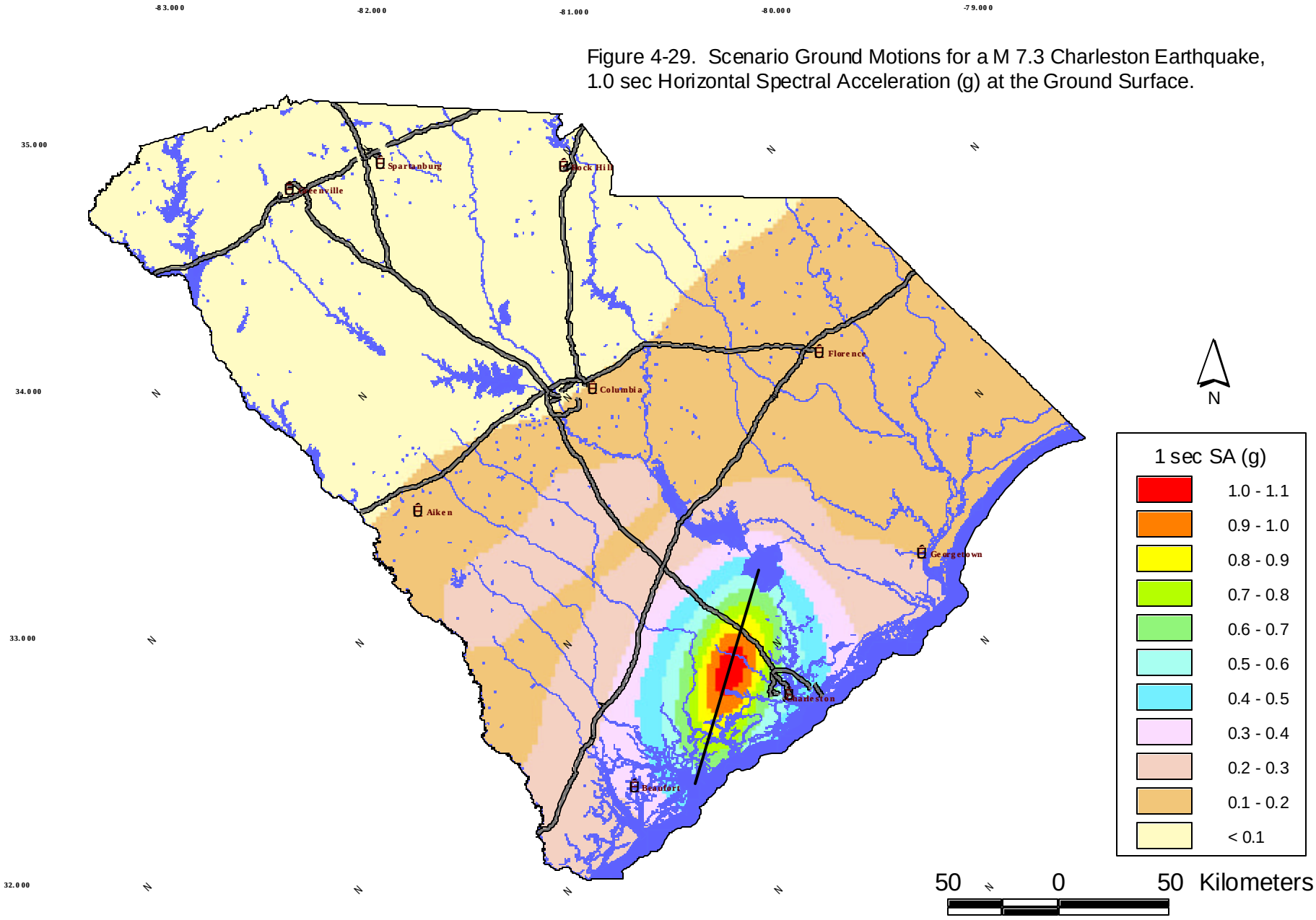

Figure 4-29. Scenario Ground Motions for a M 7.3 Charleston Earthquake, 1.0 sec Horizontal Spectral Acceleration (g) at the Ground Surface.

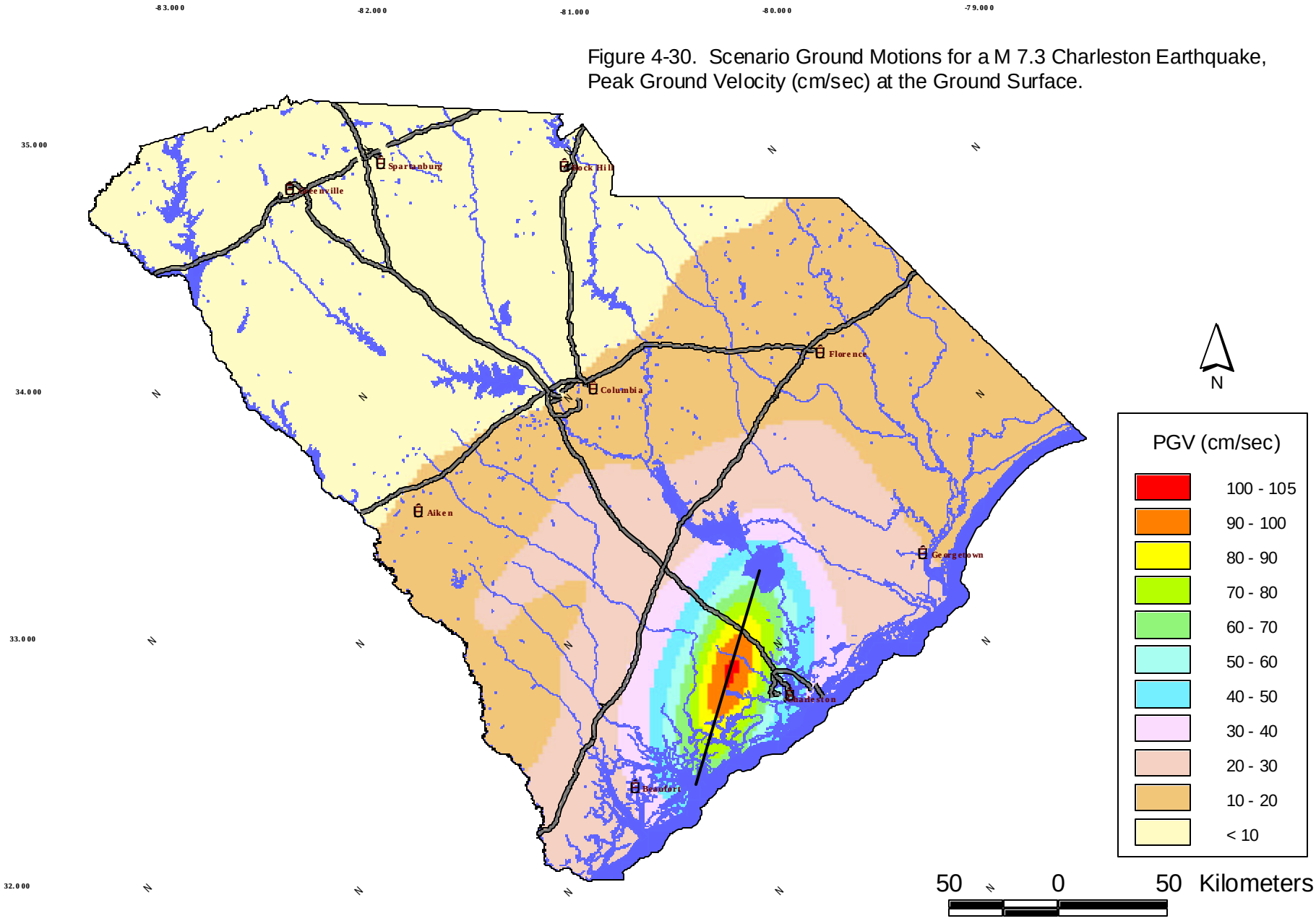

Figure 4-30. Scenario Ground Motions for a M 7.3 Charleston Earthquake, Peak Ground Velocity (cm/sec) at the Ground Surface.

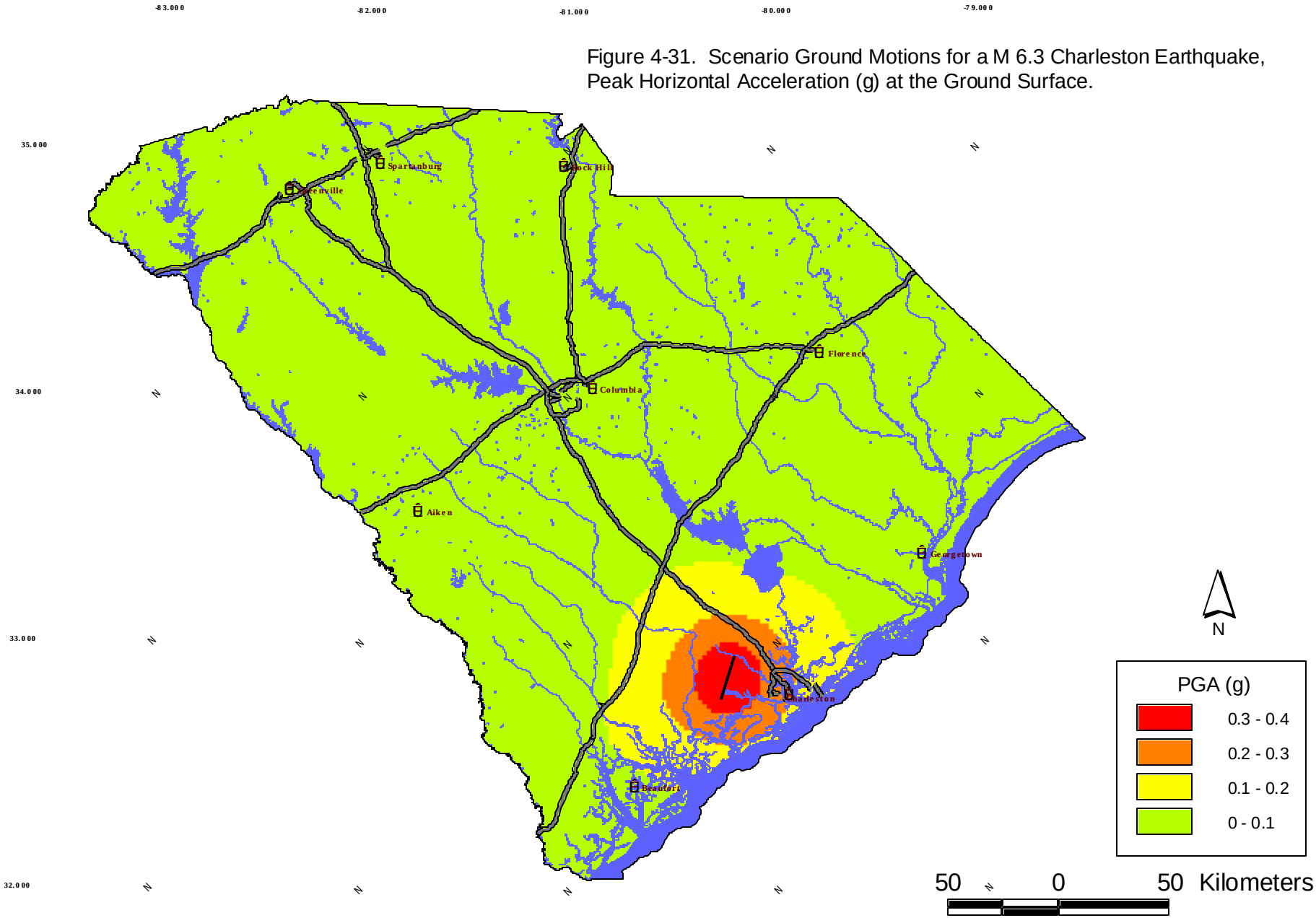

Figure 4-31. Scenario Ground Motions for a M 6.3 Charleston Earthquake, Peak Horizontal Acceleration (g) at the Ground Surface.

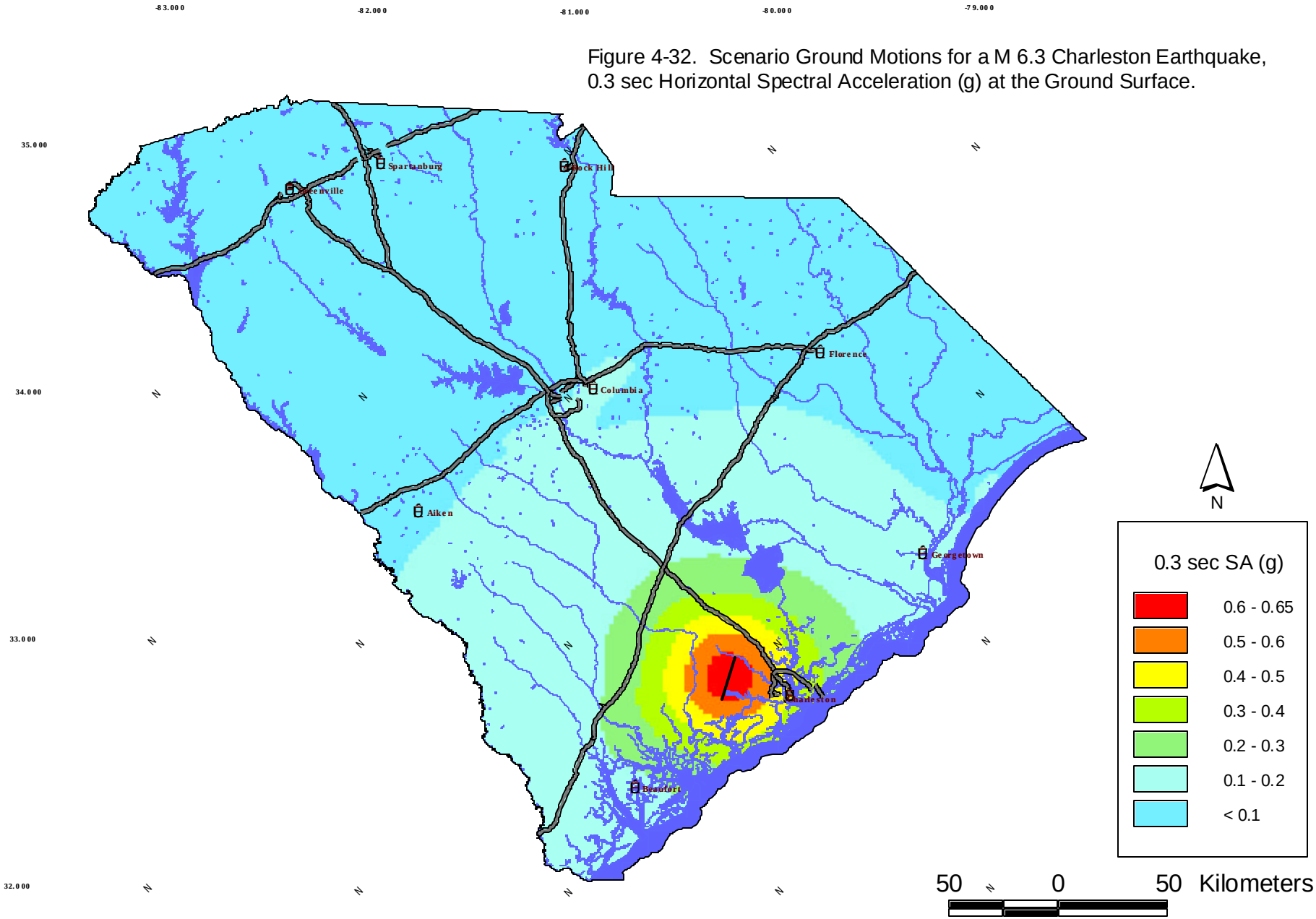

Figure 4-32. Scenario Ground Motions for a M 6.3 Charleston Earthquake, 0.3 sec Horizontal Spectral Acceleration (g) at the Ground Surface.

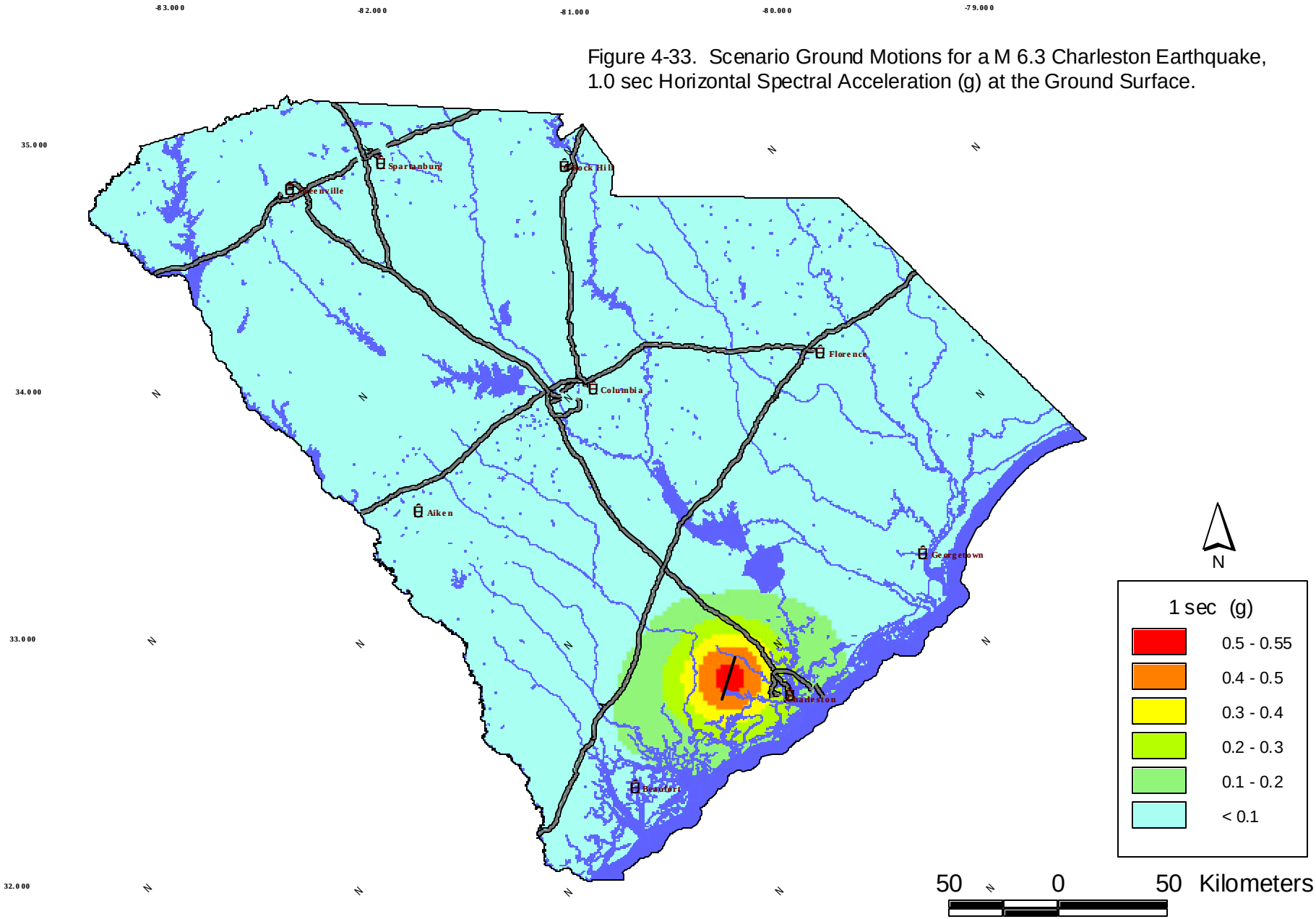

Figure 4-33. Scenario Ground Motions for a M 6.3 Charleston Earthquake, 1.0 sec Horizontal Spectral Acceleration (g) at the Ground Surface.

Figure 4-34. Scenario Ground Motions for a M 6.3 Charleston Earthquake, Peak Ground Velocity (cm/sec) at the Ground Surface.

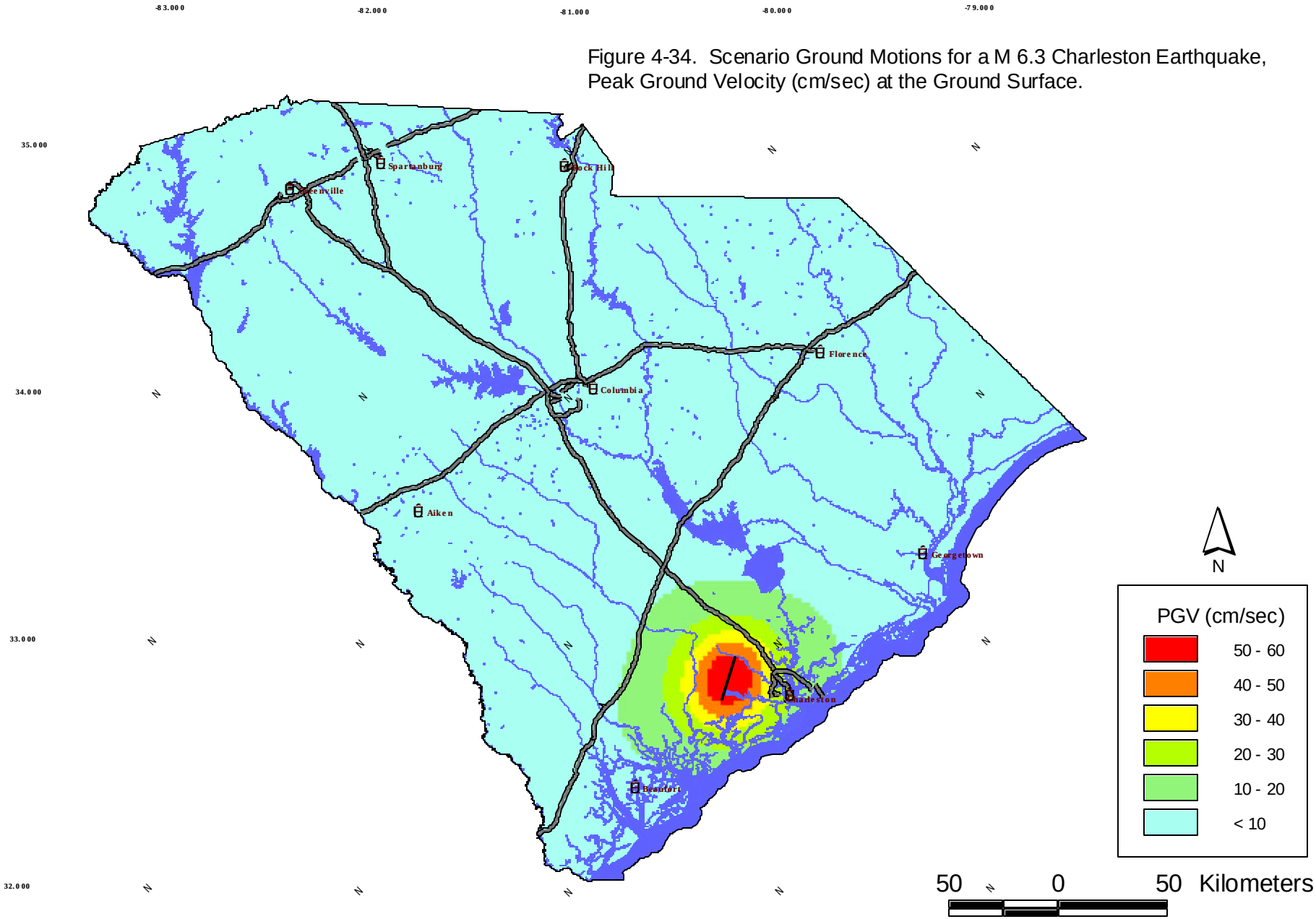

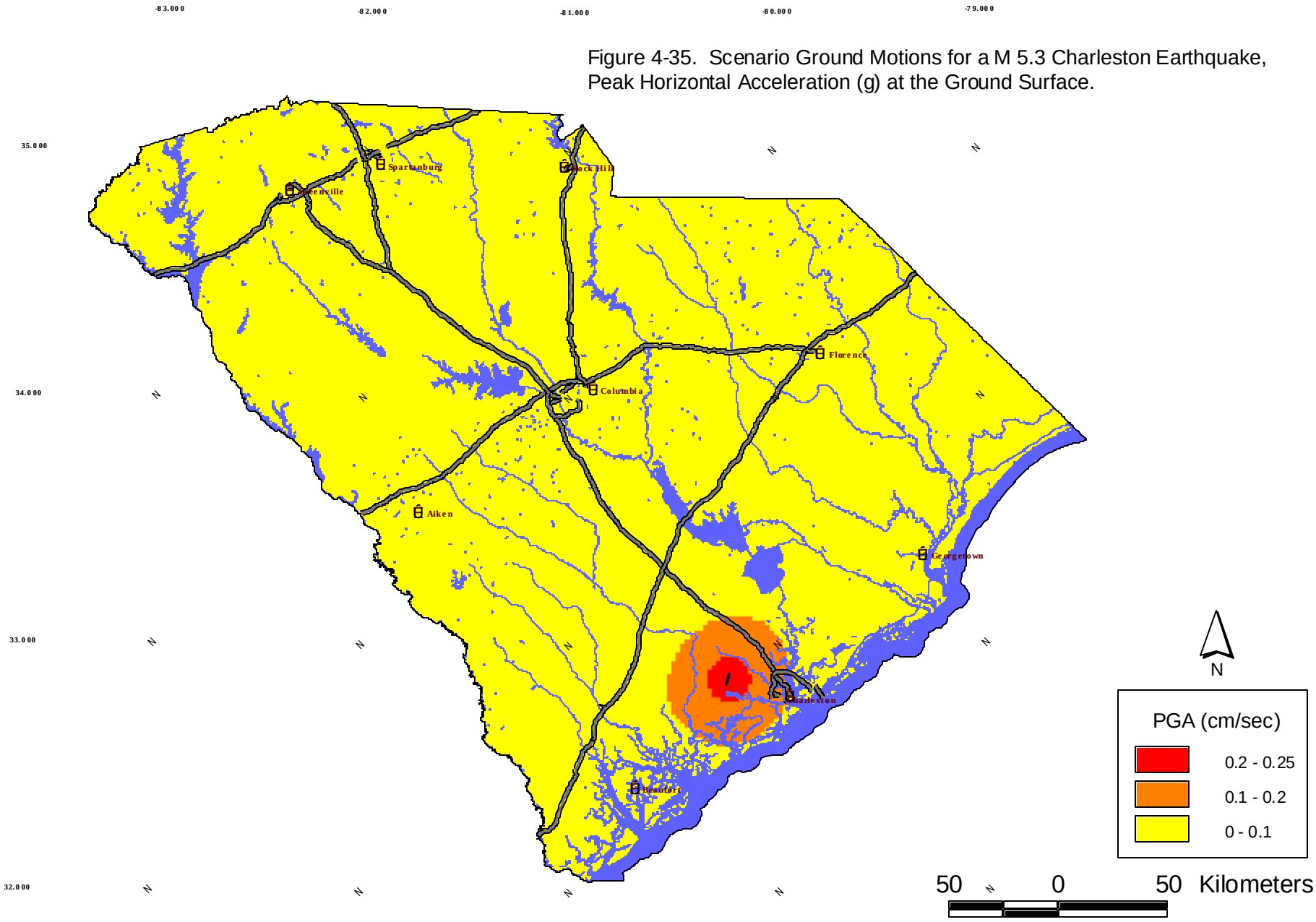

Figure 4-35. Scenario Ground Motions for a M 5.3 Charleston Earthquake, Peak Horizontal Acceleration (g) at the Ground Surface.

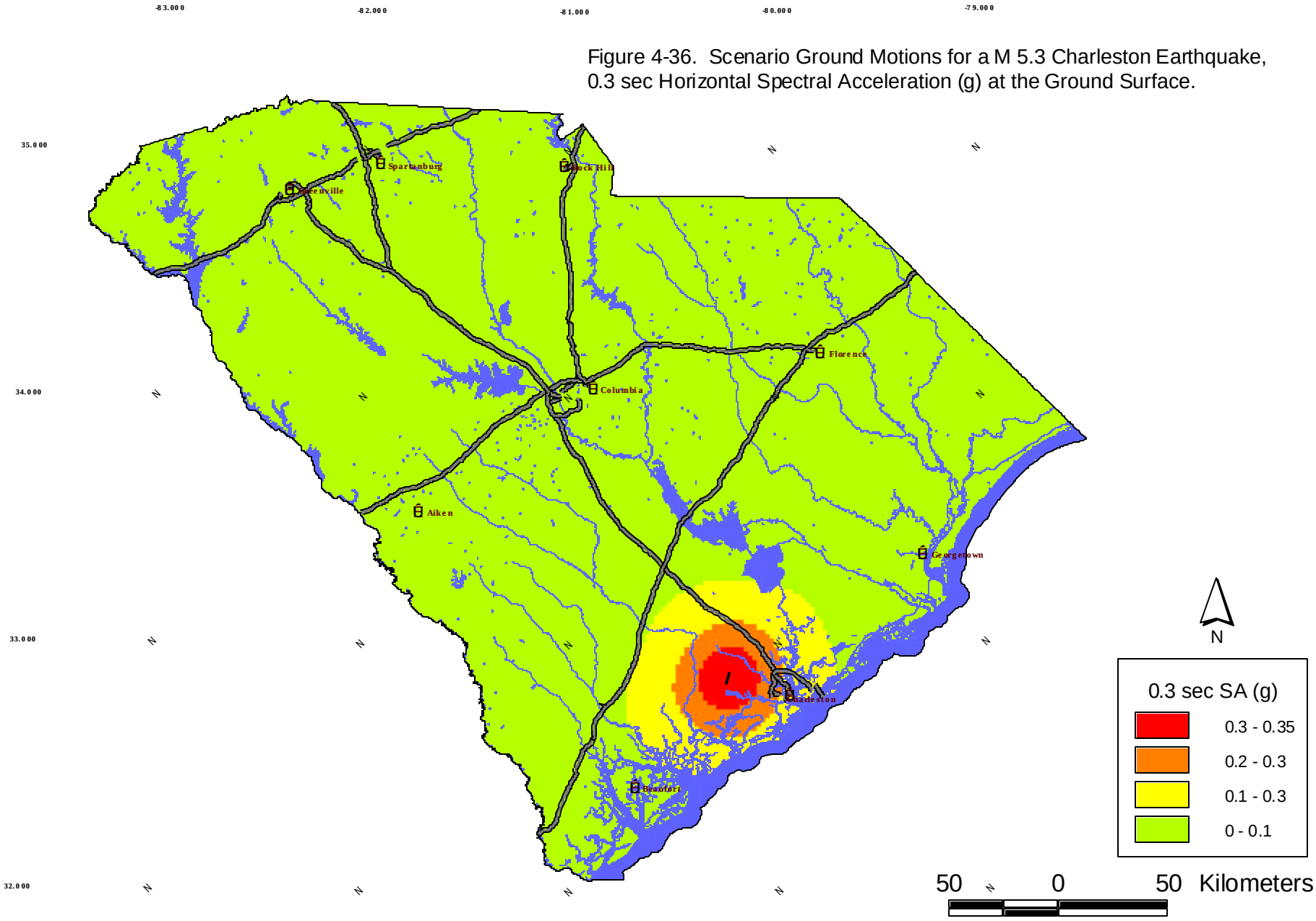

Figure 4-36. Scenario Ground Motions for a M 5.3 Charleston Earthquake, 0.3 sec Horizontal Spectral Acceleration (g) at the Ground Surface.

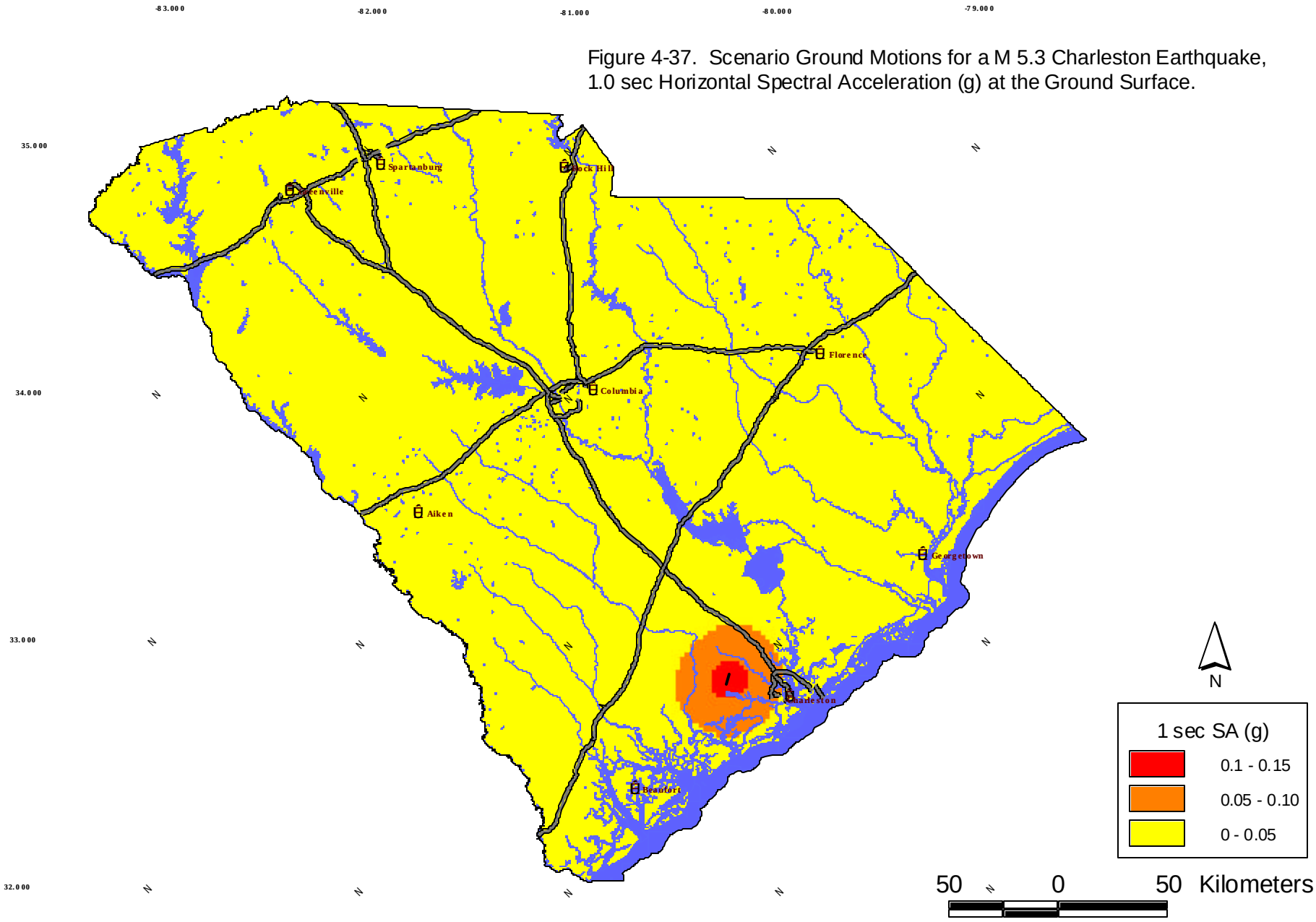

Figure 4-37. Scenario Ground Motions for a M 5.3 Charleston Earthquake, 1.0 sec Horizontal Spectral Acceleration (g) at the Ground Surface.

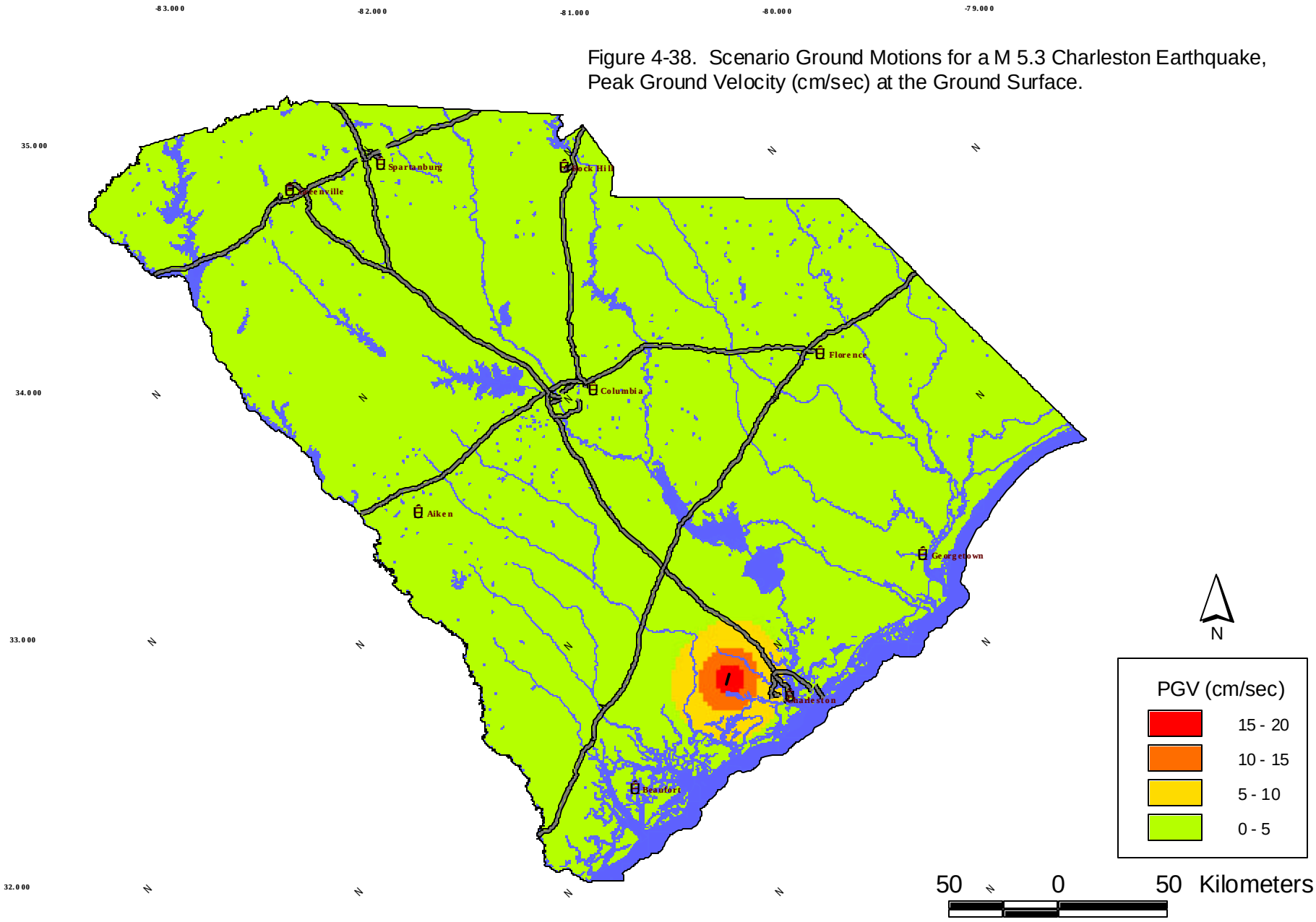

Figure 4-38. Scenario Ground Motions for a M 5.3 Charleston Earthquake, Peak Ground Velocity (cm/sec) at the Ground Surface.

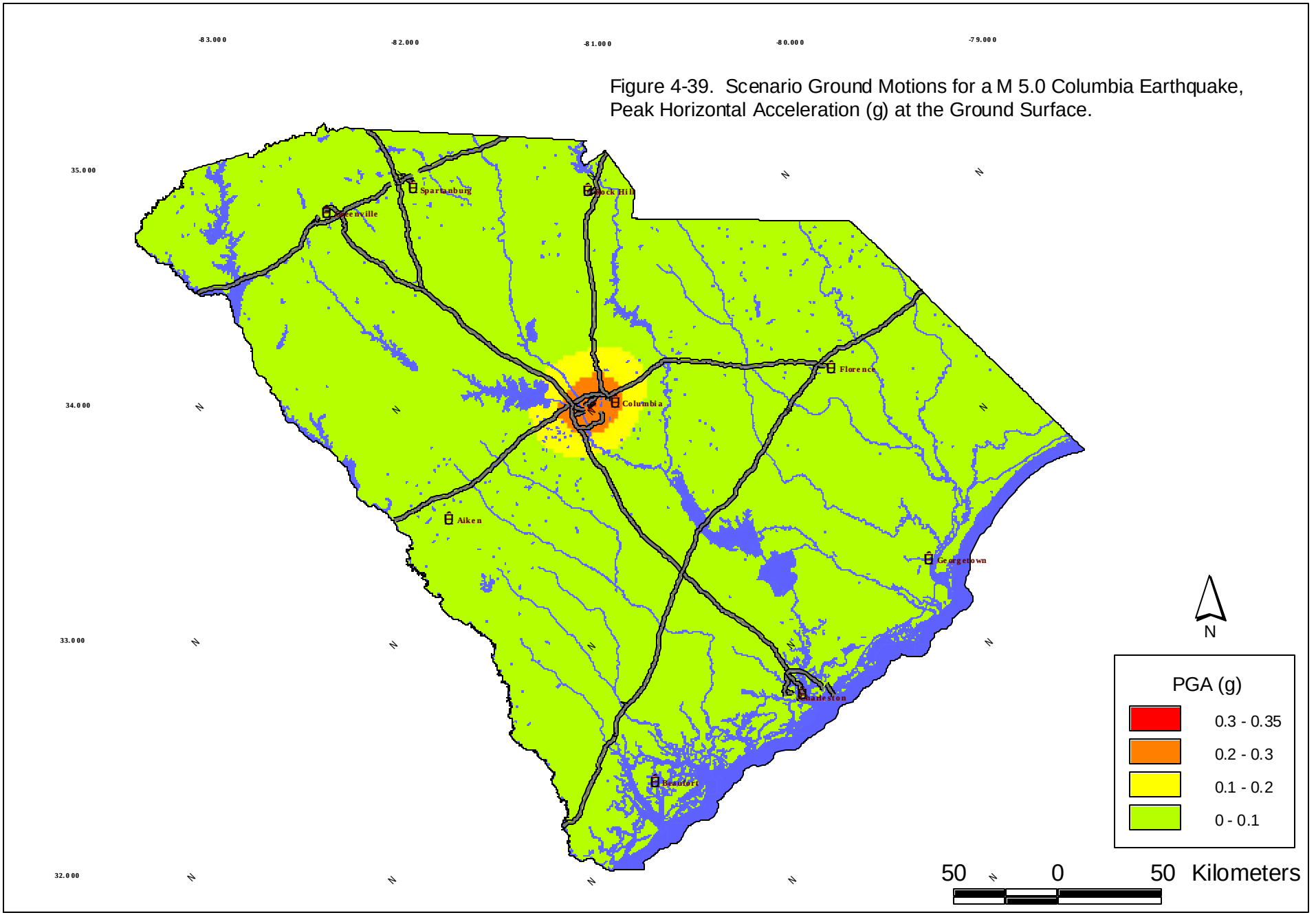

Figure 4-39. Scenario Ground Motions for a M 5.0 Columbia Earthquake, Peak Horizontal Acceleration (g) at the Ground Surface.

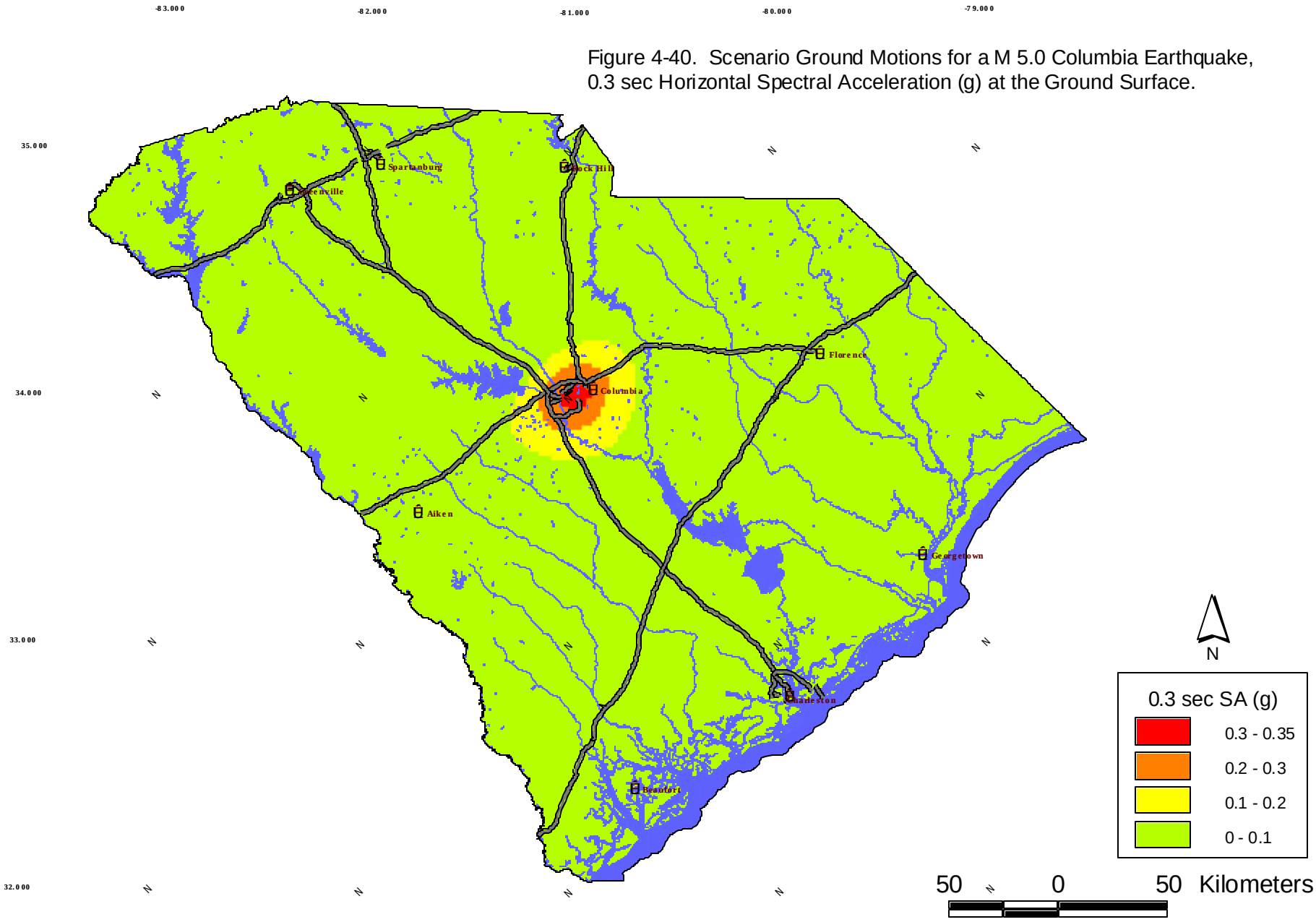

Figure 4-40. Scenario Ground Motions for a M 5.0 Columbia Earthquake, 0.3 sec Horizontal Spectral Acceleration (g) at the Ground Surface.

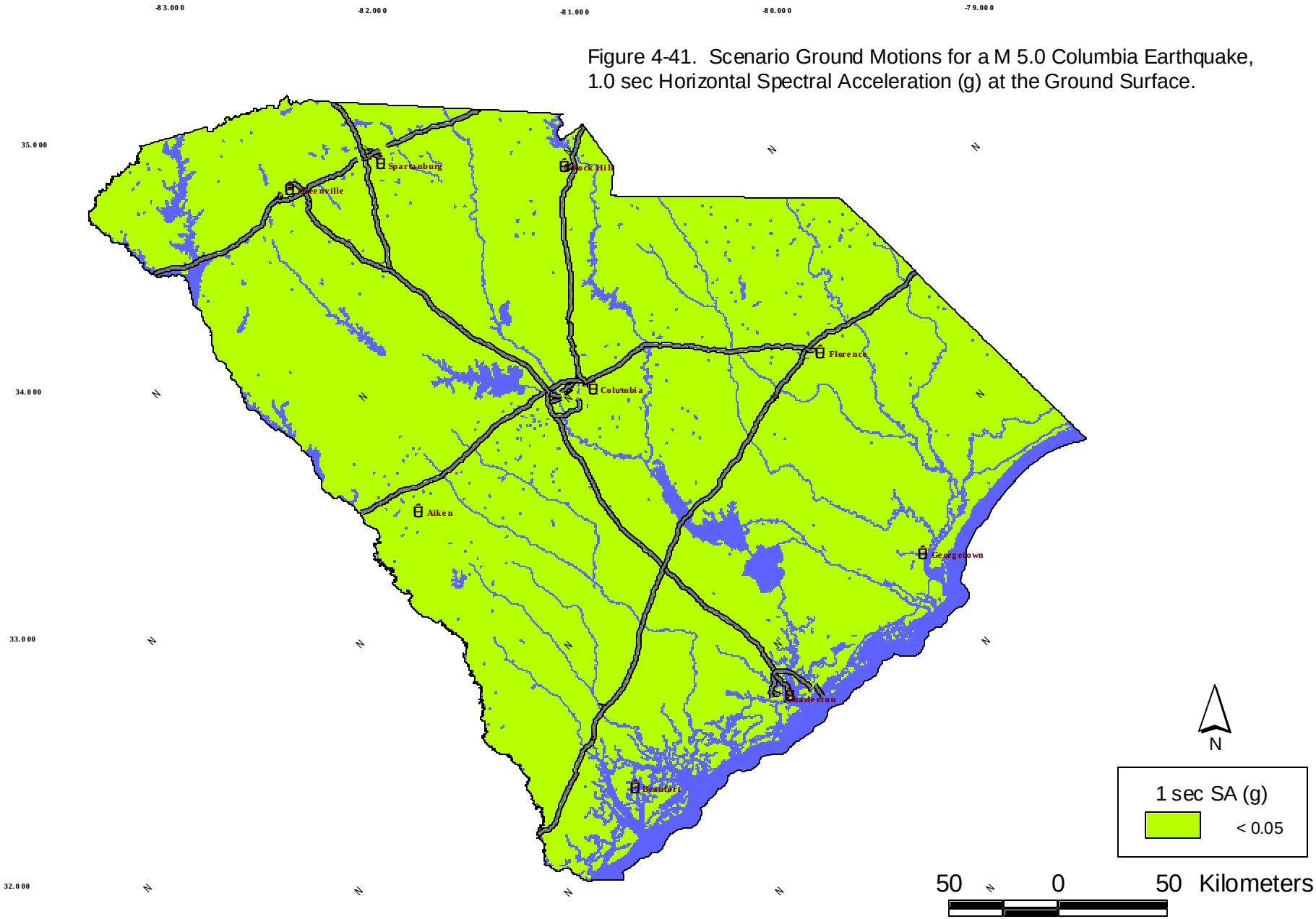

Figure 4-41. Scenario Ground Motions for a M 5.0 Columbia Earthquake, 1.0 sec Horizontal Spectral Acceleration (g) at the Ground Surface.

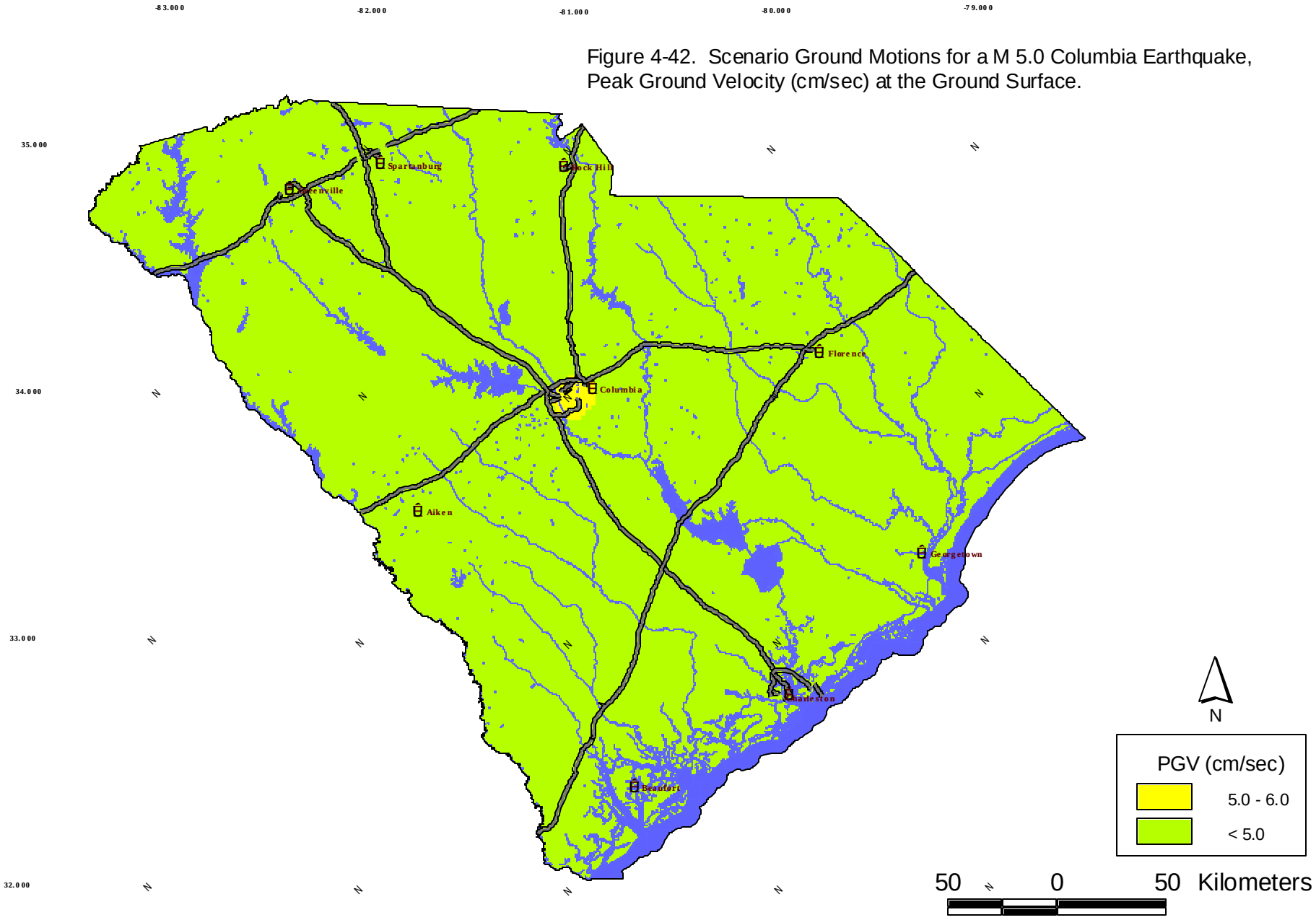

Figure 4-42. Scenario Ground Motions for a M 5.0 Columbia Earthquake, Peak Ground Velocity (cm/sec) at the Ground Surface.

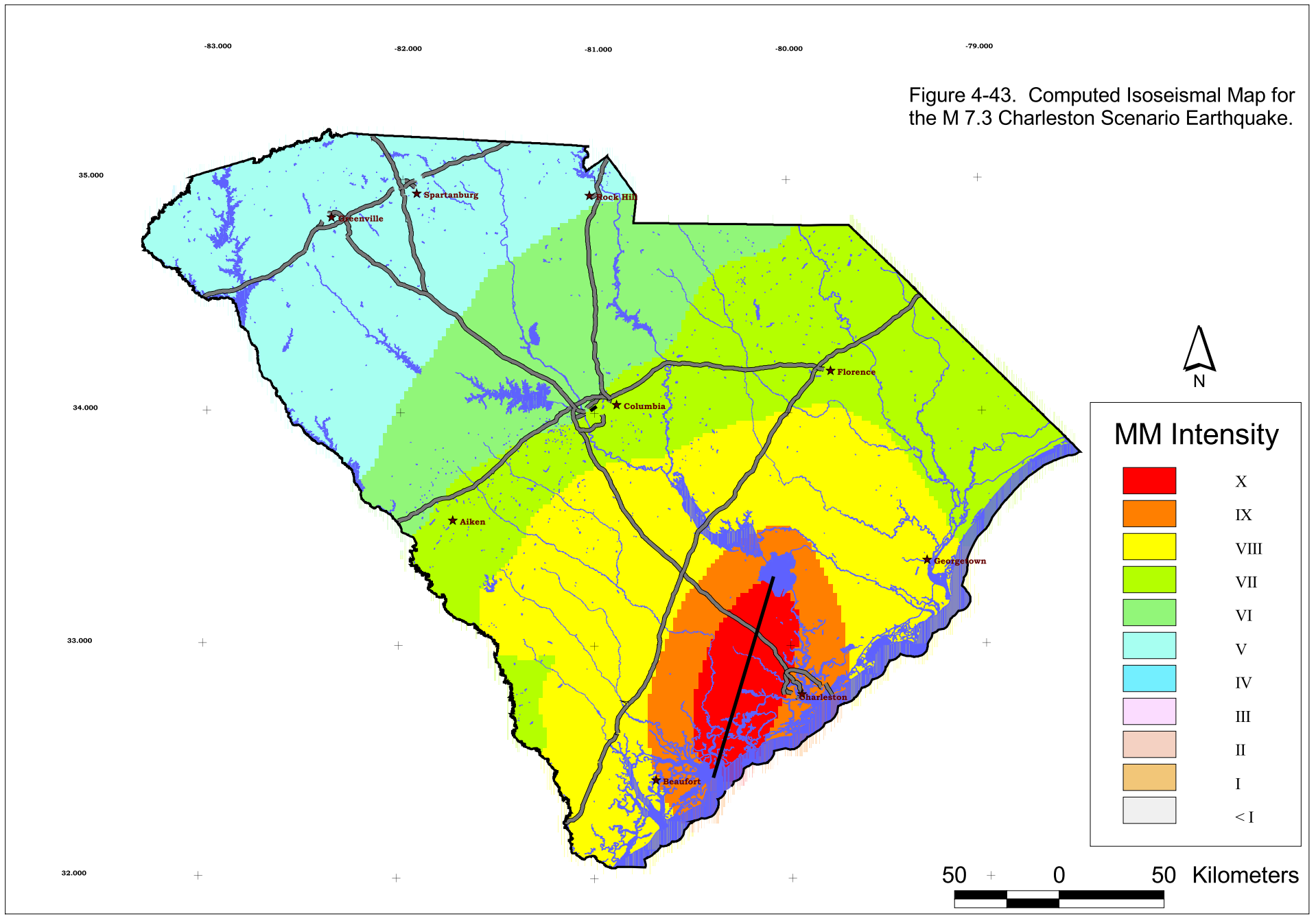

Figure 4-43. Computed Isoseismal Map for the M 7.3 Charleston Scenario Earthquake.

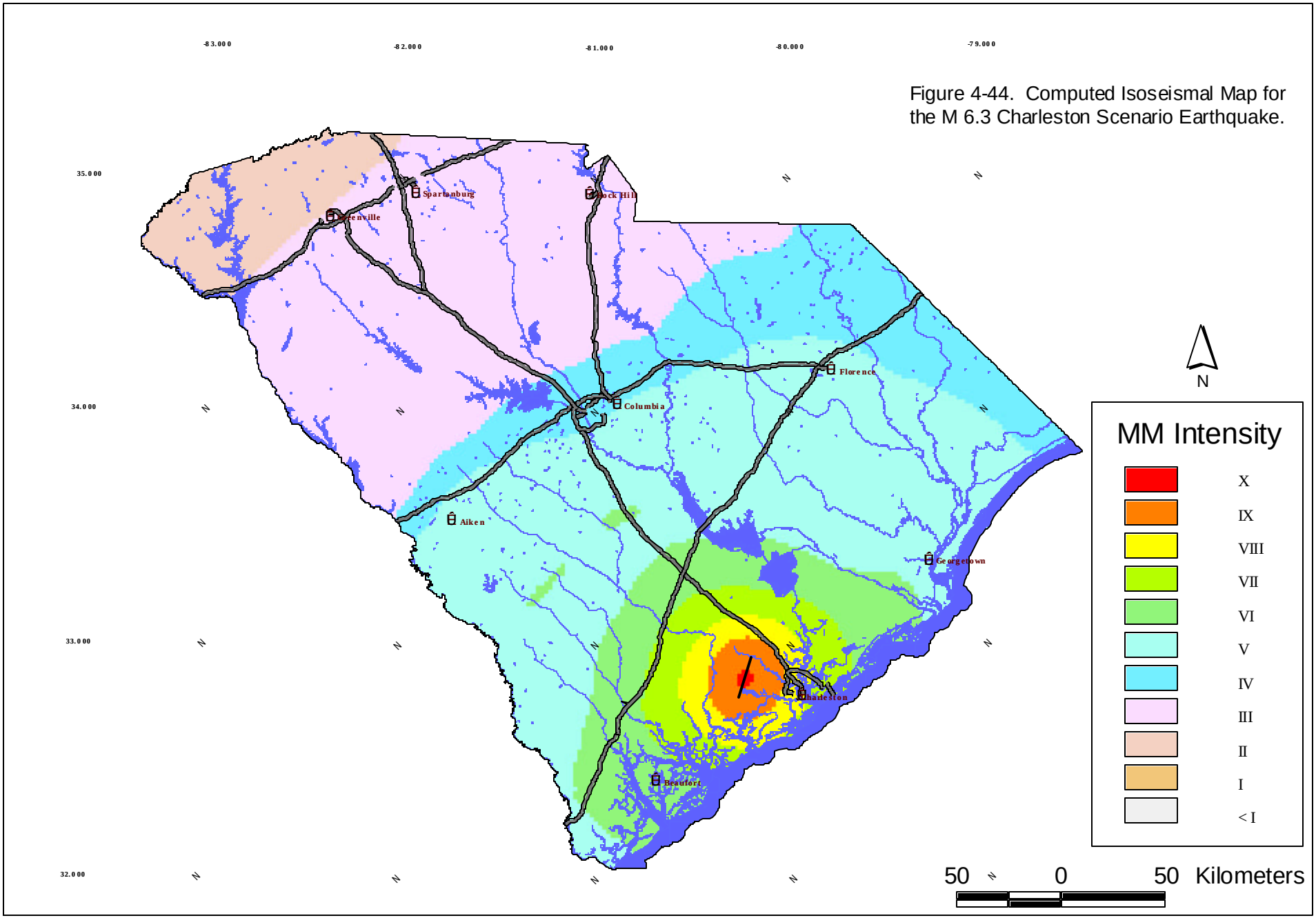

Figure 4-44. Computed Isoseismal Map for the M 6.3 Charleston Scenario Earthquake.

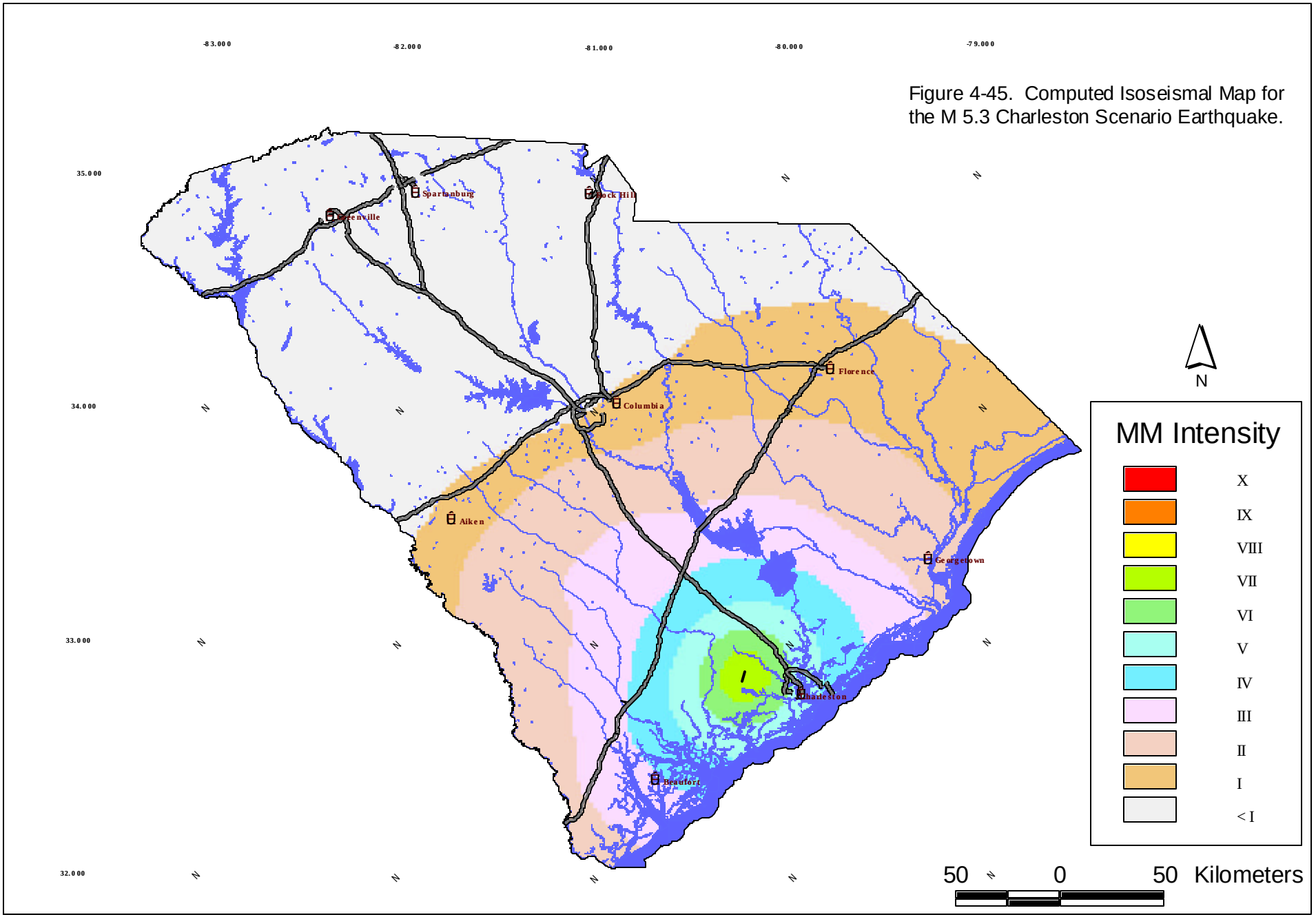

Figure 4-45. Computed Isoseismal Map for the M 5.3 Charleston Scenario Earthquake.

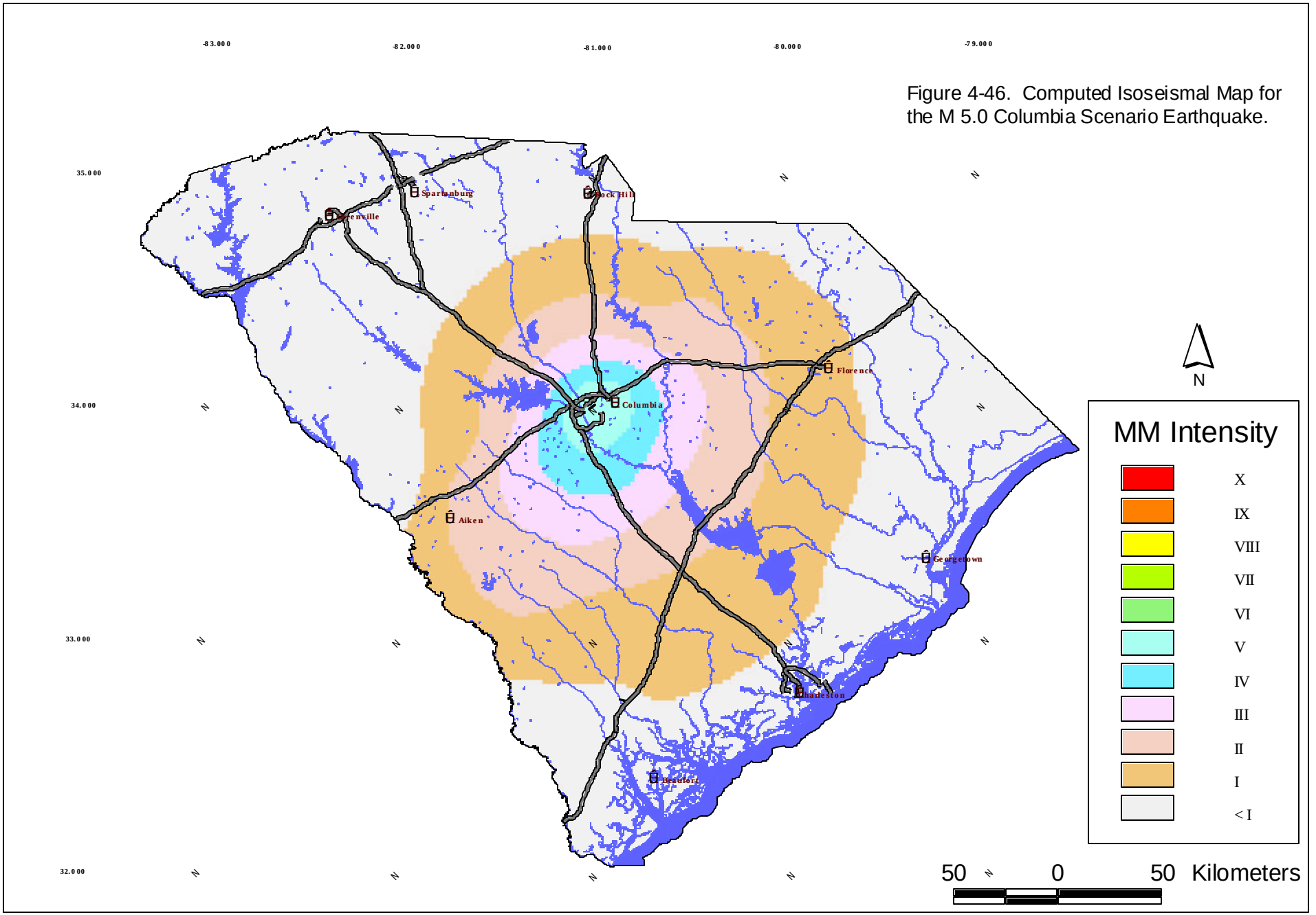

Figure 4-46. Computed Isoseismal Map for the M 5.0 Columbia Scenario Earthquake.

In this section, we describe our evaluations of the potential for liquefaction and landsliding in the State as a result of the four earthquake scenarios considered in this study. The results of these evaluations are used by HAZUS to estimate damage and other related factors (e.g., replacement costs) for lifelines and essential facilities (Section 7), hazardous materials facilities (Section 8), and dams (Section 9). The results were also used to prepare maps showing the probability and factor of safety against liquefaction for each earthquake scenario. The maps may be used to identify areas with greater or lower risks of damage from liquefaction.

5.1 LIQUEFACTION

Liquefaction is a soil behavior phenomenon in which a saturated sand softens and loses strength due to the development of high excess pore pressures during strong earthquake ground shaking (Seed and Idriss, 1971; Silver and Seed, 1971). Post-earthquake observations indicate that silts, sands, and gravels can experience settlement and lateral spread during and immediately following liquefaction. Recent earthquakes such as the **M** 7.6 Chi-Chi Taiwan; **M** 7.5 Koaceli, Turkey; **M** 6.9 Kobe, Japan; **M** 6.7 Northridge; and **M** 6.9 Loma Prieta have resulted in hundreds of billions of dollars of damage and years of reconstruction with much of the loss attributed to liquefaction-related effects. Figures 5-1 and 5-2 are of pavement and building damage, respectively, resulting directly from liquefaction of underlying soils during strong earthquakes. In South Carolina, relic liquefaction features suggest that a reoccurrence of the 1886 Charleston earthquake could result in liquefaction over a significant portion of the Coastal Plain. As part of the HAZUS study, the liquefaction potential for South Carolina was evaluated based on the general site conditions developed in Task 3.

The initial step in the liquefaction evaluation is identifying soils that are susceptible to liquefaction. Youd and Perkins (1978) categorized the susceptibility of soils according to age and depositional environment. In general, older soils have a lower potential for liquefaction. In fact, essentially all documented liquefaction has occurred within soils of Pleistocene age or younger. Thus, residuum derived by the weathering of the Paleozoic bedrock may be considered to have a negligible potential for liquefaction. Based on this, the potential for liquefaction-induced settlement and lateral spread for this study is considered negligible in the residual soils of the Piedmont and Blue Ridge provinces of South Carolina.

Other surficial soils within the Piedmont and Blue Ridge Provinces of South Carolina, most notably alluvium and man-placed fill, were also considered non-liquefieable. The following conclusions were made that support the appropriateness of excluding them from this general study. Alluvium deposits in the upstate of South Carolina are limited in width due to the narrow river basins associated with both the Piedmont and Blue Ridge provinces. Dams in these rivers have resulted in flooding of lower-lying alluvium, thus further reducing the exposed alluvium to a spatial resolution level significantly finer than used in this study. Similarly, the mapping of fill would also require a significantly finer resolution than used for this study, as well as a greatly expanded scope of work to identify fill in the field. In most cases, fill in the upstate is placed above the water table, and therefore, no risk of liquefaction will exist in those fills. Overall, it is for these reasons that it was considered appropriate to exclude non-residual soils in the consideration of liquefaction potential for the Piedmont and Blue Ridge. For evaluation of individual sites in this part of South Carolina, a site-specific study would be appropriate to

determine if the risk of liquefaction is increased due to underlying saturated alluvium and/or fill, if present.

For the Coastal Plain of South Carolina, younger sediments, including deposits considered man-placed fill, recent alluvium and Pleistocene sediments, are exposed at the ground surface. Research in the Coastal Plain has documented extensive evidence of liquefaction within these younger soils (Cox and Talwani, 1983; Cox, 1984; Obermeier *et al.*, 1987; Elton and Hadj-Hamou, 1988; Martin and Clough, 1990; Rajendran and Talwani, 1993; Shaeffer, 1996). The liquefaction evidence primarily consists of observed sandblows (also known as sandboils). Sandblows are created when a buried liquefied sand erupts to the ground surface during or immediately after an earthquake. The process of a sandblow creates a vertical column of sand through overburden soil and also creates a depression or craterlet in the ground surface as pore pressures dissipate. Figure 5-3 is a craterlet from the 1886 Charleston earthquake.

The first field research of paleoliquefaction features in South Carolina was conducted by Cox (1984) and this effort led to the discovery of a sandblow approximately 40 km west of Charleston. Since 1984, a total of 54 sandblows have been identified in coastal South Carolina extending from Myrtle Beach to across the Georgia state line near Savannah (Talwani and Schaeffer, 2001). It is recognized that not all of the documented paleoliquefaction features result from earthquakes associated with the Charleston source zone.

5.2 LIQUEFACTION RISK IN COASTAL PLAIN SEDIMENTS

The evaluation of a soil's resistance to liquefaction involves the estimation of both the capacity to resist liquefaction as well as the demand placed on the soil by ground shaking (Youd and Idriss, 2001).

5.2.1 Resistance to Liquefaction

The default approach in HAZUS is to assign the soil's resistance to liquefaction based on the surficial geology according to the risk levels assigned for different geologic conditions given by Youd and Perkins (1978). The soil demands in HAZUS are estimated using expected peak horizontal acceleration at the soil surface, a simplified approach using generic parameters introduced by Seed and Idriss (1971). As a refinement to the HAZUS default, consideration was given to adapting accepted engineering practice for determining site-specific liquefaction resistance. Site-specific evaluation of liquefaction resistance involves use of empirical correlations between the observed occurrence of liquefaction and the results of field measurements. Accepted field measurements include the standard penetration test (Seed and Idriss, 1971; Seed *et al.*, 1976; Seed and Idriss, 1982; and Seed *et al.*, 1983), the cone penetration test (Robertson and Campanella, 1985), and shear-wave velocity measurements (Andrus and Stokoe, 2000). All of these field measurements provide an indication of the soil's relative density. Relative density along with saturation conditions, effective stress, and grain size determine the soil's resistance to liquefaction, in terms of a cyclic resistance ratio (CRR).

For this study, the CRR for the soils in the Coastal Plain was determined using the shear-wave velocity profiles developed in Task 3 and the estimated fines content (i.e., content of soil particles smaller than the 0.075 mm) shown in Table 5-1. The shear-wave velocity profiles are

based on actual data from South Carolina, and thus, their use is considered a refinement in comparison to the default HAZUS approach. Use of the more widespread approach in estimating cyclic demands such as standard penetration and cone penetration tests would have involved developing median values of blow count and tip resistance as well as statistical models for their uncertainties across the site response category regions (Figure 3-5), possibly necessitating subdivisions as well as overlapping regions. The availability and maturity of statistical models for the variability of shear-wave velocities and layer thickness and nonlinear dynamic material properties were compelling arguments for implementing a shear-wave velocity approach to estimate cyclic capacities. The fact that too few measurements of cone tip resistance and/or blow count currently exist for soils below the Fall Line to develop reasonable statistical models was also a strong consideration. One advantage of this approach is that development of representative profiles is part of Task 3, and thus some economy in time could be achieved by their use. It is recognized that other engineering approaches for determining the liquefaction resistance of soils may be considered more applicable on a site-specific basis. It may also be feasible to consider use of other field measurements, such as SPT or CPT data, for more refined HAZUS analysis in areas of specific interest. In future studies, it may be desirable to evaluate the liquefaction resistance using correlations with either the SPT or CPT in areas where substantial data are available.

A particularly attractive advantage in using the shear-wave velocity approach in liquefaction assessment is that it is straightforward and it directly accommodates profile parametric uncertainty in a statistically rigorous manner. Within category variability (spatial variation within the site response areas, Figure 3-5), shear-wave velocity, as well as nonlinear dynamic material properties, can be incorporated in a manner consistent with developing the site amplification factors and ground motions, arriving at median and fractile estimates of liquefaction potential that are consistent with median and fractile estimates of ground motions. This is particularly important in loss estimation as HAZUS is fundamentally based on both ground motions and liquefaction (deformation), requiring the same fractile level for both hazards. The approach implemented in this project accomplishes this objective in a statistically rigorous manner.

The equation for determining the CRR from shear-wave velocity is empirical, and based on case history studies at sites that did and did not liquefy during earthquakes (Andrus and Stokoe, 2000). The equation is:

$$CRR = 0.022\,(K_C\,V^*_{S1}/100)^2 + 2.8\,[1/V^*_{S1} - K_C\,V_{S1})\text{-}1/V^*_{S1}] \cdot MSF \qquad (5\text{-}1)$$

$$MSF = (\mathbf{M}/7.5)^{-2.56} \qquad (5\text{-}2)$$

where V_{S1} is the stress-corrected shear-wave velocity, V^*_{S1} is the limiting upper value of V_{S1} for cyclic liquefaction occurrence that depends on fines content and K_C is a correction factor for cementation and aging. Because there is currently no widely accepted method for estimating K_C as well as its variability across the category areas (Andrus and Stokoe, 2000), it was taken as 1 for this study. The fines contents in Table 5-1 are conservatively assumed, based on our team's

experience in South Carolina. The actual fines content is expected to vary with depth and location.

Table 5-1
Estimated Fines Content for Determining Resistance to Liquefaction

Site Response Category	Fines Content (%)	V_{S1}^{*} (m / sec)
MB	20	208
SRS	20	208
C	5	215

5.2.2 Liquefaction Demand

Cyclic demands are expressed as the ratio of the average seismically-induced shear-stress to the vertical effective overburden stress within a liquefiable zone, generally within about 50 ft (15.2 m) of the ground surface:

$$CSR = \frac{\tau_{xy}}{\sigma'_{v}} \qquad \text{(Seed and Idriss, 1971)} \qquad (5\text{-}3)$$

In practice, demands are usually computed using approximate and generic relations between surface peak acceleration and at-depth cyclic shear stress (Seed and Idriss, 1971; Seed *et al.*, 1983; Youd and Idriss, 1997).

The ratio of capacity (CRR) to demand (CSR) is termed the factor of safety (FS) against liquefaction. Liquefaction is predicted to occur when FS is at or below 1, and not to occur when it exceeds 1. To provide a more rational basis for assessing risk levels, Juang *et al.* (2000, 2001) cast the deterministic factor of safety into an expression for the probability of liquefaction (P_L). This mapping function is given by:

$$P_L = 1/(1 + (FS/0.78)^{3.5}) \qquad (5\text{-}4)$$

It is based on the field performance data compiled by Andrus and Stokoe (2000) and accommodated the occurrence of sites that should have liquefied but did not, as well as those that did and provides the mechanism for translating liquefaction hazard into liquefaction risk. The Building Seismic Safety Council recommends a margin for the factor of safety against liquefaction of 1.2 to 1.5 for the simplified approach (Seed and Idriss, 1971). The corresponding probabilities are about 20% to 10% (Juang *et al.*, 2001). A factor of safety of 1 corresponds to a probability of about 30%.

For this study, the average CSR for the soil susceptible to liquefaction is determined during the site response analyses. Conditions which determine the CSR are: (1) cyclic shear stresses

induced by the earthquake throughout the liquefiable zone, (2) σ_{vo} – the total vertical overburden stress, and (3) σ'_{vo} – the effective vertical overburden stress. Calculation of the total and effective stress conditions requires estimation of the density of the overlying material. The following empirical correlation between shear-wave velocity and mass density (Mayne and Rix, 1993; Mayne and Rix; 1995; Hegazy and Mayne, 1995; and Burns and Mayne, 1996) was used to calculate the stress conditions:

$$\rho \text{ (mass density)} = 0.8 \log (V_s) \quad (5\text{-}5)$$

5.2.3 Computation of Liquefaction Hazard

To accommodate spatial variability in dynamic material properties within the site response categories below the Fall Line, both CRR and CSR estimates were computed, along with the amplification factors (Section 4.4). For each site response category and depth range (Table 4-7), 30 CRR and CSR values were computed using the RVT equivalent-linear site response methodology (Appendix C) at each expected hard rock peak acceleration (Table 4-6). Median and sigma estimates were then computed for the factor of safety (FS) and probability of liquefaction (P_L) (Equation 5-4), reflecting uncertainty in dynamic material properties across each site response category area. These median and fractile estimates of liquefaction susceptibility are consistent with the median and fractile estimates of the site amplification factors, both of which are conditional on expected (median) rock outcrop peak acceleration. As an example of the conditional estimates of the median factor of safety and probability of liquefaction, Figure 5-4 shows results for the Charleston site response category for the depth range of 2,000 to 4,000 ft and **M** 7.3. As a result of the randomization process, the curves are smooth, reflecting stable estimates, with a steep slope at low rock peak acceleration values and flattening out above 0.4 g. A factor of safety of 1 (probability of liquefaction of about 30%) is reached at about 0.3 g rock motion, which corresponds in this case to a median soil peak acceleration of about 0.26 g. Similar trends are seen for the other categories and depth ranges.

5.2.4 Liquefaction-Induced Settlement and Lateral Flow (Displacement)

On the basis of the computed FS, both the liquefaction-induced settlement and the lateral flow can be estimated. Considering the generalizations used to characterize the subsurface conditions, the settlement and flow estimates for this study are considered relative estimates that reflect both some variation in ground conditions and the level of ground shaking. Estimates of liquefaction-induced settlements and/or lateral flow for design purposes should be based on site-specific information and applicable empirical/theoretical relationships (e.g., Lee and Albaisa, 1974; Tokimatsu and Seed, 1987; and Ishihara and Yoshimine, 1992).

For this study, the assignment of the liquefaction-induced settlement is based on the computed factor of safety (FS) against liquefaction according to Table 5-2. The assignment of lateral flow is based on the relationship developed for HAZUS from work by Youd and Perkins (1978). The relationship, shown in Figure 5-5, is between the inverse of FS for liquefaction and the lateral flow displacement, where the PGA is the peak horizontal ground acceleration resulting from the scenario earthquake and PGA(t) is the minimum peak horizontal acceleration to induce

liquefaction. The lateral flow displacement (LFD) from Figure 5-5 is adjusted for earthquake magnitudes other than Mw = 7.5 using the following relationship:

$$LFD = LFD_{7.5} \times [0.0086\ M^3 - 0.0914\ \mathbf{M} - 0.9835]$$

Table 5-2
Liquefaction-Induced Settlement

Factor of Safety	Probability for Liquefaction	Liquefaction Hazard	Settlement (inches)
< 0.6	> 0.73	Very High	12
0.6 to 0.8	0.50 - 0.73	High	6
0.81 to 1.2	0.19 - 0.50	Moderate	2
0.121 to 1.5	0.10 - 0.19	Low	1
1.51 to 1.8	0.05 - 0.10	Very Low	0
> 1.8	< 0.05	None	0

5.3 SCENARIO EARTHQUAKE LIQUEFACTION

Based on the approach previously described, maps showing estimates of the P_L and FS for each of the four scenarios were produced. The map development was similar to the approach used for ground motions (Section 4.5.2). The P_L was a function of expected hard rock PGA only (Section 5.2.3), site response category, and soil depth. Soils whose thickness was 10 ft (3.0 m) or greater were considered to have a potential for liquefaction.

In Figures 5-6 and 5-7, the P_L is shown for both the high and low stress drop rupture models of the **M** 7.3 Charleston scenario. As discussed in Section 4.5.1.2, these mapped results were compared to the actual distribution of liquefaction features observed in 1886 (Figure 4-8) to weight the two stress drop rupture models. The high stress drop 50-km-long rupture generates a significantly larger area of liquefaction than was observed in 1886 (Section 4.5.1.2).

Figures 5-8 to 5-11 and 5-12 to 5-15 show the P_L and FS for the four scenarios, respectively. A $P_L \geq 30\%$ extends from Beaufort to the south and north to Lake Moultrie for the **M** 7.3 scenario (Figure 5-8). A FS of < 0.8 corresponding to high and very high liquefaction risk (Table 5-2) covers an area slightly larger than the area of intense craterlet activity in 1886 (Figure 4-8).

For the **M** 6.3 scenario, a P_L of 30% and greater is localized in the vicinity of the rupture (Figure 5-9). Similarly a FS < 0.8 occurs only along the modeled fault (Figure 5-13). In contrast, for the **M** 5.3 Charleston and **M** 5.0 Columbia scenario earthquakes, liquefaction is estimated to be unlikely (Figures 5-10, 5-11, 5-14, and 5-15). This is consistent with observations of past earthquakes worldwide where there are little, or no, case histories of liquefaction for earthquakes with magnitudes less than **M** 5.3 (Andrus and Stokoe, 2000; Loertscher and Youd, 1994).

5.4 EARTHQUAKE-INDUCED LANDSLIDE

In addition to the movement associated with liquefaction-induced settlement and lateral flow, there is also a potential for landslides in sloping terrain, where the additional seismic forces may temporarily exceed the slope strength. Newmark (1965) originally developed estimates for earthquake-induced slope movement based on the difference between the horizontal seismic acceleration and the critical acceleration. The critical acceleration is the horizontal acceleration for a condition where the resisting force is equal to the driving force (i.e., a factor of safety of 1.0). Makdisi and Seed (1978) extended the work by Newmark and developed a relationship between the ratio of the critical acceleration to the seismic acceleration and estimated slope displacement.

Although the Newmark/Makdisi and Seed approach is typically used for site-specific evaluation of embankment or dam deformation, it may also be applied, in a simplified manner, to the more general evaluation for this study. To accomplish this, HAZUS allows input of landslide susceptibility based on work by Wilson and Keefer (1985). Specifically, the susceptibility of an area to earthquake-induced landslides is assigned based on the general steepness of slopes, the soil/rock type and the groundwater conditions. Wilson and Keefer (1985) have 11 categories, which include a category of no susceptibility and 10 levels of susceptibility (I-lowest through X-highest). Figure 5-16, which is based on published literature (Radbruch *et al.*, 1982 and Nystrom *et al.*, 1996) and the results of our general subsurface characterization, presents our classification of South Carolina according to landslide susceptibility. The critical accelerations for the different categories (I through X as described by Wilson and Keefer, 1985) are presented in Table 5-3.

Table 5-3
Table of Yield Accelerations for Landslide Susceptibility

Susceptibility	None	I	II	III	IV	V	VI	VII	VIII	IX	X
Critical Acc (g)	0.00	0.60	0.50	0.40	0.35	0.30	0.25	0.20	0.15	0.10	0.05

Source: Loma Prieta Collection, EERC, UC Berkeley

Figure 5-1. Liquefaction-induced settlement of an embankment adjacent to a bridge abutment taken after the 1989 Loma Prieta earthquake.

Source: Steinbrugge Collection, EERC, UC Berkeley

Figure 5-2. Apartment buildings undergoing bearing-capacity failure due to underlying liquefied sand taken after the 1964 Niigata earthquake.

Source: USGS Collection

Note: Depth of craterlet is about 1 m; width is about 2 to 3 m. The white material around the craterlet is vented sand. The black wall of the craterlet is humate-enriched sand (i.e., A-horizon) that was located at and near the ground surface at the time of the earthquake.

Figure 5-3. Craterlet formed during the 1886 Charleston earthquake.

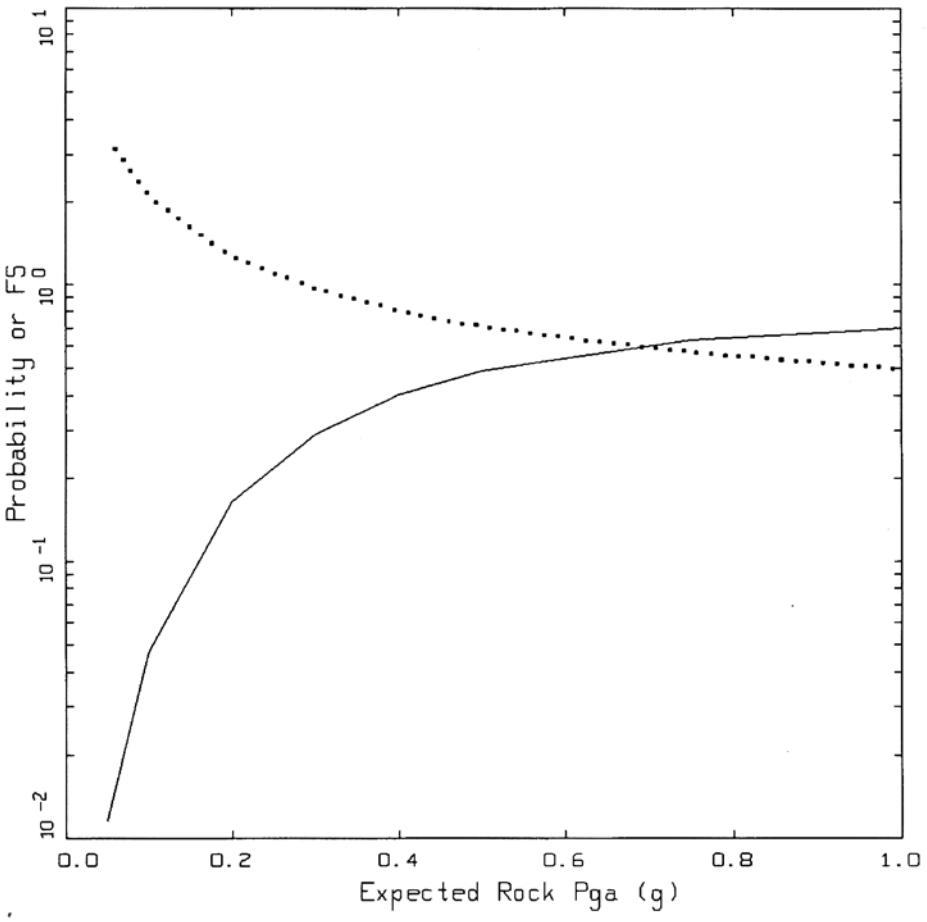

Figure 5-4. Median estimates of the factor of safety against liquefaction and probability of liquefaction, conditional on expected hard rock outcrop peak acceleration for Charleston site response category 7, 2,000 to 4,000 ft.

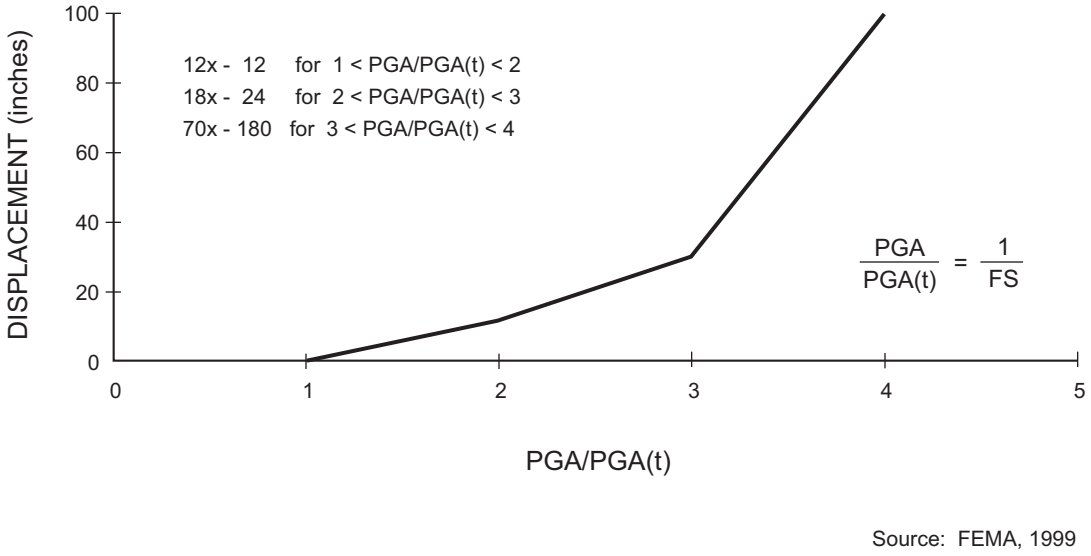

Source: FEMA, 1999

Figure 5-5. Lateral spreading displacement relationship.

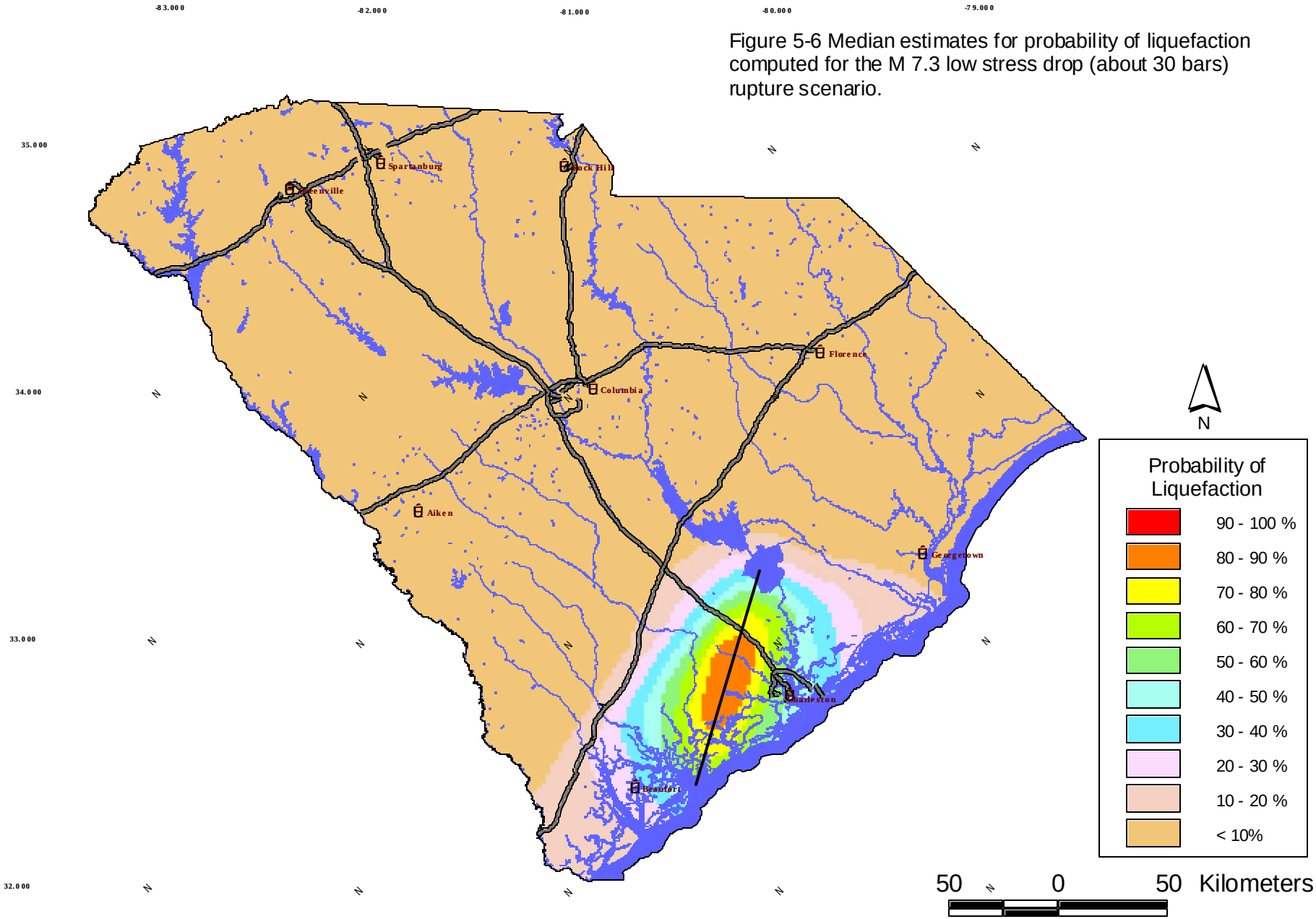

Figure 5-6 Median estimates for probability of liquefaction computed for the M 7.3 low stress drop (about 30 bars) rupture scenario.

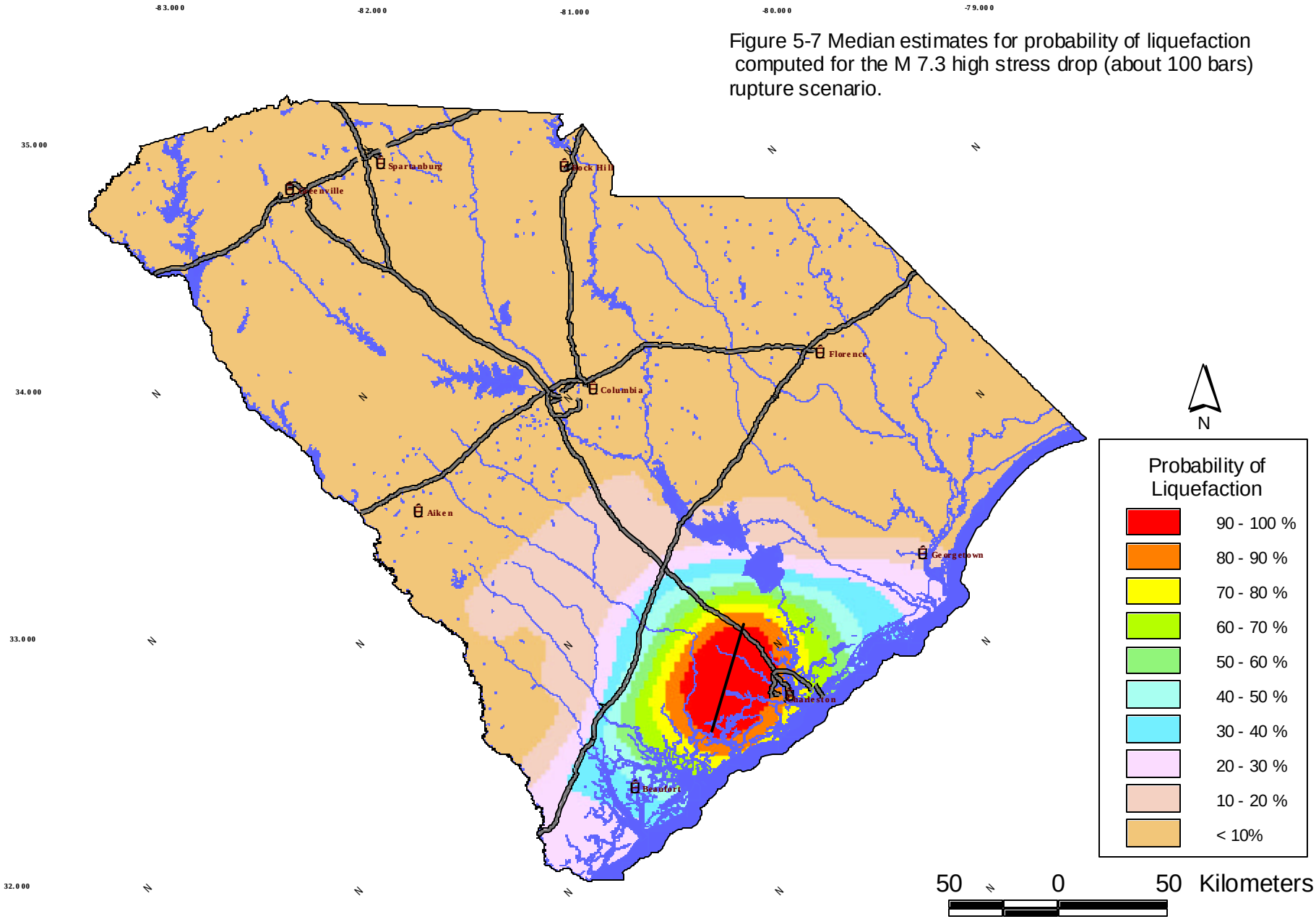

Figure 5-7 Median estimates for probability of liquefaction computed for the M 7.3 high stress drop (about 100 bars) rupture scenario.

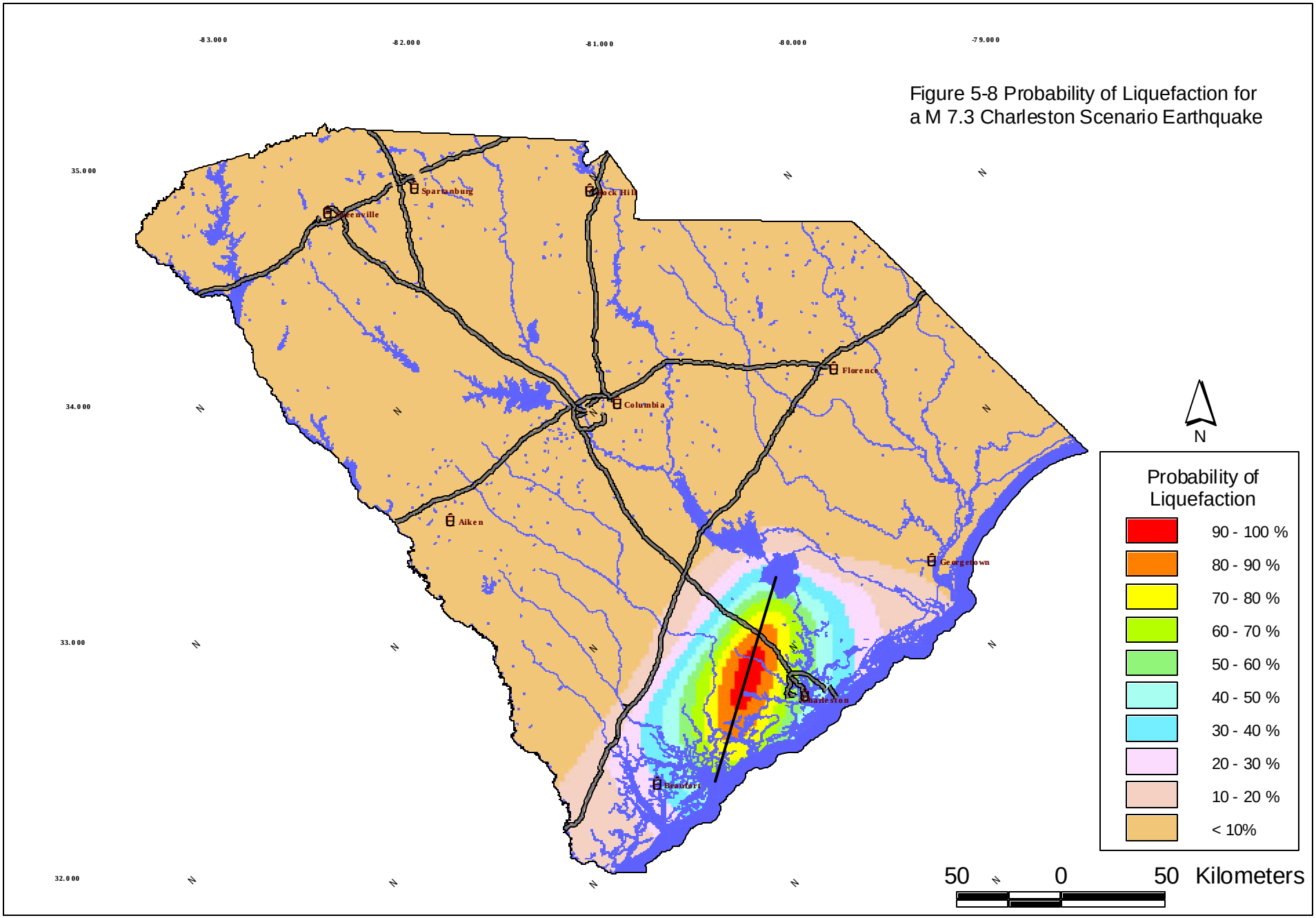

Figure 5-8 Probability of Liquefaction for a M 7.3 Charleston Scenario Earthquake

Figure 5-9 Probability of Liquefaction for a M 6.3 Charleston Scenario Earthquake

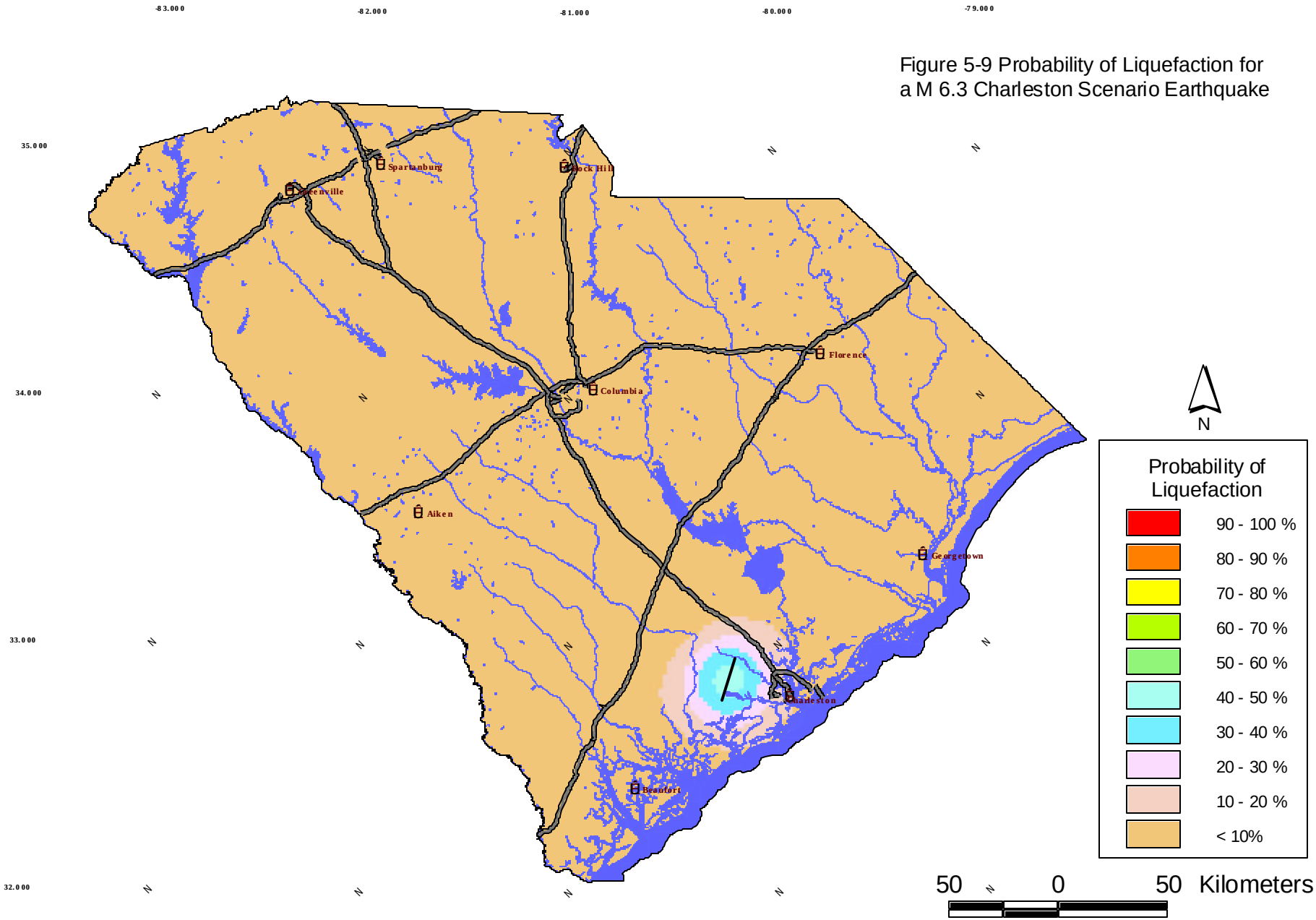

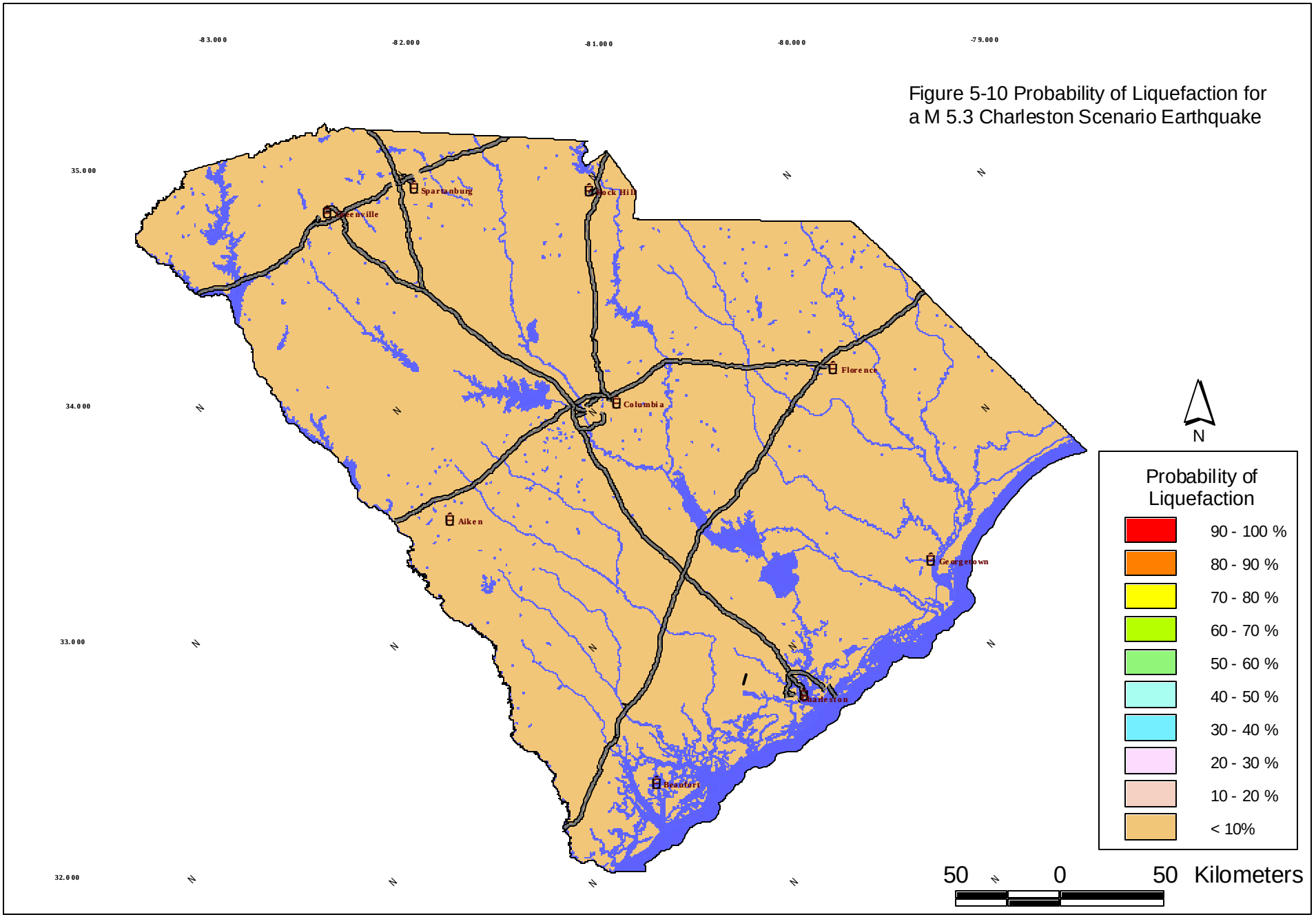

Figure 5-10 Probability of Liquefaction for a M 5.3 Charleston Scenario Earthquake

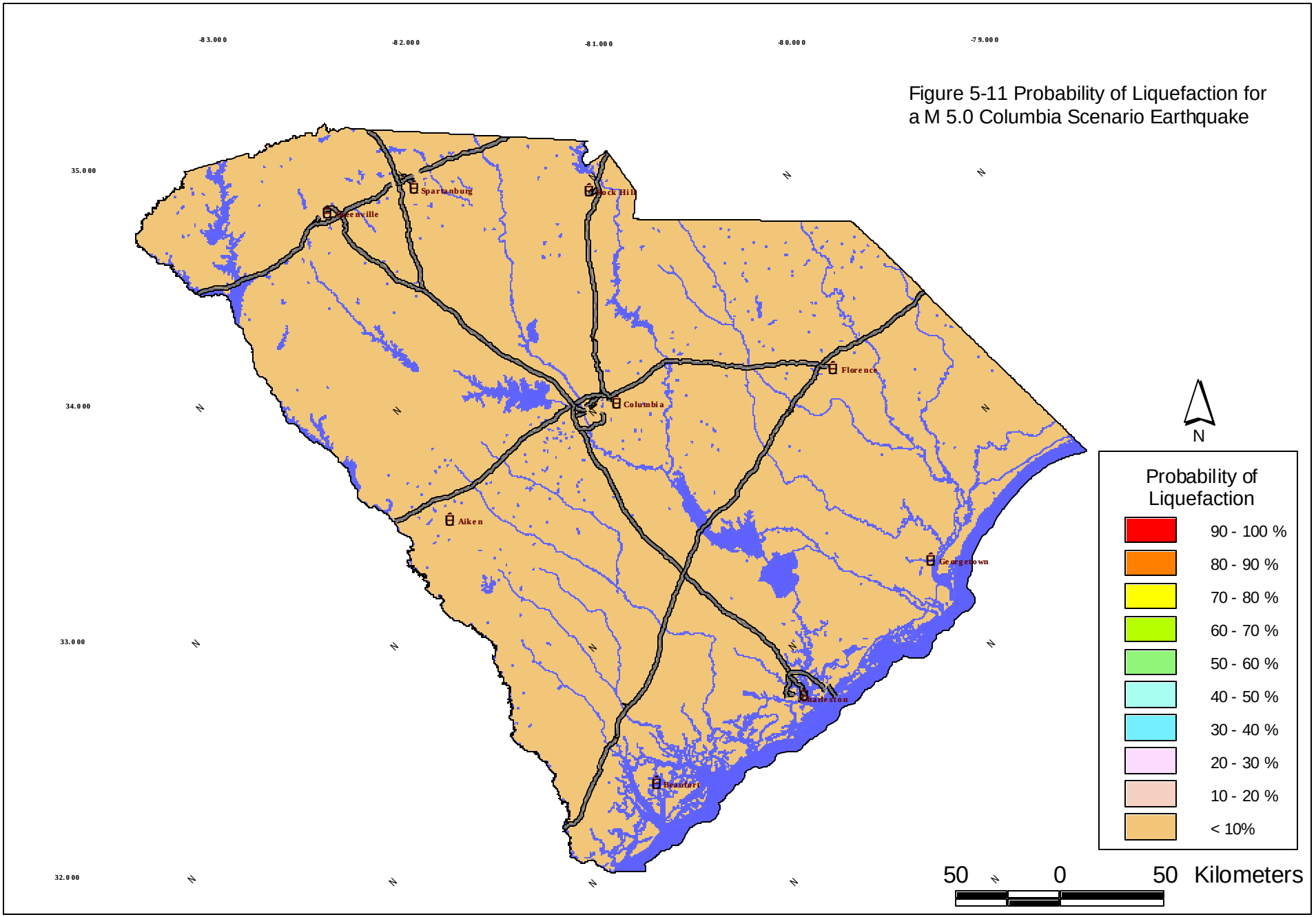

Figure 5-11 Probability of Liquefaction for a M 5.0 Columbia Scenario Earthquake

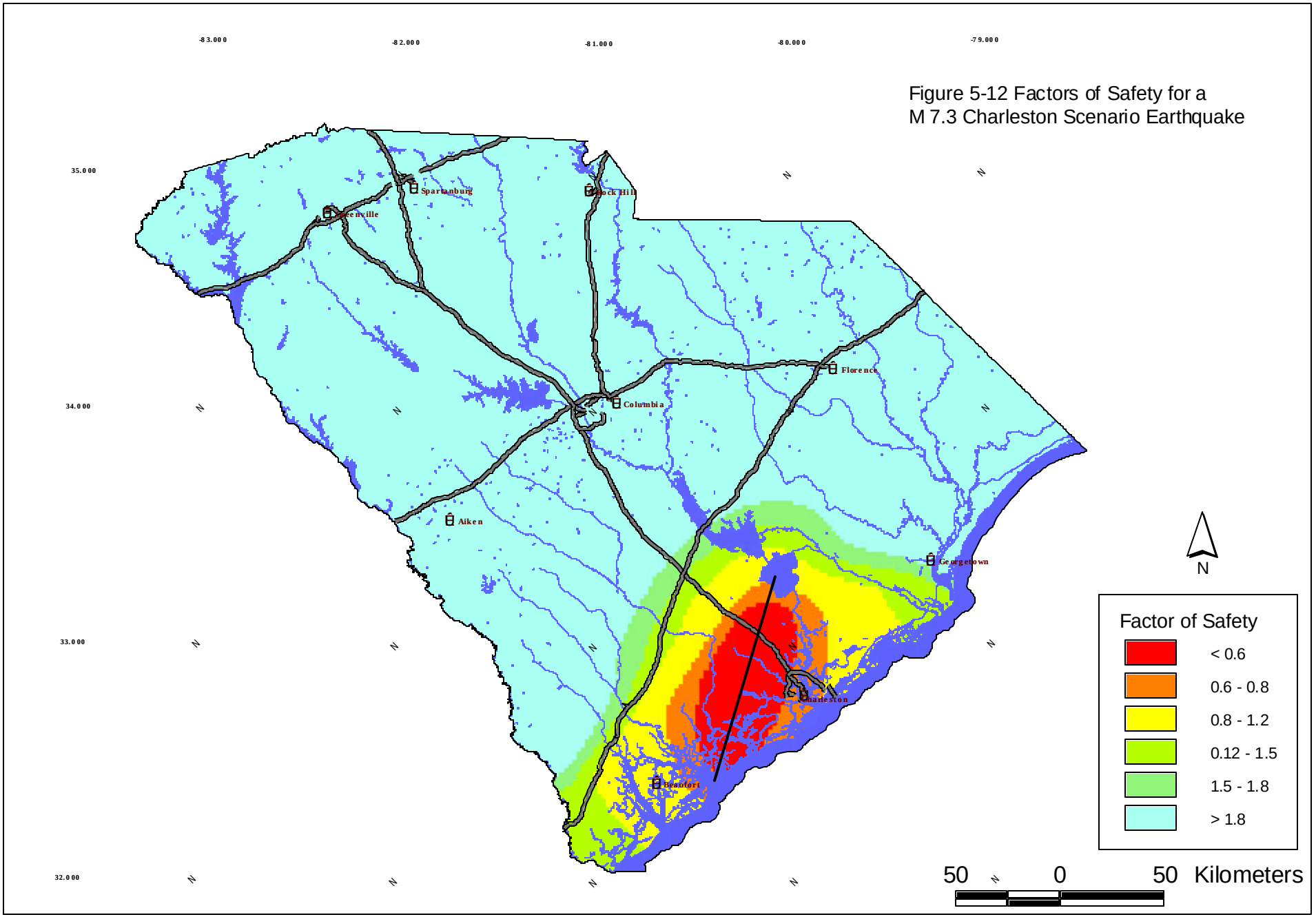

Figure 5-12 Factors of Safety for a M 7.3 Charleston Scenario Earthquake

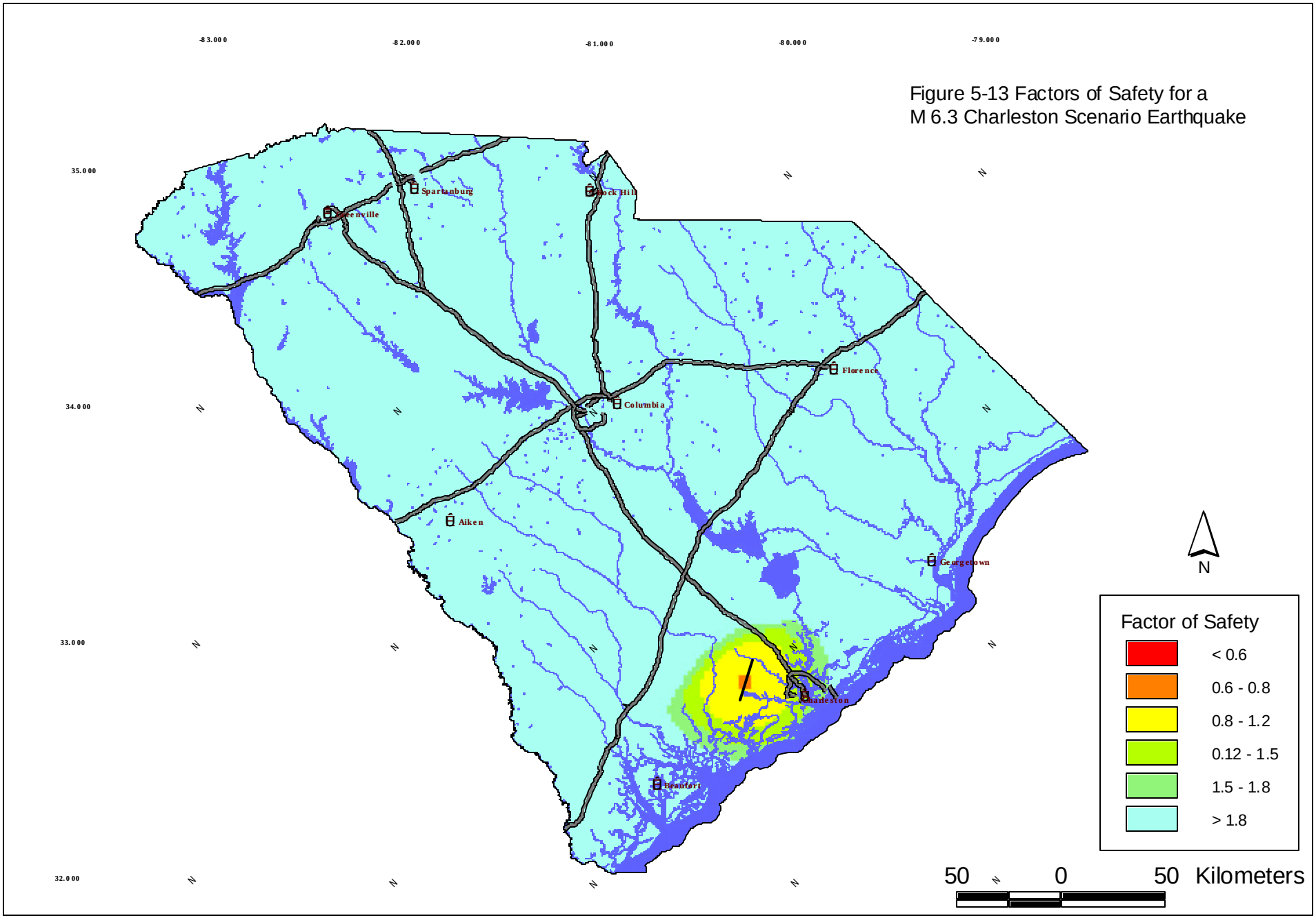

Figure 5-13 Factors of Safety for a M 6.3 Charleston Scenario Earthquake

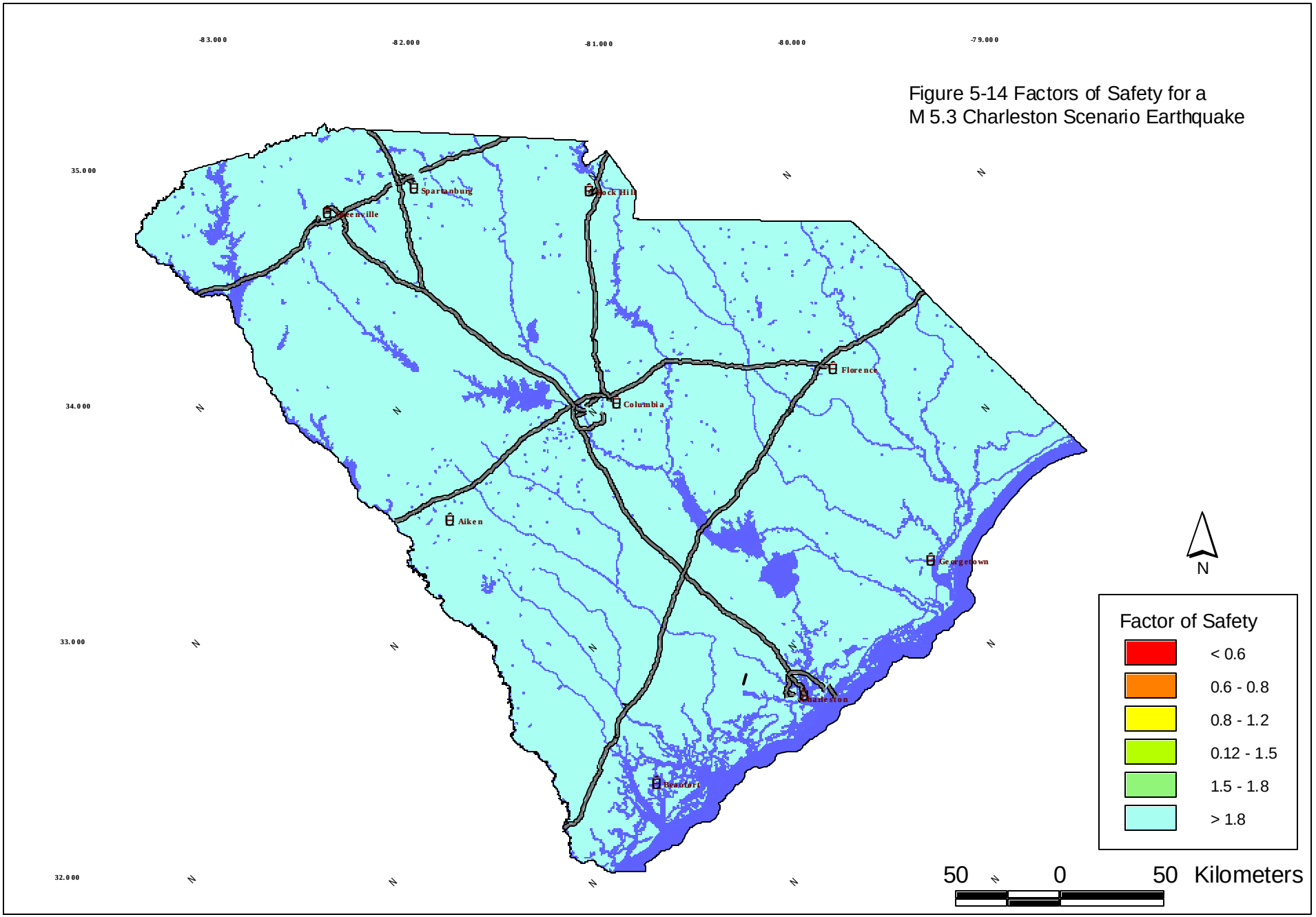

Figure 5-14 Factors of Safety for a M 5.3 Charleston Scenario Earthquake

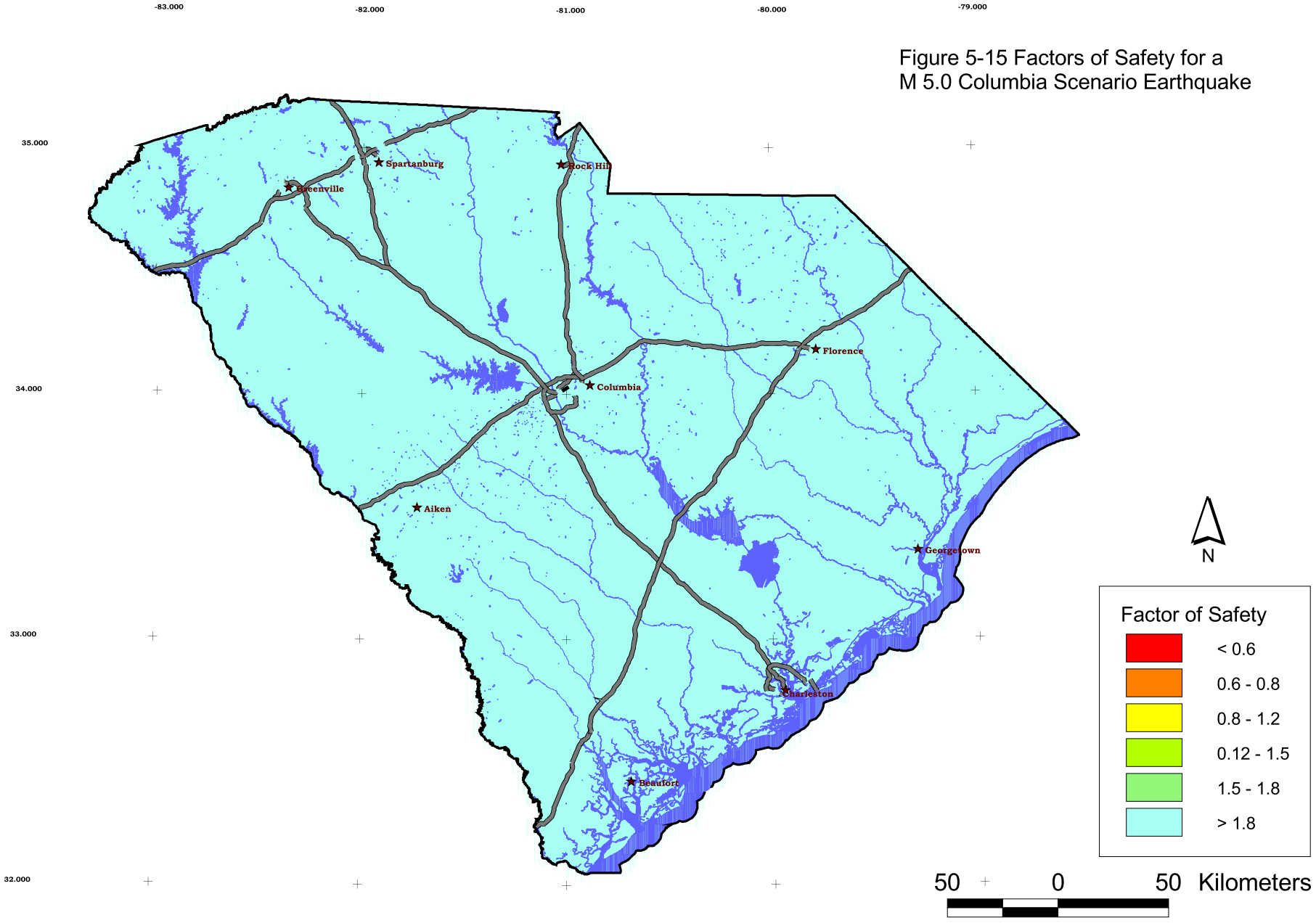

Figure 5-15 Factors of Safety for a M 5.0 Columbia Scenario Earthquake

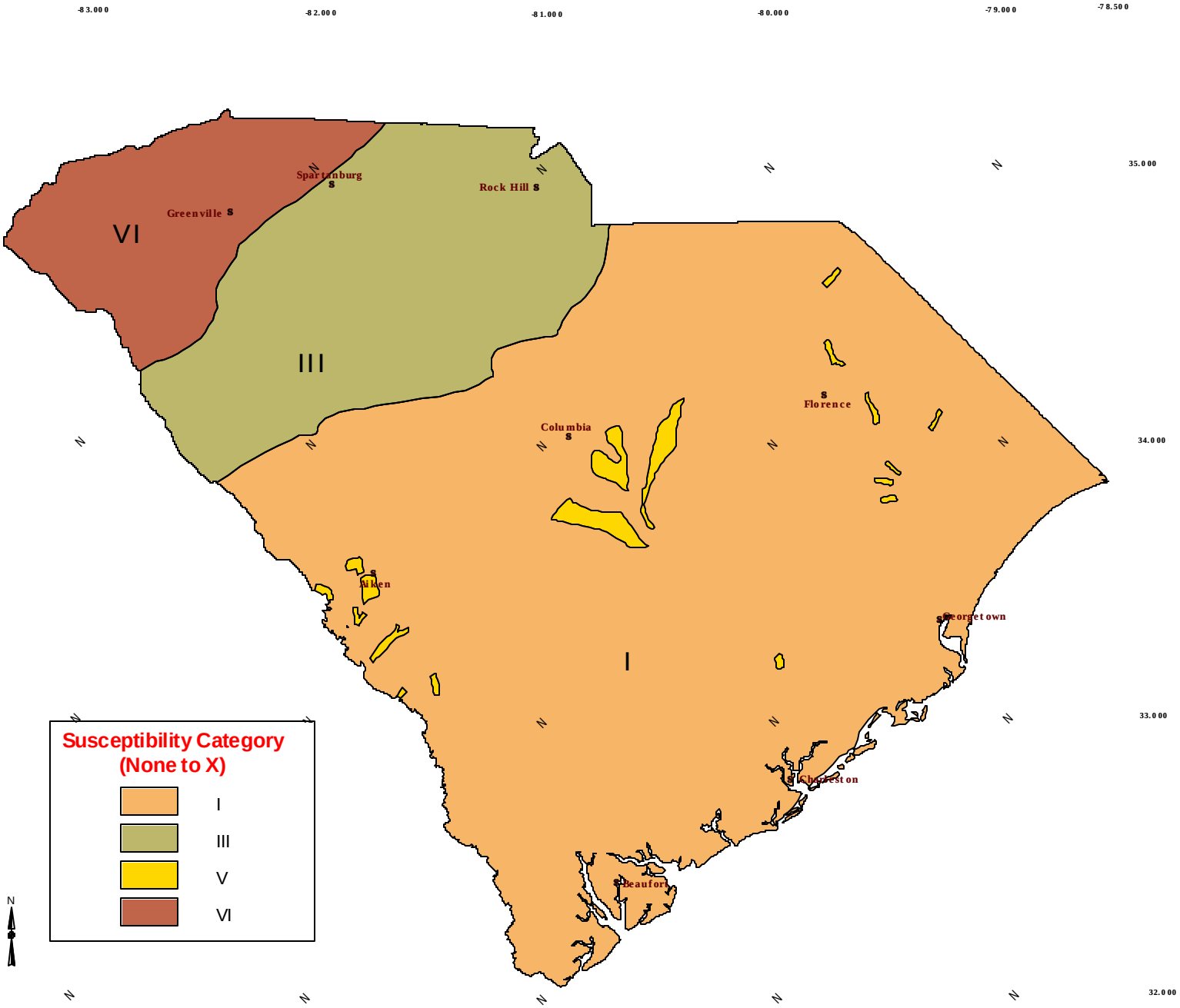

Figure 5-16. Landslide susceptibility map.